UNIVERSITEIT VAN PRETORIA
UNIVERSITY OF PRETORIA
YUNIBESITHI YA PRETORIA

Towards genetic interrogation of putative amino acid transporters in *Plasmodium falciparum* parasites

Marché Maré

18001719

Submitted in partial fulfilment of the degree:

Magister Scientiae in Biochemistry

Faculty of Natural and Agricultural Sciences

Department of Biochemistry, Genetics and Microbiology Division of Biochemistry

University of Pretoria

12 December 2023

DECLARATION OF ORIGINALITY

University of Pretoria

Faculty of Natural and Agricultural Sciences

Department of Biochemistry, Genetics, and Microbiology

Full names of student: Marché Maré

Student number: 18001719

Declaration

1. I understand what plagiarism is and am aware of the University's policy in this regard.
2. I declare that this project proposal is my original work. Where other people's work has been used (either from a printed source, Internet, or any other source), this has been properly acknowledged and referenced in accordance with requirements.
3. I have not used work previously produced by another student or any other person to hand in as my own.
4. I have not allowed and will not allow anyone to copy my work with the intention of passing it off as his or her own.

Signature: 

Date: 04/12/2023

Tables of Contents:

List of Figures

List of Tables

Abbreviations

AAAP	Amino acid/auxin permease family
ACT	Artemisinin-based combination therapy
ApiAT	Apicomplexan amino acid transporter
ATc	Anhydrotetracycline
DD	Destabilisation domain
ddNTPs	Dideoxynucleotides
DDT	Dichlorodiphenyltrichloroethane
DHODH	Dihydroorotate dehydrogenase
dNTP	Deoxynucleotide
eIF2α	Eukaryotic initiation factor 2α
EPM	Erythrocyte plasma membrane
FC	Fold change
GC	Guanylyl cyclase
gDNA	Genomic DNA
GlcN-6-P	Glucosamine-6-phosphate
glmS	*glmS* ribozyme
GOI	Gene of interest
hDHFR	Human dihydrofolate reductase
hpi	Hours post invasion
IDC	Intraerythrocytic development cycle
IMC	Inner membrane complex
IRS	Indoor residual spraying
KS	Knock sideway
Neo^R	Neomycin resistance

NPPs	New permeability pathways
NSS	Neurotransmitter:sodium symporter
PCR	Polymerase chain reaction
PVM	Parasitophorous vacuolar membrane
RE	Restriction enzyme
rpm	Revolutions per minute
Shld-1	Shield
SLI	Selection-linked integration
T2A	Skip peptide
TAE	Tris-acetate-EDTA
TetR	Tet repressor protein
TGD	Targeted gene deletion
WHO	World Health Organisation
WT	Wild type

Acknowledgements

I would like to express my heartfelt gratitude to my supervisor, Dr Jandeli Niemand, whose unwavering support, guidance, and understanding have been instrumental throughout the duration of my MSc project. Her dedication, expertise, and continuous effort have significantly influenced both the project's quality and my personal and professional development. A special thank you goes to my co-supervisor, Prof Lyn-Marié Birkholtz, whose valuable input, and scientific perspective have brought depth and richness to my research, contributing greatly to the project's overall excellence.

Heartfelt thanks also go out to my friends, Shanté da Rocha, Sizwe Tshabalala, Jean Thomas, Martha Muruya, Henrico Langeveld, Dana Schultz, Daniel Opperman and Christea van Zyl, whose wisdom, care, and active involvement have not only enriched the academic aspect but have also added immense personal fulfillment to this journey. Their support, companionship, and enduring friendship have been an indispensable part of my life, and I cherish the memories we've created together. Furthermore, to each member of the Malaria Parasite Molecular Laboratory (M^2PL) team, I extend my gratitude for your contributions, encouragement, and belief in my capabilities.

I am deeply grateful to my parents, Delia and Franscouis Maré, for their unending love and unconditional support, serving as a source of strength and motivation that empowered me to overcome challenges and strive for excellence in my work. I am equally grateful to my brother, Franco Maré. I am truly fortunate to have such an amazing support system. Above all else, I give thanks to God for His guidance and blessings throughout this journey.

Lastly, I acknowledge the National Research Foundation for funding this degree through the NRF Grantholder-linked bursary.

Summary

Malaria is a life-threatening tropical disease that caused 619 000 malaria-associated deaths in 2021. Although malaria is a curable disease, the causative agent, the *Plasmodium falciparum* parasite, continuously develops antimalarial resistance, making current chemotherapeutics ineffective. Nutrient acquisition in the *Plasmodium* parasite is essential for the proliferation and development of the obligatory intracellular parasite. The parasites are amino acid auxotrophs, and amino acids are mostly obtained from haemoglobin digestion, with additional amino acids, such as isoleucine and methionine, obtained from the extracellular environment. The uptake of these extracellular amino acids requires transport across multiple membranes surrounding the parasite. Between the asexual and gametocyte life stages, a dynamic shift in the expressed transportome was observed, as seen by the expression of all 11 putative amino acid transporters in asexual parasites, whereas gametocytes only express four of these amino acid transporters constitutively. Of the four putative amino acid transporters expressed in gametocytes, two transporters from the neurotransmitter:sodium symporter family are constitutively expressed in *P. falciparum* asexual parasites and gametocytes, and we hypothesize that these are essential for asexual proliferation and sexual differentiation in *P. falciparum* parasites.

Here, our objective was to develop genetically modified parasite lines to investigate the essentiality of two putative amino acid transporters, Pf3D7_0515500 and Pf3D7_1132500, in *P. falciparum* asexual parasites and gametocytes. The essentiality of the two putative transporters was probed by generating irreversibly truncated, non-functional proteins through targeted gene deletion. However, if the amino acid transporter proteins are essential for asexual stage parasites, no integrants will be obtained, which prevents the evaluation of its essentiality in gametocyte stages using the same system. Therefore, an inducible knockdown system was also investigated to conditionally alter gene expression levels of the amino acid transporters through the action of a *glmS* ribozyme. The required recombinant plasmids for both systems were generated as confirmed with Sanger sequencing. Following transfection, parasites with episomal uptake of the plasmids were obtained. Although no integrants for the SLI-TGD system were obtained, a population of parasites transfected with SLI-*glmS* plasmids developed neomycin resistance. The integration confirmation PCR for the recovered parasite populations did not confirm genomic integration at the GOI locus, however for NF54-Pf3d7_0515500-*glmS*-GFP green fluorescence was detected, possibly indicating integration of the recombinant

plasmid at another locus. In the future, whole genome sequencing could be considered to determine where genomic integration occurred, and ultimately characterise these proteins.

1. Literature review

1.1. Malaria

Malaria is a significant global health concern, with economic and socio-economic impacts on several countries. Although malaria is preventable and treatable, it remains deadly. In 2021, there were an estimated 247 million malaria cases and 619 000 malaria-associated deaths, in 84 malaria-endemic countries (1). The four countries that accounted for the most malaria-related deaths, with a total of 52 % of global cases in 2021, including Nigeria, the Democratic Republic of the Congo, the Republic of Tanzania, and Niger (Figure 1.1). Underdeveloped countries, with scarce healthcare and malaria intervention aids, account for 95 % of malaria cases (2). Additionally, between 2019 and 2021, an estimated 63 000 people died from malaria due to Covid-19 related disruptions to essential malaria services (1).

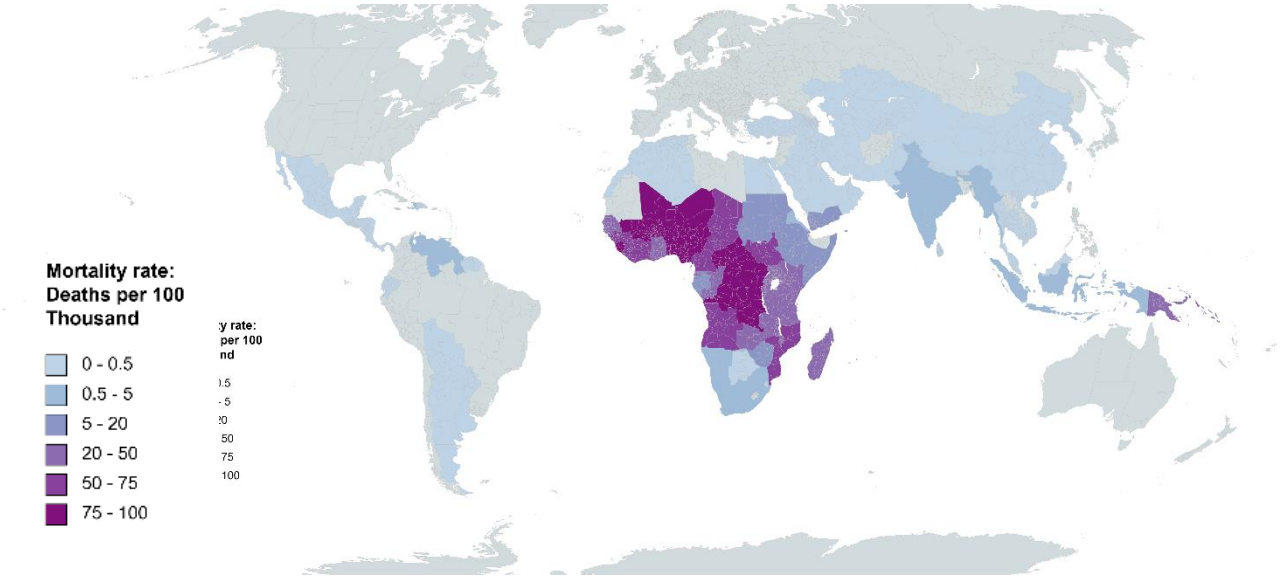

Figure 1.1: Global map of 2021 malaria mortality rate distribution.
Geological distribution of estimated malaria deaths in 2021 per 100 thousand. Image adapted from WHO Malaria Report 2022, for deaths recorded in 2021 per population denominators. Image produced in MapChart (https://www.mapchart.net).

Malaria is caused by protozoan parasites of the genus *Plasmodium*, transmitted to the human host by female *Anopheles* spp. mosquitoes infected with *Plasmodium* spp. In South Africa, malaria is transmitted along the border areas of Limpopo, Mpumalanga and KwaZulu-Natal by mosquito vectors *Anopheles funestus* and *Anopheles gambiae* that transmit the *Plasmodium falciparum* parasite to the human host (3).

There are currently six known *Plasmodium* species that can infect humans: *P. falciparum*, *Plasmodium vivax*, *Plasmodium ovale curtisi, Plasmodium ovale wallikeri*, *Plasmodium malariae*, and *Plasmodium knowlesi* (4, 5). Of these, *P. falciparum* and *P. vivax* result in the highest number of infections and subsequent deaths. Unlike other species of *Plasmodium*, *P. falciparum* parasites infect mature erythrocytes, causing intense haemolysis and sequestration of infected erythrocytes resulting in severe complications such as organ dysfunction, metabolic acidosis, and respiratory distress (6-10). By contrast, *P. vivax* can only invade the small percentage of reticulocytes found in the blood (8, 10) and only 2 % of the global malaria cases estimated in 2021 were caused by *P. vivax* infection (1).

1.2. *P. falciparum* life cycle

In the human host, the *P. falciparum* parasite's life cycle (Figure 1.2) consists of asexual exo-erythrocytic development within the liver, followed by the asexual intraerythrocytic development cycle (IDC) and lastly sexual differentiation. During a blood meal by parasite-infected *Anopheles* mosquitoes, infectious sporozoites enter into human skin and migrate via the bloodstream (11), to reach the liver within two minutes (12). In the parenchymal hepatocytes, the parasite undergoes exoerythrocytic schizogony, to form merozoites. Thousands of these are released from a hepatocyte ~ 6.5 days later to invade erythrocytes, initiating the IDC (13, 14).

Upon contact with the erythrocyte, the merozoite initiates erythrocyte invasion (15), during which the parasitophorous vacuolar membrane (PVM) is formed around the parasitic plasma membrane (PPM) inside the erythrocyte. The intraerythrocytic parasite is ultimately surrounded by three membranes, the erythrocytic plasma membrane (EPM), the PVM and the PPM (15, 16). Three morphological stages of intraerythrocytic asexual development can be observed: ring, trophozoite, and schizont stages. Ring-stage parasites have a thin ring of organelle-rich cytoplasm surrounding a clear centre composed of a few organelles with low metabolic activity (17, 18). The parasite develops novel mechanisms to acquire nutrients from the host plasma, and new permeability pathways (NPPs) are induced at 10 – 20 hpi to increase the permeability of erythrocytes to various carbohydrates, amino acids, and monovalent ions (19, 20). The appearance of a haemozoin pigment, the product of haemoglobin digestion in the phagosome, marks the onset of the trophozoite stage (17, 21). In the trophozoite stage (20 – 30 hpi (18)) the parasite becomes metabolically active and there is a rapid increase in the size of the parasite as extensive RNA and protein synthesis takes place. From 33 – 36 hpi, nuclear replication occurs, and a multinucleated schizont is formed. Merozoites egress occurs after cytokinesis, where up

to 32 merozoites are released at 48 hpi (22, 23). Each of the daughter merozoites, invades another erythrocyte and initiate another IDC (20).

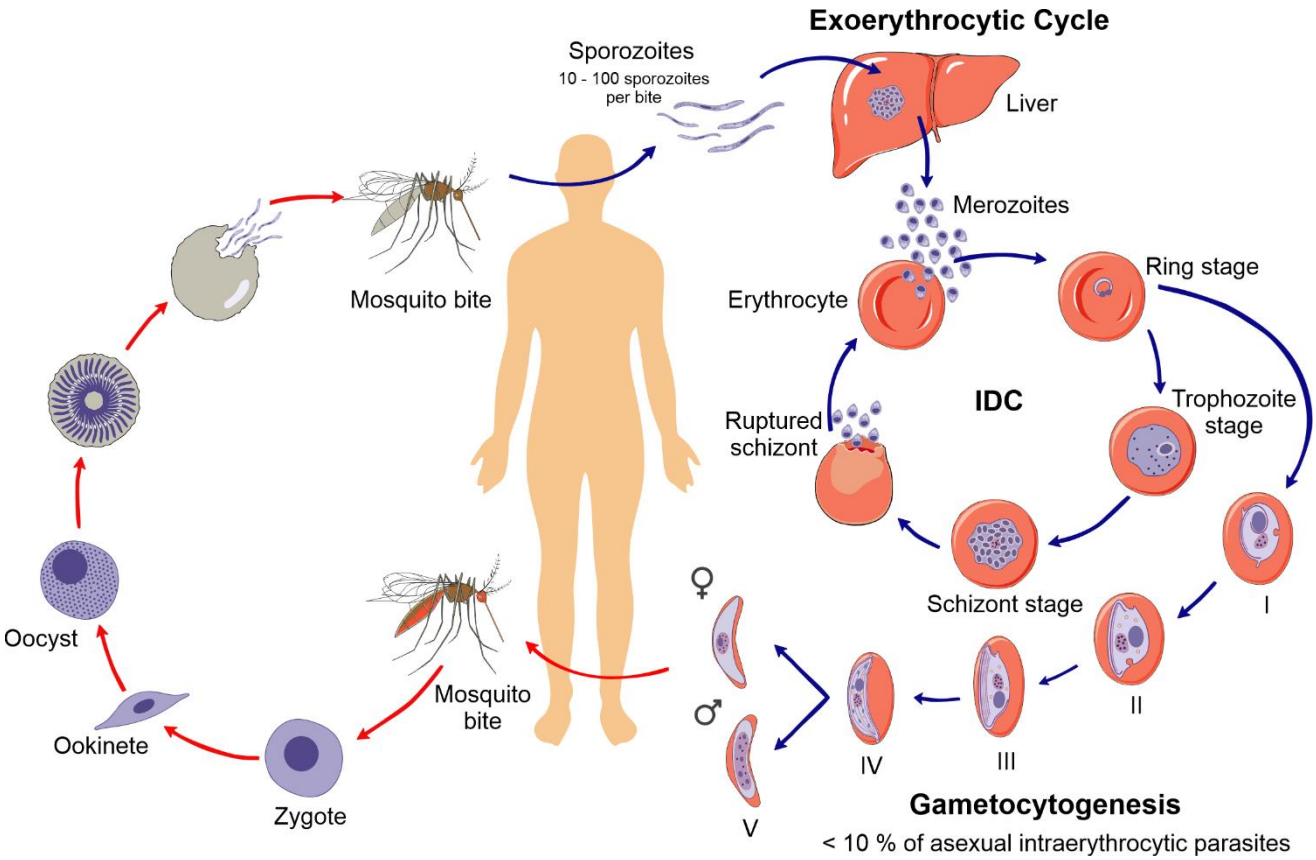

Figure 1.2: Life cycle of *P. falciparum*.
The human host is infected with *P. falciparum* sporozoites during a female *Anopheles* mosquito bite. Sporozoites, injected into the host tissue, migrate to the liver through the blood vessel and infect hepatocytes. When hepatic schizonts rupture, merozoites are released into the blood. Once the merozoites infect erythrocytes, the 48 h intraerythrocytic developmental cycle (IDC) is initiated. A subpopulation of parasites commits to sexual differentiation to form mature gametocytes, which are ingested by *Anopheles* mosquitos where fertilization occurs in the midgut to form zygotes. The zygotes develop into mobile ookinetes, which differentiate into an oocyst that matures to sporozoites. Sporozoites are released into the salivary glands of the mosquito and re-initiate the cycle of infection. Created using CorelDRAW 2020.

A small population (< 10 %) of trophozoites differentiates into male and female gametocytes, which are essential for the transmission and reinfection of the *Plasmodium* parasite (24). In *P. falciparum*, gametocytogenesis takes between 9 - 12 days and can be divided into 5 distinct morphological stages defined as stage I-V (Figure 1.2).

P. falciparum gametocyte stages I to IV are sequestered in the bone marrow to allow sexual maturation while avoiding phagocytic clearance (25). Stage I gametocytes are morphologically comparable to asexual trophozoite stage parasites. Stage II gametocytes are marked by the

deposition of specialised elongation machinery called the inner membrane complex (IMC) and have a distinct D-shape within the erythrocyte, while a stage III gametocyte has an elongated lemon shape. Stage IV gametocytes are maximally elongated by the extension of the subpellicular complex, and the characteristic “falciform” shape is observed. At stage IV, haemoglobin digestion is completed, and the host erythrocyte is reduced to a thin layer around the parasite (25).

Mature stage V male and female gametocytes have increased flexibility and re-enter the peripheral blood circulation. Female gametocytes are characterised by a small, dense nucleus and a concentrated haemozoin pigment pattern, while male gametocytes have a larger nucleus and scattered haemozoin pigment pattern. Mature gametocytes are taken up from peripheral blood when female *Anopheles* mosquitoes feed (17, 24, 26).

Within minutes of ingesting mature male and female gametocytes, gametogenesis occurs in the mosquito midgut, which is initiated by a decrease in temperature, increase in pH, and gamete activating factor, xanthurenic acid, to form micro- (male) and macro- (female) gametes (27). During microgametogenesis and exflaggelation, male gametocytes undergo three rounds of DNA replication and mitotic division, resulting in eight flagellated male gametes (28). Fertilisation occurs within 15 to 20 minutes of being taken up by the mosquito when flagellated male gametes fuse with female gametes. Diploid zygotes then undergo meiosis and differentiate into mobile ookinetes. The elongated unicellular ookinetes penetrate the midgut epithelium and the oocyst forms between the midgut epithelium and the basal lamina. The oocysts mature into sporozoites and after 8 - 16 days, the sporozoites are released into the haemolymph where they enter the salivary glands of the mosquito (28-30).

The complex life cycle of the *P. falciparum* parasite, with its dependence on the mosquito vector and human host, requires a wide range of malaria control strategies. These include various prevention strategies and chemotherapeutics to prevent and treat *P. falciparum* parasite infection.

1.3. Malaria control

A multi-layered approach is needed to control the spread of the disease by mosquitoes and to treat infections. The efficacy of most control strategies is finite due to antimalarial and insecticide resistance development, and therefore new antimalarial agents and novel drug targets are essential (31).

Vector control strategies are designed to decrease the transmission of *Plasmodium* parasites by either reducing mosquito numbers or preventing biting. Vector control strategies include long-lasting insecticidal bed nets and indoor residual spraying (IRS) with insecticides. However these are threatened by vector resistance to insecticides such as pyrethroids (32). Alternatively, the mosquito population is controlled with larvicides and draining the mosquito's breeding reservoirs (33, 34). Between 2015 and 2021, the number of people protected from malaria infections with vector control strategies decreased from 112 million to 80 million, likely due to vector insecticide resistance and climate change resulting in a change of migration patterns and habitats of the *Anopheles* mosquito (1, 33, 35).

Parasite control strategies include chemoprophylaxis to prevent infection by the *Plasmodium* parasite, and chemotherapeutics reduce pathogenesis if infected. Chemoprophylaxis is used to protect travelling individuals and residents in endemic areas during seasonal malaria outbreaks (34). In South Africa, a daily dose of doxycycline or a weekly dose of mefloquine is advised (36). However, a *Plasmodium* infection that will result in the onset of malaria symptoms can still occur when chemoprophylaxis fails.

Treatment of malaria has been limited by the development of drug resistant *Plasmodium* parasites, and older antimalarial drugs, including chloroquine and antifolates, have become ineffective (37). The current gold standard for treating malaria infection is artemisinin-based combination therapy (ACT), which consists of a fast-acting artemisinin derivative and slow-acting partner drugs that significantly reduce parasite numbers while reducing the risk of resistance (1). Although independent cases of artemisinin resistance have been reported in southeast Asia and Africa (38), ACTs only fails when resistance against both artemisinin and the partner drug develop. Antimalarial drug resistance, which develops during the replicative asexual stages, can only be spread when the non-pathogenic mature gametocytes are transmitted to the mosquito vector. Therefore, the incorporation of transmission blocking or dual active drugs, targeting the asexual parasite stages and gametocytes, is an important component in chemotherapeutics to prevent the spread of resistance (39). Dual-active antimalarials currently in the drug development pipeline include Cipargamin (KAE609). Another combination therapy active against liver stages, asexual parasites and gametocytes is Ganaplacide (KAF156) combined with lumefantrine and is being tested in patients (40).

Vaccines have been notoriously difficult to develop to prevent parasite infections. The pre-erythrocytic vaccine, RTS, S/AS01$_E$, based on the *P. falciparum* circumsporozoite protein only has 36 % efficacy and was approved for widespread use among children in malaria affected

sub-Saharan Africa in 2021. This vaccine targets the sporozoite stage of *P. falciparum* by blocking hepatocyte infection, thus preventing the re-entry of the parasite into the bloodstream, and forming intraerythrocytic stages (41, 42). Another pre-erythrocytic vaccine candidate targeting the circumsporozoite protein, R21 along with the adjuvant Matrix-M, has now been approved by the WHO (43).

New chemotherapeutic targets are consistently needed to combat the spread of antimalarial and insecticide resistance (44, 45). Therefore, extensive knowledge is needed about the *Plasmodium* parasite's biology to identify new chemotherapeutic targets.

1.4. Membrane transport proteins

Membrane transport proteins are crucial for various physiological processes such as nutrient uptake, the generation and maintenance of the transmembrane electrochemical gradients and the removal of metabolic waste and drugs (46). These proteins are classified into three groups based on their functional characteristics and mechanism of action: carrier proteins, channel proteins, and pumps (Figure 1.3).

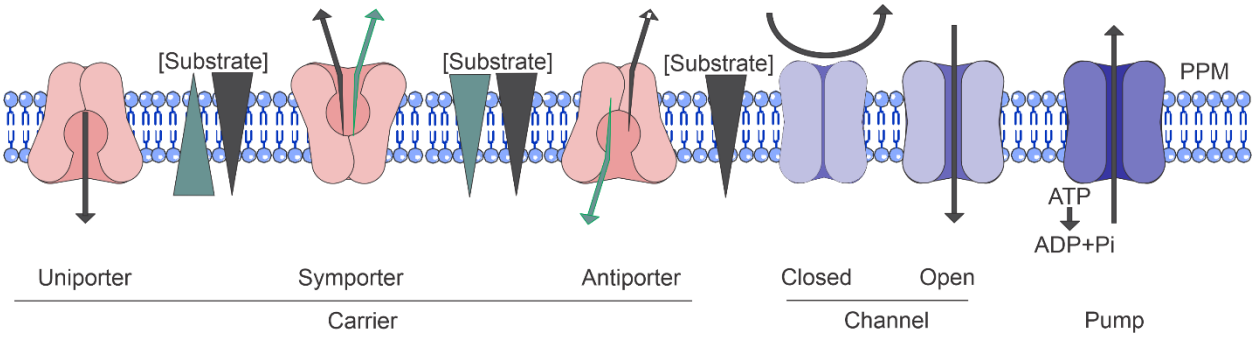

Figure 1.3: Membrane transport protein classes.
Three main classes of membrane transporters are channels, carriers, and pumps. Carriers undergo conformational change upon substrate binding and use the electrochemical gradients of H^+ or Na^+ to transport substrates down or against their electrochemical gradient. Channels transport substrates down their electrochemical gradient through an aqueous passage. Pumps, powered by ATP hydrolysis, transport substrates against their electrochemical gradients.

Carrier proteins undergo a conformational change upon binding to a specific substrate to transport these solutes across the bilipid membrane, and these proteins can be further classified into three subclasses uniporters, symporters, and antiporters. While uniporters facilitate the transport of a single solute down its electrochemical gradient, symporters and antiporters transport two or more substrates simultaneously. Symporters and antiporters use the energy stored in one or more of their substrate's electrochemical gradients (such as H^+ and Na^+) to drive the transport of another substrate against its electrochemical gradient (47). Channel

proteins are aqueous pores that are open, to constitutively allow rapid transport of solutes, or closed and first needs a physiological signal to induce a conformational change to open the pore and allow rapid transport of small solutes (with a specific size and charge) down their electrochemical gradient. Lastly, ATP-powered pumps are active transporters that use ATP hydrolysis to generate energy and transport solutes across the phospholipid membrane against the electrochemical gradient (48).

Plasmodium falciparum parasite infected erythrocytes have an increase in the rate of substrate uptake compared to uninfected erythrocytes. The parasite transports sugars, amino acids, vitamins, metabolites, waste products, and ions across the various membranes for successful replication (49-51). For this reason, the *P. falciparum* parasite changes the EPM and the PVM by trafficking membrane transport proteins from the parasite to the surrounding membranes to adjust the permeability and allow the transport of substrates (52).

The *P. falciparum* transportome consists of 19 channels, 69 carriers and 29 pumps, and is encoded by 3 % of the parasite's genome. This is reduced compared to the vector, *A. gambiae* (5 %) and the host, *Homo sapiens* (4 %). Transporters with overlapping functions were lost through evolutionary adaptation of the parasite in the relatively nutrient rich environments of the mosquito midgut and human blood (47). Notwithstanding this limited repertoire of transport proteins, mutations in these transport proteins are used to confer drug resistance, even if it affects the natural function. For example, mutations in the chloroquine resistance transporter (PfCRT) allow chloroquine-resistant parasites to export the antimalarial from the food vacuole and prevent the binding of chloroquine to its haem and haemozoin targets, rendering the drug inactive (45, 53). Furthermore, multidrug resistance appears due to mutations in the cyclic amine resistance locus (PfCARL) transporter localised to the Golgi apparatus, while amplification of the multidrug resistance protein 1 (*pfmdr1)* gene confers a decreased sensitivity to a broad range of antimalarial classes (54, 55).

By contrast, several *P. falciparum* membrane transport proteins are possible direct therapeutic targets (47). The P-type Na^+ transporter ATPase 4 (PfATP4) maintains low intracellular Na^+ concentrations by exporting Na^+ with the simultaneous import of H^+ (56). Multiple, chemically diverse inhibitors target PfATP4, resulting in disrupted Na^+ efflux and deacidification of the parasite cytoplasm leading to parasite death (57-59), including Cipargamin. Whilst the other membrane proteins have not progressed so far in the drug discovery process, there are several membrane proteins with *in vitro* validation as antimalarial targets (40, 60). The V-type H^+ ATPase are essential for maintaining the pH and inward negative membrane potential of

infected erythrocytes (61) and is the target of the antimalarial clinical candidate triaminopyridine (62). The Niemann-Pick type C1-related protein (PfNCR1) localises to the PPM and inhibition of this essential lipid/sterol:H^+ symporter by MMV009108 and MMV019662 results in disrupted lipid homeostasis and parasite death (63). The hexose transporter 1 (PfHT1) responsible for glucose import into the parasite is the target of MMV009085, amongst other compounds (64, 65). Lastly, the formate-nitrite transporter (PfFNT) responsible for lactate export is inhibited by MMV007839 and MMV000972 (66).

To expand the list of possible membrane transport proteins as potential druggable targets, one needs to identify a metabolite that is transported by the parasite, via a transport protein that is genetically validated as essential for parasite survival. Given that *in vitro* cultivation of asexual *P. falciparum* parasites requires extracellular medium containing various amino acids including cysteine, glutamate, glutamine, isoleucine, methionine, proline and tyrosine (67), amino acid transport and the membrane transporters responsible may provide new avenues of investigation.

1.5. Sources of amino acids

Amino acids form an integral part of all cells, and in addition to serving as building blocks in protein synthesis, they are also crucial for whole cell homeostasis, cell signalling, gene regulation and development (68). The *P. falciparum* parasite is auxotrophic for the majority of amino acids and can only synthesise six of the 20 amino acids *de novo*, namely aspartate, asparagine, glutamate, glutamine, proline, and glycine (69). Of these, asparagine plays a major role in protein synthesis, as it is one of the most abundant amino acids in *Plasmodium* proteins (70).

Plasmodium falciparum parasites have two mechanisms to acquire amino acids: digestion of haemoglobin found in the host erythrocytes, and uptake of free amino acids from the blood plasma or external medium (71). During the asexual stages of the parasite's life cycle, *P. falciparum* parasites ingest and degrade 75 % of the host haemoglobin (72). Whilst haemoglobin degradation allows the parasite to acquire amino acids needed for biochemical processes, the rate of this degradation is almost equal to the rate of amino acid efflux from the infected erythrocyte (73). Therefore, it is suggested that haemoglobin digestion is most likely needed to maintain osmotic balance inside the host cell and to create space for the asexual parasite to grow (74). On average, only 16 % of the amino acids obtained from haemoglobin digestion are converted to parasite proteins, thus, additional free amino acids are exported to

the extracellular medium (75-77). However, since haemoglobin is completely lacking in isoleucine and has low levels of glutamate, methionine, glutamine and cysteine, these free amino acids must additionally be taken up from the extracellular environment (67).

Intraerythrocytic *P. falciparum* parasites therefore have increased transport of amino acids such as tryptophan, glutamine, and glutamate (78, 79). Additionally, alanine competes with methionine and isoleucine for uptake through a nonspecific mechanism for neutral amino acids (80). As *P. falciparum* gametocytes remain within the same erythrocyte for several days, the amino acid requirements of gametocytes can differ from those of asexual parasites, especially when the host haemoglobin reservoir becomes depleted as gametocytes mature (17). Therefore, the importance of the amino acid transporters responsible for this increased amino acid transport during the *P. falciparum* life cycle will be investigated.

1.6. Amino acids transporters

The *P. falciparum* genome contains 11 putative amino acid transporters (47). Five of these belong to the ApiAT family, known as uniport transporters of aromatic and large neutral amino acids in *Toxoplasma gondii* (81). Furthermore, there are three predicted members of the amino acid/auxin permease family (AAAP) and three predicted neurotransmitter:sodium symporter (NSS) family members (Table 1.1) (46).

A comparison of amino acid transporter gene expression profiles showed differential expression of these genes during the different life stages of *P. falciparum* parasites. Interestingly, asexual parasites express all 11 of these putative amino acid transporters, while gametocytes only express some (Table 1.1) (46, 82, 83). During gametocyte maturation, four amino acid transporters, *pf3d7_0104700* (ApiAT9), *pf3d7_1208400* (AAT2), *pf3d7_0515500* (NSS2 or GEP1) and *pf3d7_1132500* (NSS3) showed constitutive expression, while relative downregulation of the other transporters is observed.

High-throughput transposon mutagenesis, which involves the random insertion of *piggyBac* transposons into a genome to produce a loss of function phenotype, was used to investigate the essentiality of various genes during the asexual life stages of *P. falciparum* parasites. Based on this, three of the 11 putative amino acid transporters were predicted to be essential for asexual proliferation of *P. falciparum* parasites (Table 1.1) (84).

Table 1.1: Predicted expression profiles and essentiality of putative amino acid transporter during *P. falciparum* intraerythrocytic life cycle.

Name	Sub-family	Gene name	Expression profiles				Essentiality				
				Gametocyte stage			Asexual			Gametocyte stage	
			Asexual	I/II	III/IV	V	piggy-Bac	Direct *Pf*	Other models	Direct *Pf*	Other models
Major facilitator superfamily-related	ApiAT2/ MFR4	*Pf3d7_0914700*						[1]		[1]	Pb[6]
Major facilitator superfamily-related	ApiAT4/ MFR5	*Pf3d7_1129900*						[1]		[1]	Pb[6]
Novel putative transporter 1	ApiAT8/ NPT1	*Pf3d7_0104800*						[1]	Pb[3]	[1]	Pb[6]
Major facilitator superfamily-related	ApiAT9/ MFR2	*Pf3d7_0104700*						[1]	Pb[3]		Pb[5]
Multidrug-resistant modulator	ApiAT10/ MFR3	*Pf3d7_0312500*						[1]	Pb[3]	[1]	Pb[6]
Amino acid transporter	AAT1	*Pf3d7_0629500*							Pb[7]		Pb[7]
Amino acid transporter	AAT2	*Pf3d7_1208400*							Pb[3]		
Membrane protein	AAAP3	*Pf3d7_1231400*						[2]	Pb[3]		
Putative transporter	NSS1	*Pf3d7_0209600*							Pb[3]		
Gametogenesis essential protein 1	NSS2/ GEP1	*Pf3d7_0515500*							Py[4]		Py[4]
Amino acid transporter	NSS3	*Pf3d7_1132500*							Py[4]		

Transcriptional expression profiles of putative amino acid transporters during asexual proliferation and gametocyte maturation, with high Log(fold change (FC)) being red and low Log(FC) being blue (85). Essentiality of amino acid transporters (piggyBac (84) and independent focused studies ((82)[1], (86)[2], (87)[3], (88)[4], (89)[5], (90)[6], (91)[7]) essential genes in orange, and non-essential genes in green.

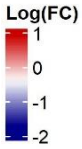

Some of these results were confirmed with alternative genetic modification techniques. *Pf3d7_1231400* (AAAP3) was confirmed to be essential in asexual *P. falciparum* parasites and *P. berghei* gametocytes (86). Additionally, the five putative ApiAT amino acid transporters expressed in asexual stage *P. falciparum* parasites were confirmed to be non-essential, as they had partial redundancy and allowed complementary amino acid transport. These ApiAT transporters are also fully redundant during *P. falciparum* gametocytogenesis although the ortholog for *pf3d7_0104800* (ApiAT8) is essential for *P. berghei* gametocytes (82, 89).

An ortholog to a transporter that is essential for *P. yoelii* gametocytes is *pf3d7_0515500* (GEP1) from the NSS subfamily. *Py*GEP1 is required for the signalling platform regulated by guanylyl cyclases (GC) during gametogenesis (92). However, the essentiality of the two NSS transporters, with no human orthologs, and that have been identified as constitutively expressed in asexual and gametocyte stage parasites has not been investigated directly. As the NSS subfamily accounts for 2.7 % of all FDA approved drugs (93), this project aims to investigate the functional importance of *Pf3d7_0515500* (GEP1) and *Pf3d7_1132500* (NSS3) in asexual and gametocyte stage *P. falciparum* parasites using genetic manipulation techniques.

1.7. *P. falciparum* genetic manipulation

A variety of genetic manipulation tools that can modify DNA, RNA, or protein levels have been developed to evaluate the function and essentiality of genes in the genome of the *P. falciparum* parasite (Table 1.2). DNA editing tools result in the disruption of the gene of interest (GOI) and include targeted gene deletion (TGD), conditional knockout or point mutations. TGD replace the full GOI with a truncated 5' gene fragment, leading to the expression of a truncated, nonfunctional protein (94). However, if the GOI is essential to parasite survival, the disruption of this gene will not produce viable parasites, preventing the investigation of the protein function in subsequent life stages. Alternatively, a CISPR-Cas9 system can be used to introduce point-mutations in the GOI to render it nonfunctional upon translation. Conditional knockout of the GOI can be achieved with site-specific Cre/LoxP recombinase that upon dimerisation excises the GOI from the parasite genome.

Table 1.2: Advantages and disadvantages of genetic manipulation systems in *P. falciparum*. Summarised from (94-97).

Level of editing	System	Advantages	Disadvantages
DNA	TGD	• Simple • Irreversible knockout	• Transgenic lines not obtained for essential gene targets • Not inducible
	Conditional DiCre	• Suitable for essential targets • Inducible system • Rapid effects, in the same life cycle • Irreversible gene excision	• Efficacy and speed of excision varies • Stable proteins remain for extended periods after gene excision • Not suitable for genes > 5Kb • Parental line with DiCre needed
	CRISR-Cas9	• Ideal to introduce small genomic changes (point mutations)	• Not inducible
RNA	*glmS* ribozyme	• Suitable for essential targets • Reversible knockdown	• Variable efficacy of knockdown (~ 50 – 90 %)

		• Gene tagged for localisation	
	Tet repressor protein	• Suitable for essential targets	• Requires passive selection that has low efficacy and is slow
Protein	Destabilisation domain	• Suitable for essential targets • Rapid effect on protein	• Varying levels of destabilisation • Shield ligand is expensive, can be cytotoxic • Not suitable for secreted proteins
	Knock sideways	• Rapid effect on protein	• Some proteins cannot be mislocalised incl. membrane proteins • Requires parent line with localiser

The relative gene expression can also be altered at the mRNA level, through inducible *glmS* ribozyme or Tet repressor protein (TetR) systems. The activated *glmS* ribozyme (catalytic RNA molecule), results in instability and degradation of the GOI mRNA and prevents protein expression (97). To ensure that the findings of the GOI *glmS* knockdown are due to the activation of the *glmS* ribozyme, a mutated version of the ribozyme that prevents catalytic activity (M9) is used as a control line (95, 97). The TetR system is based on the introduction of a TetR-binding aptamer in the 5' UTR of the GOI. Here, in the absence of anhydrotetracycline (ATc), TetR binds to the aptamer and prevents translation of the GOI (95).

Systems that influence protein stability and function include the destabilisation domain (DD) system, which induces misfolding and destabilisation of proteins in the absence of the ligand Shield (Shld-1) (98). Proteins can also be post-translationally mislocalised from the native site of action, theoretically preventing its intended function. In the knock sideway (KS) system, the dimerisation between the protein of interest tagged with FK506-binding protein (FKBP) and a signal tagged with FKBP rapamycin binding (FRB) results in mislocatisation of the protein when rapamycin is introduced (97). An additional KS tool that is compatible with secreted proteins, is knockER, where secreted proteins are conditionally sequestered to the ER by inducible fusion of the protein of interest with a C-terminal KDEL ER-signal sequence (99).

Various challenges have been identified when introducing these genetic manipulation systems into the parasite genome, therefore, selection-linked integration (SLI) was developed to improve the success of generating transgenic lines. The SLI system uses a dual-selection process. Episomal uptake of a recombinant plasmid expressing one resistance marker (e.g. human dihydrofolate resistance (hDHFR)) can be selected with the addition of the antifolate compound, WR99210. However, a second selection marker, for example, neomycin resistance (Neo^R) is used that will only express once homologous recombination occurs under the endogenous

promoter of the GOI. This allows the selection of integrants by adding G418, a neomycin derivative. In SLI constructs, the Neo^R gene is separated from the GOI fragments by a skip peptide (T2A), allowing for the translation of the mRNA into two separate proteins (94).

Previously, the essentiality of the five ApiAT transporters in asexual stage *P. falciparum* parasites and gametocytes was successfully investigated with SLI-TGD and inducible SLI-*glmS* transgenic lines (82). Here, we aimed to generate SLI-TGD and SLI-*glmS* transgenic lines that could be used to investigate the essentiality of two NSS putative amino acid transporters, *pf3d7_0515500* and *pf3d7_1132500,* that were identified as constitutively expressed in asexual and gametocyte stage *P. falciparum* parasites (83).

2. Problem statement

Malaria elimination requires that not only the disease-causing asexual stage *P. falciparum* parasites be targeted, but also the transmissible gametocyte stages. Gametocyte differentiation is coupled with extensive transcriptional reprogramming and a metabolic shift towards aerobic energy production, where a wider variety of amino acid dipeptides are used by the parasite compared to asexual stages. Protein synthesis, which are a validated biological target in early gametocytes, require amino acids as building blocks. These amino acids are mostly obtained from haemoglobin digestion, however, as haemoglobin does not contain sufficient levels of all the required amino acids, additional amino acids must be sourced from the host. The uptake of amino acids from the extracellular environment requires transport across multiple membranes, enabled by one of the 11 putative amino acid transporters found in the parasite's genome. Of these putative amino acid transporters, only 4 are constitutively expressed in gametocytes. Furthermore, the essentiality of two constitutively expressed transporters, from the NSS symporter family, remains unknown in gametocyte stage *P. falciparum* parasites.

3. Aim, hypothesis, and objectives

3.1. Aim

Generate transgenic lines to investigate the importance of putative amino acid transporters Pf3D7_0515500 and Pf3D7_1132500 during *P. falciparum* asexual proliferation and gametocyte differentiation.

3.2. Hypothesis

Genetic manipulation of Pf3D7_0515500 and Pf3D7_1132500 is accomplished with targeted gene deletion and *glmS* ribozyme conditional knockdown.

3.3. Objectives

I. Generate recombinant SLI-TGD plasmids for *pf3d7_0515500* and *pf3d7_1132500*.
II. Select for integration of SLI-TGD for both putative amino acid transporters.
III. Generate recombinant SLI-*glmS*/-M9 plasmids for *pf3d7_0515500* and *pf3d7_1132500*.
IV. Select for integration of SLI- *glmS*/-M9 for both putative amino acid transporters.

Conference Poster Presentation:

Oral Presentation: "Towards genetic interrogation of putative amino acid transporters in *Plasmodium falciparum* parasites". BGM Research Day, University of Pretoria, 30 November 2023.

Oral Presentation: "Reverse genetic analyses of amino acid transporters in early gametocyte stages of *Plasmodium falciparum* parasites". 8th Southern Africa Malaria Research Conference 2023, RH Hotel, Sunnyside, Pretoria, 1 – 3 August 2023.

Marché Maré, Shanté da Rocha, Savannah Watson, Lyn-Marie Birkholtz and Jandeli Niemand. "The effect of *in vitro* carbon source concentrations on asexual *Plasmodium falciparum* parasite proliferation". SASBMB, Virtual, 24-26 Jan 2022.

Marché Maré, Elisha Mugo, Lyn-Marie Birkholtz and Jandeli Niemand. "Targeted gene disruption of putative amino acid transporters Pf3D7_0515500 and Pf3D7_1132500 in *Plasmodium falciparum* gametocytes". 7th Southern Africa malaria research conference, Virtual, 2- 4 August 2022.

Marché Maré, Elisha Mugo, Lyn-Marié Birkholtz and Jandeli Niemand. “Towards genetically modified *Plasmodium falciparum* parasites for functional evaluation of amino acid transport in gametocytes”. BGM Research Day, University of Pretoria, 1 December 2022.

4. Method

4.1. *In silico* analysis

The transmembrane domains of Pf3D7_0515500 and Pf3D7_1132500 (PlasmoDB) were predicted from the amino acid sequences obtained from PlasmoDB using TOPCON (https://topcons.cbr.su.se/pred/). In addition, a hydropathy plot was generated with the Kyte-Doolittle hydrophobicity scale with a window size of 21, where positive values correspond to hydrophobic regions and negative values correspond to hydrophilic regions, to confirm possible membrane-spanning regions (100). The conserved family domains as indicated by InterPro (http://www.ebi.ac.uk/interpro/) was identified within the amino acid sequence of these two putative amino acids.

4.2. Ethical clearance

Parasite cultivation was carried out in the Malaria Parasite Molecular Laboratory (M^2PL), a certified level 2 biosafety facility at the University of Pretoria (Department of Agriculture, Forestry and Fisheries registration number 39.2/University of Pretoria - 19/160). All *in vitro* experiments specific to this project have ethical approval from the University of Pretoria, Faculty of Natural and Agricultural Sciences Ethics Committee (reference number NAS023/2022 and 180000094) and ethical clearance for the *in vitro* cultivation of *P. falciparum* parasites in human erythrocytes was obtained (reference number 506/2018) under Prof. Lyn-Marié Birkholtz.

4.3. *In vitro* cultivation of asexual *P. falciparum* parasites

Plasmodium falciparum (NF54) strain was maintained in fresh human erythrocytes (various types of blood) at 5 % haematocrit in complete culture media consisting of RPMI-1640 medium (Sigma Aldrich, USA) containing L-glutamine and supplemented with 25 mM HEPES (pH 7.5, Sigma Aldrich, USA), 0.2 mM hypoxanthine (Sigma Aldrich, USA), 0.024 mg/mL gentamycin (Fresenius Kabi Manufacturing, South Africa), 23.81 mM sodium bicarbonate (Sigma Aldrich, USA), 0.2 % (w/v) D-glucose (Merck, South Africa) with 5 g/L Albumax II Bovine Serum Albumin (Thermo Fisher Scientific, USA, alternative to human serum) (101).

An asexual *P. falciparum* parasite culture was maintained in 75 cm^2 flasks at 37 ºC with moderate shaking (60 revolutions per minute (rpm)) to ensure maximal single merozoite invasion events (102), under hypoxic conditions (5% O_2, 5% CO_2, 90% N_2, Afrox, South Africa).

Parasitaemia, defined as the percentage of infected erythrocytes, was routinely determined by counting ~ 500 erythrocytes of a thin blood smear stained with Rapi-Diff (Merck, South Africa) and visualised with a 1000X magnification YS2-H light microscope (Nikon, Japan). All parasite images were taken with an Eclipse 50i microscope with digital sight (Nikon, Japan). Routinely, the erythrocytes were pelleted by centrifugation at 3500 *xg* for 3 min (Heraeus® Megafuge 40 centrifuge, Thermo Fisher Scientific, USA) and the spent medium was aspirated and replaced with fresh pre-warmed (37 ºC) complete culture medium. The asexual cultures were maintained at ~ 8 % parasitaemia for ring- or ~ 4 % parasitaemia for trophozoite-stage parasites.

Asexual parasite cultures were synchronised with iso-osmotic D-sorbitol exposure to obtain cultures with the same developmental stages (> 90% ring-stage) for stage-specific experiments (103). Infected erythrocytes with trophozoite- or schizont-stage parasites are permeable to sorbitol due to the presence of the NPPs, resulting in increased entry of osmotic pressure into the cell, causing cell lysis (104). Cultures consisting mainly of ring-stage parasites were incubated in pre-warmed (37 ºC) 5 % (w/v) D-sorbitol (Sigma-Aldrich, USA) at 37 ºC for 10 min. After incubation, the parasites were pelleted by centrifugation at 3500 *xg* for 3 min (Heraeus® Megafuge 40 centrifuge, Thermo Fisher Scientific, USA), and the supernatant was aspirated. The residual D-sorbitol was removed by washing the parasite culture with incomplete culture medium [RPMI-1640 medium (Sigma Aldrich, USA) containing L-glutamine and supplemented with 25 mM HEPES (pH 7.5, Sigma Aldrich, USA), 0.2 mM hypoxanthine (Sigma Aldrich, USA), 0.024 mg/mL gentamycin (Fresenius Kabi Manufacturing, SA), 23.81 mM sodium bicarbonate (Sigma Aldrich, USA), 0.2 % (w/v) D-glucose (Merck, SA)]. The synchronised culture was resuspended in pre-heated (37 ºC) complete culture medium. Two rounds of synchronisation 5 h apart were performed to obtain a highly synchronised culture.

4.4. Cloning strategy to create recombinant plasmids

Two genetic manipulation techniques were used to investigate the essentiality of the putative amino acid transporters, Pf3d7_0515500 and Pf3d7_1132500 in the *P. falciparum* intraerythrocytic life cycle. In the first instance, a 5' gene fragment of the putative amino acid transporter was used in the pSLI-TGD recombinant plasmids, to allow for integration in the first portion of the GOI. Subsequently, the endogenous gene was replaced with the 5' gene fragment in the recombinant plasmid, resulting in the expression of non-functional proteins after integration. For this technique, pSLI-TGD-*Pf3d7_0515500*, and pSLI-TGD-*Pf3d7_1132500* were generated as summarised in (Figure 4.2).

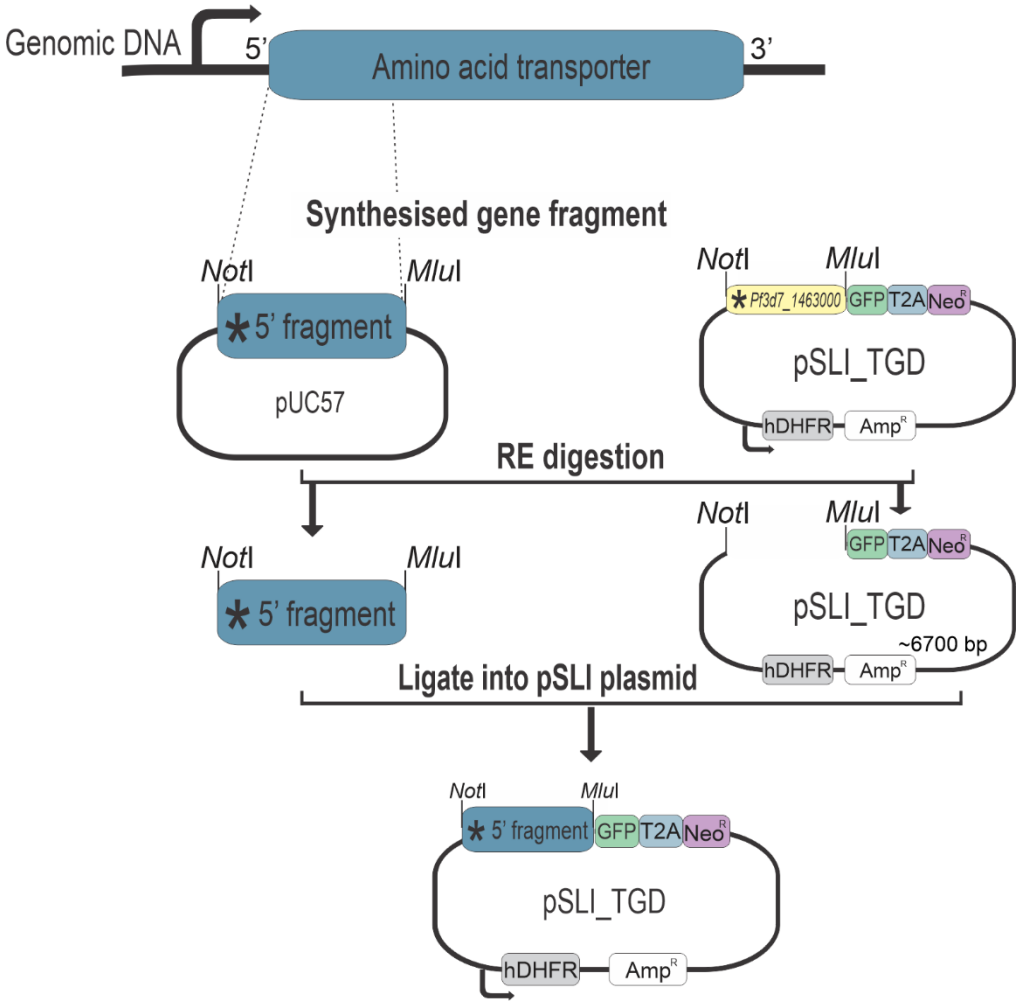

Figure 4.1 Cloning strategy to generate pSLI- TGD recombinant plasmids.
The 5' gene fragments were synthesised by Gene Universal and the pUC57 plasmid, with the respective gene fragments were transformed into competent *Escherichia coli* cells, to create *E. coli* stocks and to isolate plasmids. Concurrently, SLI-plasmids with ampicillin resistance (Amp^R), Neomycin resistance (Neo^R), and human dihydrofolate reductase resistance (hDHFR) were isolated from *E. coli* stocks. Asterisk (*) represents a stop codon.

Secondly, a conditional *glmS* knockdown was generated with a 3' gene fragment, to insert the *glmS* ribozyme at the 3' terminus of the GOI and subsequently investigate the function of the amino acid transporters by conditionally altering the mRNA transcripts of the transporter genes (Figure 4.2). Four different plasmids were generated, with each gene associated with a non-functional *glms* (M9) control: pSLI-*glmS*-*Pf3d7_0515500*, pSLI-M9-*Pf3d7_0515500*, pSLI-*glmS*-*Pf3d7_1132500* and pSLI-M9-*Pf3d7_1132500*.

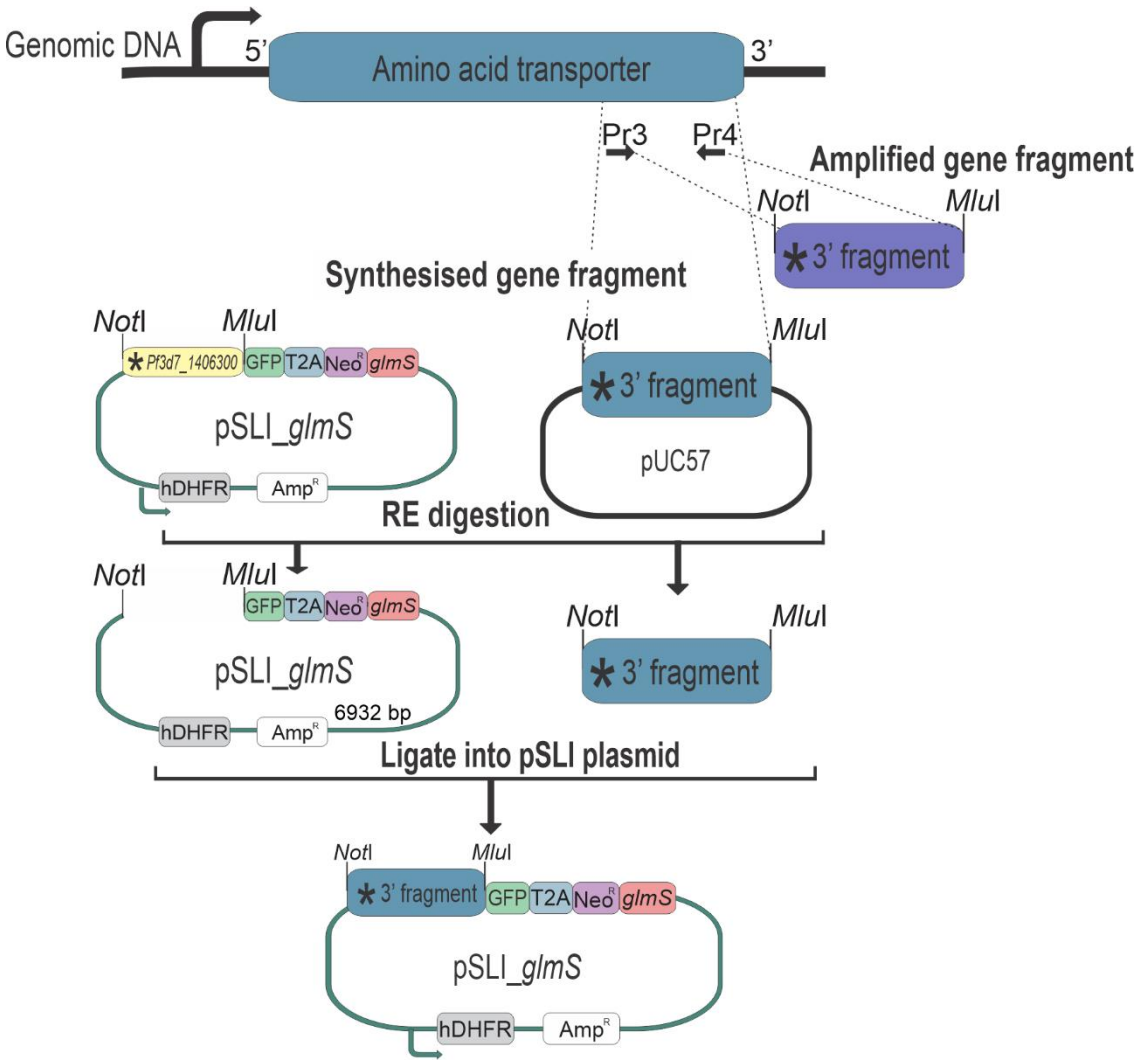

Figure 4.2 Cloning strategy to generate pSLI-*glmS* recombinant plasmids.
The selected gene fragment of amino acid transporters was amplified using gene specific primer pairs. Additionally, the gene fragments were synthesised by Gene Universal and the pUC57 plasmid, with the respective gene fragments were transformed into competent *E. coli* cells, to create E. coli stocks and to isolate plasmids. Concurrently, SLI-plasmids with ampicillin resistance (Amp^R), Neomycin resistance (Neo^R), and human dihydrofolate reductase resistance (hDHFR) were isolated from *E. coli* stocks. Asterisk (*) represents a stop codon.

4.4.1. Production of 5' and 3' gene fragments of *Pf3d7_0515500* and *Pf3d7_1132500*

For both the 5' fragments, as well as the 3' fragment of *Pf3d7_0515500*, the gene fragments required for downstream cloning were commercially synthesised. By contrast, the 3' fragment of *Pf3d7_1132500* was amplified from gDNA.

4.4.1.1. Gene fragment synthesis

The nucleotide sequences of *Pf3d7_0515500* and *Pf3d7_1132500* were obtained from PlasmoDB and used to design the gene fragments that were synthesised. Nucleotide sequences of ~ 350 bp corresponding to the 5' coding strand and ~ 400 – 800 bp corresponding to the 3' coding strand for each putative transporter were identified. These selected gene fragments with restriction enzyme sites, *Not*I (5'-GCGGCCGCTAA-3') and *Mlu*I (5'-ACGCGT-3'), and an additional stop codon (TAA) at the 5' end of the gene fragment, were submitted to Gene Universal (USA) for synthesis. The gene fragments were synthesised into pUC57 plasmids, containing ampicillin resistance and lacking intrinsic *Not*I and *Mlu*I restriction sites. The lyophilised plasmids received from Gene Universal were transformed into *E. coli* cells to generate working stocks.

4.4.1.2. Genomic DNA isolation

For downstream PCR amplification experiments, genomic DNA (gDNA) was isolated from a culture containing asexual NF54 *P. falciparum* (> 5 % parasitaemia of mostly trophozoite-stage parasites) using the Quick-gDNA Blood Miniprep kit (Zymo Research, USA). The isolation kits make use of chaotropic lysis buffers to release gDNA from the infected erythrocytes by solubilising membrane bound proteins and disrupting the hydrophobic effect of water molecules in the cell membranes (105). A volume of 200 µL infected erythrocytes was mixed with 800 µL of chaotropic lysis buffer through vortexing and left at room temperature for 10 min. Subsequently, the mixture was transferred to Zymo-Spin IIC columns and centrifuged at 10000 *xg* for 1 min in a Minispin centrifuge (Eppendorf, Germany) to separate and extract the gDNA that selectively binds to silica resin columns. Pre-wash buffer (200 µL) was added to the silica column and centrifuged at 10000 *xg* for 1 min, whereafter 500 µL wash buffer was added to the column and centrifuged as above. Purified gDNA was eluded from the silica column by incubating 50 µL elution buffer, at room temperature for 5 min, in the column and centrifuging it for 30 sec at 14100 *xg*. The quality and concentration of the purified DNA was determined spectrophotometrically with a NanoDrop One^{C} spectrophotometer (Serial number: 949416, Thermo Fisher Scientific, USA) by measuring the UV light absorbance of nucleic acids due to the resonance structure of purines and pyrimidines at 260 nm. The purity of each sample was determined by the absorbance ratios A_{260}/A_{280} and A_{260}/A_{230}, with a ratio close to 1.8 – 2.0 regarded as pure dsDNA free of contaminants such as proteins (A_{260}/A_{280}) and aromatic

compounds containing phenolic rings (A_{260}/A_{230}) respectively. Purified DNA was stored at 4 ºC until use.

4.4.1.3. Gene fragment amplification

Primers (Table 4.1) for the amplification of the 3' fragment of *Pf3d7_1132500* from *P. falciparum* gDNA was designed using primer designing software, Benchling (www.benchling.com, open-source). *Not*I (5'-GCGGCCGC-3') and *Mlu*I (5'-ACGCGT-3') restriction enzyme sites were added to the forward and reverse primers, respectively, along with four additional nucleotides at the ends of these sites, to allow enzyme digestion and subsequent ligation of the amplified gene fragment in the SLI vectors. The forward primer also contained a stop codon (TAA) to prevent gene fragment expression prior to genomic integration. The specificity of the primers to the genes of interest was determined using the BLAST tool on PlasmoDB.

Table 4.1: Primer sequences for 3' gene fragment amplification.

Primer code	Forward/ Reverse	Primer sequence (5' – 3' orientation)	Product length
Pr3	F	cgatgcggccgcTAACATATTCTCCAAAAACTTACACCAATGTGGTGC	868
Pr4	R	cgatacgcgtTTCATTTTTATCTATTCTTTTTTTTTTTTTTTTTGTGT	

*Restriction sites, *Mlu*I and *Not*I as underlined, and four nonspecific nucleotides were added to primer sequences. The forward primer introduces a stop codon, as indicated in red.

The amplification of the gene fragment was carried out using an Applied Biosystems 2720 Thermal Cycler (Applied Biosystems, USA) with each reaction containing 1x KAPA Ready mix and buffer [KAPA Taq DNA polymerase (0.5 U/25 µL), dNTPs (0.2 mM), MgCl2 (1.5 mM)], 10 pmol of each primer (Table 4.1) and 20 – 40 ng of gDNA isolated as described in 4.4.1.2. PCR conditions consisted of initial denaturation of 5 min at 95 ºC, followed by 30 cycles of denaturation of 30 sec at 95 ºC, primer annealing of 1 min at 55 ºC, extension of 1 min at 68 ºC and a final extension of 5 min at 68 ºC.

A portion of the PCR products were analysed on a 1 % (w/v) agarose gel (Bioconcept, Switzerland)/Tris-Acetate-EDTA (TAE, 0.04 M Tris-acetate, 1 mM EDTA, pH 8) in TAE running buffer at 110 V for 45 min. Each sample was loaded with 2 µL 6x Purple Loading Dye (New England Biolabs, UK) and 5 µL GeneRuler™ 1 kb DNA ladder (Promega, USA) was used as a molecular marker. The gel was stained with ethidium bromide (0.5 µg/mL). DNA bands were visualised with a Gel Doc Go Imaging system (Bio-Rad, USA) at 302 nm. Gel images were analysed using Image Lab 3.0 (Bio-Rad, USA).

The remaining PCR products were subjected to RE digestion to generate sticky ends for subsequent ligation reactions. Here, the PCR products were incubated with 6 U *Not*I-HF (high fidelity, New England Biolabs, UK) and 6 U *Mlu*I-HF (high fidelity, New England Biolabs, UK) in 1x CutSmart buffer 3.1 (New England Biolabs, UK) for 3 h at 37 ºC (2720 Thermal Cycler, Applied Biosystems, USA).

The digested gene fragments were purified using a NucleoSpinGel and PCR Clean-up kit (Macherey-Nagel, Germany). For each 100 µL of PCR products, 200 µL binding buffer was added. The solution was transferred to a High Pure filter column provided in the kit and centrifuged for 30 sec at 11000 *xg* after which the flow through was discarded and two wash steps were performed with 700 µL wash buffer and centrifugation for 30 sec at 11000 x*g.* Excess wash buffer was removed by centrifuging the column for 2 min at 11000 x*g.* DNA was eluted by incubating 30 µL elution buffer in the column at room temperature for 1 min, followed by centrifuging the column for 1 min at 11000 x*g*. The concentrations of the digested fragments were determined spectrophotometrically, as described above.

4.4.2. Preparation of heat-shock competent *Escherichia coli* cells

DH5α *E. coli* cells were used to generate $CaCl_2$ competent cells, as these cells have mutated endA1, an endonuclease that degrades foreign plasmids, and recA, which prevents recombination between cloned and native genes (106). $CaCl_2$ competent *E. coli* DH5α cells were prepared from thawed DH5α *E. coli* stocks (stored at -70 ºC) and cultured overnight in 5 mL Luria-Bertani (LB) liquid medium (1 % (w/v) tryptone (Glentham Life Sciences, UK), 0.5 % (w/v) yeast extract (Glentham Life Sciences, UK) and 1 % (w/v) NaCl (Sigma-Aldrich, USA), pH 7.5) containing 50 µg/ml ampicillin (VWR Life Sciences, USA) with agitation (180 rpm) at 37 ºC (MRC LM-570 incubator, Israel). The saturated overnight culture was diluted in a ratio of 1/50 in LB liquid medium and incubated with agitation at 37 ºC until the optical density (OD_{600}) of 0.8 OD_{600}/mL was reached (measured every 30 min using a NanoDrop One^C spectrophotometer (Serial number: 949416, Thermo Fisher Scientific, USA)). Cells were harvested during the log growth phase to ensure viable cells were collected. Subsequently, cells were chilled on ice for 15 min and centrifuged at 1865 x*g* for 30 min at 4 ºC in an SL 8R centrifuge (Thermo Scientific, USA). The supernatant was discarded, and the pellet was resuspended in 25 mL ice-cold 0.1 M $CaCl_2$ (Merck, South Africa) and centrifuged as before. The supernatant was again decanted and then the cells were resuspended in 2.5 mL ice-cold 0.1 M $CaCl_2$ and 375 µL 13 % (v/v)

glycerol (Sigma-Aldrich, USA) and incubated on ice for 1 h, after which the cells were aliquoted into 100 µL and stored at -80 ºC until use.

4.4.3. Transformation of $CaCl_2$ competent cells

Competent cell aliquots prepared as above (4.4.2) were placed on ice to thaw, after which 10 ng DNA was added to the thawed cells and incubated on ice for 30 min, followed by heat shock for 90 s at 42 ºC (AccuBlock Digital Dry baths, Labnet International Inc., USA). Repulsion between negative bacterial cells and the negative backbone of the DNA can be overcome by divalent cations such as calcium ions binding linear or circular DNA to the bacterial cells. The binding of divalent cations also increases membrane permeability, therefore making transformation 4 – 6 times more effective (107, 108). Treatment of cells with temperature imbalances such as heat-shock further reduces the repulsion between the foreign DNA and the cell membrane, thus leading to the incorporation of DNA into the cytosol (109). Subsequently, the reaction was incubated on ice for 2 min after which the entire mixture was transferred to 900 µL pre-warmed LB liquid medium containing 50 µg/mL ampicillin supplemented with 20 mM glucose and incubated with shaking (180 rpm) for 30 min at 37 ºC (MRC LM-570 incubator, Israel). Of the transformation mixture, 100 µL was plated onto 1 % LB-agar-ampicillin plates (1 % (w/v) agar in LB liquid medium containing 100 µg/mL ampicillin) and incubated overnight at 37 ºC in a stationary incubator. A blank control, transformation without plasmid, was included in the transformation experiments. The isolated single colonies obtained in the plates were subsequently inoculated into LB-ampicillin liquid medium and grown overnight at 37 ºC with agitation (180 rpm).

4.4.4. Plasmid isolation

Plasmid DNA was isolated from transformed *E. coli* DH5α cell cultures that were incubated overnight with agitation (180 rpm) at 37 ºC in 10 mL of LB medium containing 50 µg/mL ampicillin. A portion of the culture, 5 mL, was centrifuged at 11000 x*g* (Minispin Eppendorf centrifuge, Germany) for 30 s and the pellet was resuspended in ice-cold 250 µL suspension buffer containing 0.1 mg/ml RNAse through the vortex. An SDS/alkaline lysis buffer, 250 µL, was added to the suspension and the solution was incubated for 5 min at room temperature to release DNA from cells. After the addition of 300 µL neutralisation buffer, the sample was centrifuged for 10 min at 11000 x*g* in a Minispin centrifuge to pellet precipitated proteins, genomic DNA and cell debris. The supernatant was transferred to a High Pure filter column

provided in the kit and centrifuged for 1 min at 11000 x*g*. Subsequently, the flow through was discarded and 500 µL wash buffer containing ethanol was added to wash out contaminants such as salts and metabolites. The column was centrifuged for 1 min at 11000 x*g* and the flow through was discarded, after which the column was centrifuged for a second time to remove residual wash buffer. The plasmid DNA was eluted in 50 µL prewarmed elution buffer (5 mM Tris/Cl, pH 8.5) by centrifugation for 1 min at 11000 x*g.* The concentration of purified plasmid DNA was determined spectrophotometrically as described above and stored at -20 ºC until use.

Subsequently, ~0.5 – 1.0 µg DNA was digested with 6 U *Not*I-HF (high fidelity, New England Biolabs, UK) and 6 U *Mlu*I-HF (high fidelity, New England Biolabs, UK), as described in 4.4.1.3. The digested constructs were separated on a 1 % (w/v) agarose/TAE gel stained with 0.5 µg/mL ethidium bromide and the desired DNA fragments were excised from the gel on a UV illuminator with minimal UV exposure time. For each 100 mg of the excised gel, 200 µL binding buffer from the NucleoSpinGel and PCR Clean-up kit (Macherey-Nagel, Germany) was added to the sample and the gel was dissolved in the buffer for 10 min at 50 ºC. The digested gene fragments were purified as per the manufacturer's instructions described in 4.4.1.3. The concentrations of the digested fragments were determined spectrophotometrically, and subsequent ligation reactions were performed.

4.4.5. Ligation

The gene fragments of *Pf3d7_0515500* and *Pf3d7_1132500* were ligated to the digested vector backbones with 400 U of T4 DNA ligase (New England Biolabs, USA) in 1x Ligase buffer (New England Biolabs, USA) to produce recombinant plasmids. The T4 DNA ligase synthesises phosphodiester bonds in dsDNA breaks by esterification of a 5'- phosphoryl to a 3'- hydroxyl group (110). All ligation reactions contained at least a 5:1 insert to vector ratio, with a final concentration of 50 ng vector backbone added to each reaction. The insert concentration used for the reaction was calculated as follows:

$$\frac{\text{ng of vector x kb size of insert}}{\text{kb size of vector}} \times \text{insert: vector molar ratio} = \text{ng of insert}$$

The entire 10 µL ligation reaction was incubated at room temperature for 30 min, after which it was incubated overnight at 4 ºC and used to transform 100 µL DH5α *E. coli* competent cells as described in 4.4.3. The transformation reactions were plated onto LB-agar-ampicillin plates and incubated overnight.

4.4.6. Colony screen PCR

Colonies containing the recombinant plasmid have an ampicillin resistance gene that allows for the survival of recombinant colonies in the presence of ampicillin. Between 5 and 8 possible recombinant colonies were randomly selected from the LB-agar-ampicillin plates, inoculated into 100 µL LB-ampicillin medium (LB supplemented with 50 µg/mL ampicillin) and grown for 3 h at 37 ºC in a shaking incubator (180 rpm). Next, a PCR was performed with the backbone specific primers, listed in Table 4.2, to confirm by size estimation whether the gene fragments were present.

Each PCR used to amplify gene fragments was performed using an Applied Biosystems 2720 Thermal Cycler (Applied Biosystems, USA) and contained 1x KAPA Ready mix [KAPA Taq DNA polymerase (0.5 U/25 µL), KAPA Taq buffer, dNTPs (0.2 mM), $MgCl_2$ (1.5 mM)], 10 pmol of each primer (Table 4.2) and 1 µL of bacterial culture. The amplification of the gene insert fragments was achieved with a denaturation step of 95 ºC for 5 min, followed by 30 cycles of denaturation at 95 ºC for 30 sec, annealing at 58 ºC for 30 sec and extension at 68 ºC for 1 min. The final elongation of the amplified DNA by *Taq* polymerase occurs at 72 ºC for 1 min. The results of colony screen PCR were visualised on a 1 % (w/v) agarose/TAE gel.

Table 4.2: Primer sequences used for colony screen PCR and DNA sequencing.

Primer ID	Primer code	Forward/ Reverse	Primer sequence (5' – 3' orientation)
Lz_116	Pr1	F	AGCGGATAACAATTTCACACAGGA
Lz_114	Pr2	R	ACAAGAATTGGGACAACTCCAGTGA

*The primer sequences are specific to the backbone and flank the gene insert within the SLI plasmid. Primer Lz_116 is located upstream of the insert region, and primer Lz_114 is located downstream of the insert, specific to the GFP sequence.

After positive transformants were confirmed, recombinant bacterial cultures were transferred to 10 ml of LB-ampicillin and grown overnight at 37 ºC with shaking at 180 rpm. Plasmid DNA was isolated from the saturated overnight culture as per manufacturer's instructions (NucleoBond Xtra Mini purification kit, Machery Nagel, Germany), and between ~ 0.5 and 1.0 µg plasmid DNA was subjected to RE mapping, as described in 4.4.1.3, to verify the fragment size found in the vector.

4.4.7. Sanger sequencing

Sanger sequencing was performed to confirm the orientation and sequence of the gene fragments inserted into the vectors. Sanger sequencing incorporates fluorescently-labelled dideoxynucleotides (ddNTPs) during DNA replication, which causes chain termination. The

different coloured ddNTPs can be detected to determine the nucleotide sequence of the replicated DNA.

Each 20 µL sequencing reaction consists of ~ 300 ng plasmid DNA, 2x BigDye Buffer (4 µL) and 1x BigDye reaction mix (2 µL) from the Big Dye Sequencing kit (Applied Biosystems, USA) and 5 pmol of either forward or reverse primers (Table 4.2, Lz_114, and Lz_116). Replication reactions were performed in an Applied Biosystems 2720 thermal cycler (Applied Biosystems, USA) with the following conditions: initial denaturation of 1 min at 95 ºC, followed by 25 cycles of denaturation of 10 sec at 95 ºC, primer annealing of 5 sec at 58 ºC, and extension of 4 min at 60 ºC. The sequencing products were cleaned by ethanol precipitation to remove unincorporated fluorescent nucleotides that can lead to high background readings. The products were incubated in an ice-cold solution of 0.1x the volume sodium acetate (3 M, pH 5.2) and 3x the volume 98 % (v/v) ethanol and incubated on ice for 15 min. The samples were centrifuged at 11000 *xg* for 35 min at 4 ºC, after which the supernatant was removed, and the pellet was washed with 250 µL ice-cold 70 % (v/v) ethanol and centrifuged at 11000 *xg* for 15 min at 4 ºC. The pellet was retained and all ethanol was removed by evaporation in a Vacuum Concentrator (Bachofer, Germany) for 7 min. The sequencing samples were submitted for analysis at the University of Pretoria's FABI AGCT Sequencing facility. The ABI3500xL Genetic analyser (Applied Biosystems, USA) was used to determine the sequence and analysed with Benchling (www.benchling.com, open-source).

4.5. Large scale recombinant plasmid isolation

The recombinant plasmids, as confirmed with Sanger sequencing, were transformed into competent DH5α *E. coli* cells as described in 4.4.3. Transformed cultures were grown at 37 °C overnight (O/N) in LB-agar-ampicillin plates, then transferred to 5 mL of freshly prepared LB-amp medium (50 µg/mL ampicillin) and grown at 37 °C O/N in a shaking incubator at ~ 180 rpm. After this, 3 mL of the saturated culture was used to inoculate 200 mL LB-amp medium (50 µg/mL ampicillin) and grown O/N as described above. Recombinant plasmids were isolated from saturated DH5α *E. coli* cells with an optical density greater than 1.8 as measured with a NanoDrop One^{C} spectrophotometer (Thermo Fisher Scientific, USA), using the NucleoBond Xtra Midi kit (Macherey-Nagel, Germany). A concentration of ~ 100 - 200 µg recombinant plasmid was obtained for future transfections.

The eluded recombinant plasmid DNA was concentrated by adding 3.5 mL of ice-cold 100 % (v/v) isopropanol, resuspended by vortex for 6 – 10 s and pelleted at 15000 *xg* for 30 min at

4 °C. Ice-cold 70 % (v/v) ethanol (1 mL) was added to the pellet and centrifuged as above for 15 min. The ethanol was removed, and the pellet dried in a heating block at 50 °C. Once dried, the pellet was resuspended in 250 µL pre-heated $dddH_2O$ and stored at -20 °C. The concentration of plasmid DNA was measured spectrophotometrically. The gene fragment sizes in the isolated recombinant plasmids were confirmed by RE mapping, as described in 4.4.1.3.

A day before transfection, ~ 100 - 250 µg of the respective recombinant plasmid DNA was precipitated with ethanol as previously described (4.4.7), and dried in a sterile BSL2 flow hood to allow resuspension of the plasmid pellets into 250 µL Cytomix (120 mM KCl (Merck, South Africa), 0.15 mM $CaCl_2$ (Merck, South Africa), 2 mM EGTA (Sigma-Aldrich, USA), 5 mM $MgCl_2$ (Merck, South Africa), 10 mM K_2PO_4 (Merck, South Africa), 25 mM HEPES (Sigma-Aldrich, USA), pH 7.6) for downstream experiments. A final concentration of 50 – 200 µg was obtained and the plasmid DNA samples were stored at 4 °C until transfection.

4.6. *P. falciparum* parasite transfection

Transfection of *P. falciparum* parasites allows the movement of the recombinant plasmids into the parasite, through transient pores in the lipid bilayer of the membranes created when applying an electric field (111). Therefore, a culture of *P. falciparum* consisting of predominantly ring-stage parasites (> 5 % parasitaemia, 5 % haematocrit, > 75 % ring culture) was used for each transfection. The cultures were centrifuged at 11000 x*g* for 3 min to separate the culture media from the erythrocytes and replace spent culture media with fresh medium 3 h prior to the transfection. At the time of transfection, the cultures were centrifuged at 11000 x*g* for 3 min to aspirate the culture medium and the parasite-containing pellet was washed once with Cytomix in a 1:1 ratio and centrifuged as above. The parasite-infected pellet (200 µL, 100 % haematocrit) was resuspended with the Cytomix-plasmid DNA mixture, as prepared in 4.5, containing 50 – 200 µg of recombinant plasmid DNA to a final volume of 450 µL. The mixtures were electroporated in pre-cooled 2 mm cuvettes in a Gene Pulser Xcell Electroporation system (Bio-Rad, USA) at a capacitance of 950 µF and a voltage of 310 V, producing optimal time constants between 10 – 20 ms.

The electroporated mixture was transferred to a culture flask containing 5 mL pre-warmed culture medium supplemented with 50 µL fresh erythrocytes (100 % haematocrit) and allowed to recover for 3 h in a hypoxic environment at 37 ºC. Then, lysed erythrocytes from the parasite suspension were aspirated after the recovered culture was centrifuged for 3 min at 3500 x*g* and the transfected cells were resuspended in 5 mL complete culture medium that was transferred

to the stationary incubator at 37 ºC under hypoxic conditions. This was regarded as day 0 of transfection.

4.7. Drug selection and confirmation of episomal uptake of plasmids

Twenty-four (day 1) and forty-eight hours (day 2) after transfection, drug pressure using 4 nM WR99210 (Jacobus Pharmaceutical Company, USA) was applied for 10 consecutive days to transfected parasites to select for episomal uptake of recombinant SLI plasmids (112, 113). As an antifolate drug, WR99210 prevents nucleic acid synthesis by inhibiting the parasite dihydrofolate reductase (DHFR). However, parasites with episomal uptake of recombinant plasmids will have the human DHFR (hDHFR) resistance marker that is not susceptible to WR99210, allowing them to synthesise folates necessary for nucleic acid synthesis and thus survive (114). The parasitaemia was determined every second day, with thin blood smears stained with RapiDiff, using light microscopy as in section 4.3.

Once the parasitaemia of the recovered culture reached > 4 % with a majority trophozoites culture, samples were collected, and genomic DNA was isolated with the Quick-DNA miniprep kit (Zymo Research, USA), according to the manufacturer's specifications. To confirm the episomal presence of recombinant plasmids, amplification of the plasmid was completed using vector backbone specific primers Lz_114 and Lz_116 (Table 4.2). Each PCR reaction consisted of 1x KAPA Ready mix and buffer, 10 pmol of each primer flanking the gene fragment insert and ~ 30 ng extracted DNA. The thermocycler conditions consisted of an initial denaturation of 5 min at 95 ºC, followed by 30 cycles of denaturation of 30 sec at 95 ºC, primer annealing of 1 min at 58 ºC, extension of 1 min at 68 ºC and a final extension of 5 min at 68 ºC. The amplified products were analysed using agarose/TAE gel electrophoresis as described above.

Following episomal uptake confirmation, a majority ring stage culture (> 75 % ring stage) were cryogenically preserved in liquid nitrogen by resuspending 250 - 500 µL infected erythrocytes (100 % haematocrit) in a 1:1 ratio with specialised freezing media (28 % (v/v) glycerol (Sigma Aldrich, USA), 3 % (w/v) sorbitol (Sigma Aldrich, USA), and 0.65 % (w/v) NaCl (Glentham, USA)). The recombinant parasite lines were referred to as NF54-epi(pSLI-TGD_*gene*) for the gene deletion system and NF54-epi(pSLI-*glmS*/-M9_*gene*) for the induce knockdown system.

4.8. Drug selection for genomic integration

Two biological cultures of NF54-epi(pSLI-TGD_*gene*) and NF54-epi(pSLI-*glmS*/-M9_*gene*) were subjected to a second drug selection cycle with 400 µg/mL neomycin derivative, G418 (Thermo

Fisher Scientific, USA). G418 prevents polypeptide synthesis and ensures that only the parasite population with genomic integration, and subsequently displayed the neomycin resistance marker under the endogenous promoter of the selected gene, survived (115). The parasite cultures were placed under drug selection for 10 consecutive days and then every second day for a total of 16 days in the stationary incubator, after which the parasites were transferred to a shaking incubator and allowed to recover in fresh culture media. Parasitaemia was monitored every second day with RapiDiff-stained blood smears as described in section 4.3. During recovery, the culture medium was replaced every 3 – 4 days, and fresh erythrocytes were added weekly to replace lysed cells and maintain a 5 % haematocrit.

4.9. Confirmation of genomic integration

Samples of the recovered parasite cultures were isolated as described in section 4.4.1.2 and screened for genomic integration once the parasitaemia reached > 4 %. To detect locus specific genomic integration, the 5' and 3' region of the native loci were amplified in a PCR reaction consisting of 1x KAPA Ready mix and buffer, 10 pmol primer pairs described in Table 4.3 (Figure 4.3) and ~ 30 ng gDNA.

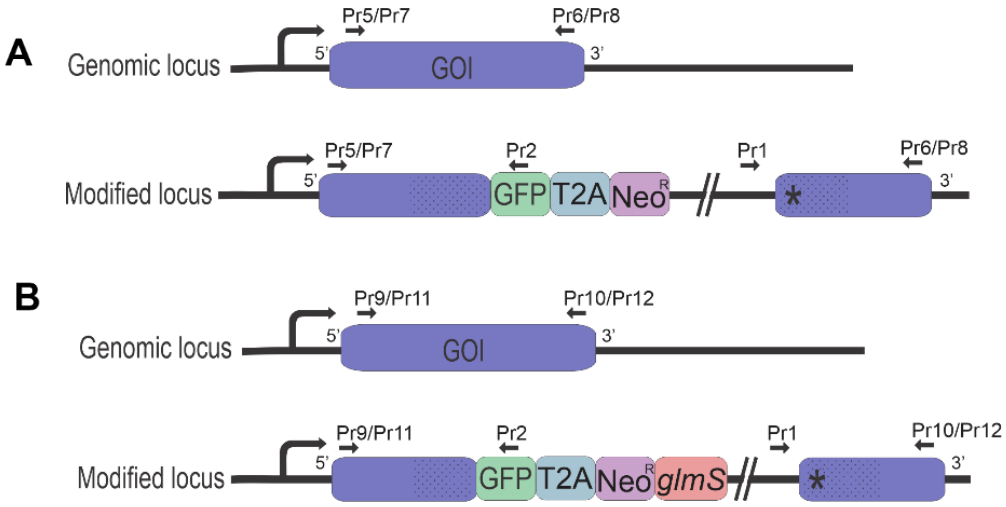

Figure 4.3: Schematic representation of primer pairs used to detect genomic integration.
Primers for screening genomic integration of **A)** NF54-*gene*-GFP and **B)** NF54-*gene*-GFP-*glmS*/-M9, listed in Table 4.3 and direction (indicated by arrows). Schematic diagram not drawn to scale.

The thermocycler conditions for NF54-*gene*-GFP drug selected parasites consisted of the following: initial denaturation of 5 min at 95 ºC, followed by 30 cycles of denaturation of 30 sec at 95 ºC, primer annealing of 1 min at 58 ºC, extension of 2 min at 68 ºC and a final extension of 5 min at 68 ºC. For conditional knockdown NF54-*gene*-GFP-*glmS*/-M9 drug selected parasites, the genomic integration confirmation PCR conditions consisted of an initial denaturation of 5 min

at 95 ºC, followed by 30 cycles of denaturation of 30 sec at 95 ºC, primer annealing of 1 min at 60 ºC, extension of 2 min at 68 ºC and a final extension of 5 min at 68 ºC. The PCR products were visualised on a 1 % (w/v) agarose/TAE gel with 0.5 µg/mL ethidium bromide. It is expected that once genomic integration has occurred, allele exchange will result in an increased amplicon size compared to the wild type (WT) genome and therefore the WT locus of transgenic parasites will not create a PCR product in the extension time described above.

The C-terminal GFP fluorescence tag will only be expressed if genomic integration occurred under the native promoter. Therefore, GFP fluorescence will confirm integration on a functional, protein level. The recovered intraerythrocytic *P. falciparum* parasite cultures (10 µL, 5 % haematocrit) were placed onto a microscope slide and sealed with a 1 mm coverslip (Menzel-Gläser, Thermo Fisher Scientific, USA) prior to imaging. Both brightfield and fluorescent images were captured with an excitation wavelength of 488 nm and emission wavelength of 500 nm using an EVOS M5000 cell imaging system (Thermo Fisher Scientific, USA) with a 100x oil immersion objective (1000x magnification). Image analysis was performed with the preloaded EVOS software.

Table 4.3: Primer pairs for genomic integration confirmation.

Parasite line		Primer code	Forward/ Reverse	Primer sequence (5' – 3' orientation)	Product length
NF54-*Pf3d7_0515500*-GFP	5'	Pr5	F	CAACCTTGTGTTTTATTCCCATGTTCATATACC	650
		Pr2	R	ACAAGAATTGGGACAACTCCAGTGA	
	3'	Pr1	F	AGCGGATAACAATTTCACACAGGA	630
		Pr6	R	CACTCGCCATATGTATAATATCATTATATGATATACC	
	WT locus	Pr5	F	CAACCTTGTGTTTTATTCCCATGTTCATATACC	1050
		Pr6	R	CACTCGCCATATGTATAATATCATTATATGATATACC	
NF54-*Pf3d7_0515500*-GFP-*glmS*/-M9	5'	Pr9	F	CTGGGAAAGCTGCCCTTAATCTC	950
		Pr2	R	ACAAGAATTGGGACAACTCCAGTGA	
	3'	Pr1	F	AGCGGATAACAATTTCACACAGGA	760
		Pr10	R	TGGAGAAATGTATAAGAAGAAAAAATATATGCATGTATC	
	WT locus	Pr9	F	CTGGGAAAGCTGCCCTTAATCTC	1060
		Pr10	R	TGGAGAAATGTATAAGAAGAAAAAATATATGCATGTATC	
NF54-*Pf3d7_1132500*-GFP	5'	Pr7	F	CCATATAAAACAAAATAGGGAACACACACATGT	650
		Pr2	R	ACAAGAATTGGGACAACTCCAGTGA	
	3'	Pr1	F	AGCGGATAACAATTTCACACAGGA	650
		Pr8	R	GAGCACAACGAATAGTTATCATATATATTACCACG	
	WT locus	Pr7	F	CCATATAAAACAAAATAGGGAACACACACATGT	1250
		Pr8	R	GAGCACAACGAATAGTTATCATATATATTACCACG	
NF54-*Pf3d7_1132500*-GFP-*glmS*/-M9	5'	Pr11	F	TATTTTACTTACATTGAATATAGTACAATTCATTTCGGTTC	1200
		Pr2	R	ACAAGAATTGGGACAACTCCAGTGA	
	3'	Pr1	F	AGCGGATAACAATTTCACACAGGA	1150
		Pr12	R	AATTAGGAAGGAGTTGGGTATGAAACCTC	

	WT locus	Pr11	F	TATTTTACTTACATTGAATATAGTACAATTCATTTCGGTTC	1200
		Pr12	R	AATTAGGAAGGAGTTGGGTATGAAACCTC	

5. Results

5.1. *In silico* analysis of Pf3D7_0515500 and Pf3D7_1132500

In silico analysis was performed to investigate the topology of the membrane transport proteins Pf3D7_0515500 and Pf3D7_1132500, using different transmembrane predictive tools. The topology predicted by TOPCON consists of a consensus profile obtained from five different predictive bioinformatic tools: OCTOPUS, Philius, PolyPhobius, SCAMPI and SPOCTOPUS. Additionally, TOPCON considers the free energy needed for amino acids in the protein to be inserted into the membrane when predicting the protein topology (116). OCTOPUS is a bioinformatic tool used to predict inside/outside and membrane/non-membrane regions in a protein (117), while Philius predicts the location of signal peptide cleavage sites and topological (cytosolic/non-cytosolic) information (118). PolyPhobius includes information from protein homologs when predicting protein topology (119), whereas SCAMPI predicts membrane protein topology based on physical data such as hydrophobicity and free energies of individual amino acids to membrane insertion (120). Lastly, SPOCTOPUS is an extension of OCTOPUS, adding signal peptide predictors to the statistical hidden Markov model used in the OCTOPUS algorithm to predict topology (121). For both genes, the consensus topological prediction is 14 transmembrane domains, with the N- and C-terminus predicted to be cytosolic, and no signal peptide sites were detected (Figure 5.1).

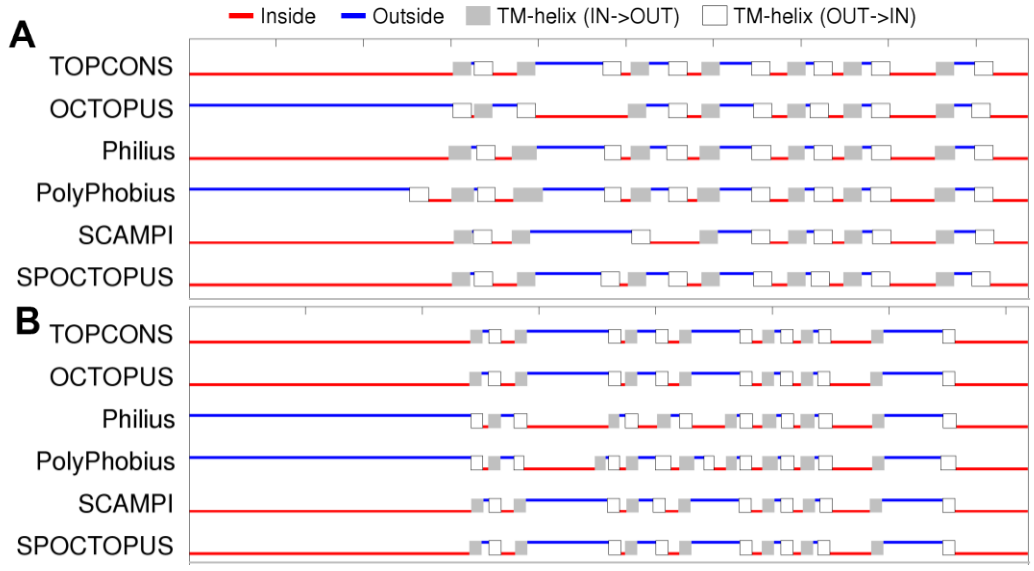

Figure 5.1: Predicted transmembrane domains for Pf3D7_0515500 and Pf3D7_1132500.
A) Pf3D7_0515500 (960 amino acids) and **B)** Pf3D7_1132500 (1439 amino acids). All programs were used with default settings. The figure was compiled using TOPCON (https://topcons.cbr.su.se/pred/).

To further validate the predicted number of transmembrane domains for Pf3D7_0515500 and Pf3D7_1132500, the Kyte-Doolittle scale was used to produce a hydropathy plot, Figure 5.2 (100). The hydropathy plot coincided with the number of predicted transmembrane domains, with 14 hydrophobic regions being identified for each amino acid transporter.

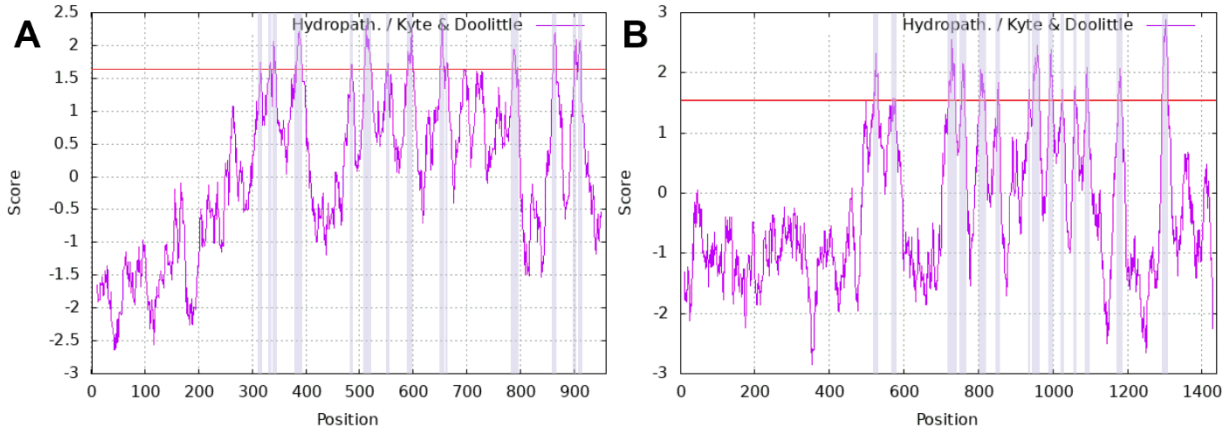

Figure 5.2: Hydrophobicity plot of amino acid transporters.
A Kyte-Doolittle plot, with window size 21, was made for **A)** Pf3D7_0515500 and **B)** Pf3D7_1132500. The red line at 1.6 depicts the threshold value for a high probability that the sequence is membrane embedded. Values above and below 0 indicate hydrophobic and hydrophilic regions, respectively. Light blue highlighted peaks represent the predicted transmembrane domain as determined by the Kyte-Doolittle method (100).

Furthermore, conserved protein family and domain predictions were done with InterPro. Both genes contained transmembrane domains associated with the NSS superfamily (IPR000175). The NSS superfamily domains are located in the center of the protein, spanning most of the predicted transmembrane helices. Therefore, it was confirmed that these transporters have the possibility of functioning as amino acid transporters, as this family couples the cotransport of Na^+ or the countertransport of K^+ with amino acid uptake (122).

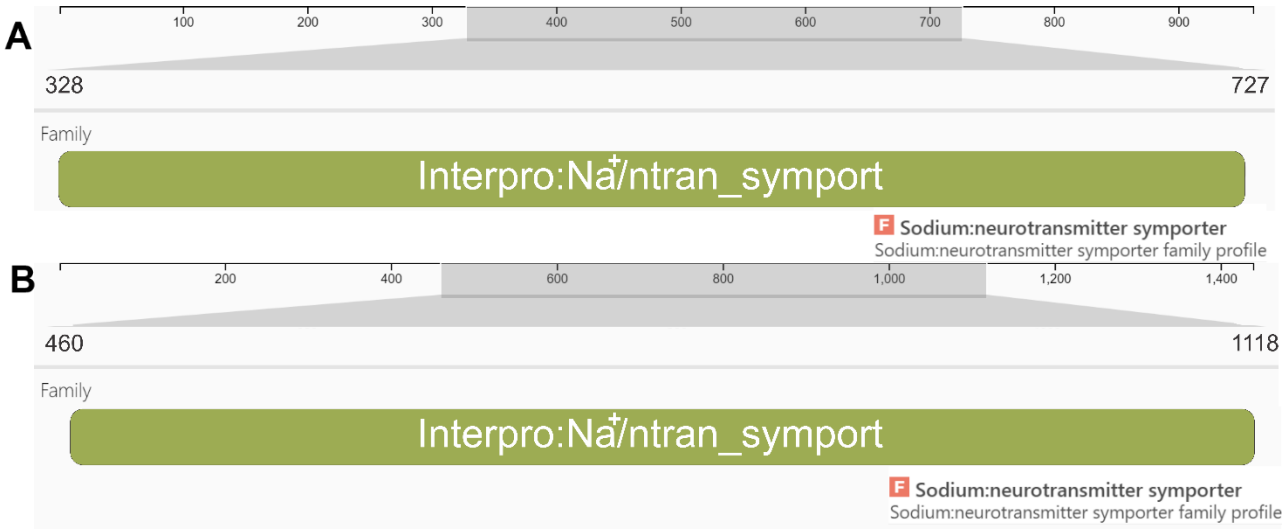

Figure 5.3: Schematic representation of Pf3D7_0515500 and Pf3D7_1132500 architecture. Predicted sodium:neurotransmitter symporter domain (IPR000175) shown in green of **A)** Pf3D7_0515500 (960 amino acids) and **B)** Pf3D7_1132500 (1439 amino acids). Obtained from InterPro (https://www.ebi.ac.uk/interpro) accessed on 6 September 2023.

5.2. *In vitro* cultivation of *P. falciparum*

The morphology and proliferation of intraerythrocytic asexual *P. falciparum* (drug sensitive strain NF54) parasites were evaluated using RapiDiff stained slides and visualised by light microscopy (Figure 5.4). During *in vitro* cultivation, asexual *P. falciparum* parasites progressed through the life cycle in 48 h, as expected. Ring stage parasites had thin chromatin structures when stained, whereas trophozoites had a visibly dark stained hemozoin crystal, the by-product of haemoglobin digestion in the metabolically active parasite. Furthermore, as parasites mature from early to late trophozoites, an increase in the size of the parasite cytoplasm is observed. The parasites next progress into the schizont stage, where DNA replication and nuclear division are indicated by individually stained nuclei within the parasite.

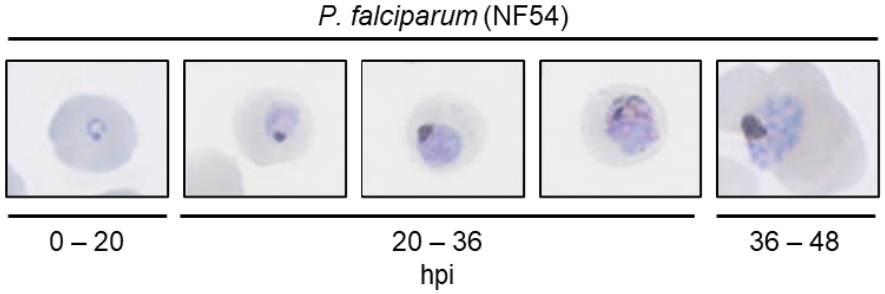

Figure 5.4: Intraerythrocytic *P. falciparum* NF54 morphology over 48 h. NF54 *P. falciparum* was RapiDiff-stained and visualised with 1000x magnification using a light microscope (Nikon, Japan). Ring stage parasites had a thin ring of visible cytoplasm, trophozoite stage parasites had a haemozoin pigment and larger parasite body, and schizonts were multinucleated.

The morphology of the parasites seen here was consistent with literature (18). It was therefore possible to maintain an NF54 *P. falciparum* asexual culture *in vitro*, and experiments for genetic manipulation of these cultures could be performed.

5.3. Cloning and validation of pSLI-TGD plasmids

The SLI-TGD system was constructed to investigate the essentiality of putative amino acid transporters, Pf3D7_0515500 and Pf37_1132500 in asexual proliferation and gametocytogenesis, as these transporters are expected to be non-essential for asexual stage parasites (Table 1.1) (84). Therefore, genetic modification of these genes with the TGD system would not prohibit asexual *P. falciparum* survival, and subsequent studies in gametocyte stages would be possible. Truncated fragments of the *Pf3d7_0515500* (288 bp) and *Pf3d7_1132500* (324 bp) genes preceding the transmembrane domains were commercially synthesised and cloned into the pSLI-TGD plasmid.

5.3.1. Cloning of 5’ gene fragments into SLI-TGD vector backbone

The 5’ gene fragments of *Pf3d7_0515500* or *Pf3d7_1132500* in the pUC57-simple plasmids, synthesised by Gene Universal, were purified from *E. coli* and restriction enzyme digestion with *Not*I and *Mlu*I was performed to isolate the *Pf3d7_0515500* (~ 280 bp) and *Pf3d7_1132500* (~ 300 bp) gene fragments (Figure 5.5A and B). Two bands, corresponding to the 5’ gene fragment synthesised, and the pUC57 plasmid backbone were obtained from the respective isolated plasmids (Figure 5.5A and B). Similarly, the SLI-TGD vector plasmid was isolated from a stock of *E. coli* cells that contained the vector plasmid and subjected to restriction enzyme digestion to verify the identity of the isolated plasmid and isolate the vector backbone. The expected band sizes for the pSLI-TGD vector (~ 6700 bp) that contains a gene fragment of *Pf3d7_1463000* (~ 1600 bp) were obtained (Figure 5.5C). Complete digestion of the plasmid was achieved as no additional band, corresponding to the uncut pSLI-TGD-*Pf3d7_1463000* was observed in the digested reaction. The band, corresponding to the pSLI-TGD backbone, was excised from the agarose gel, and purified for future ligation reactions.

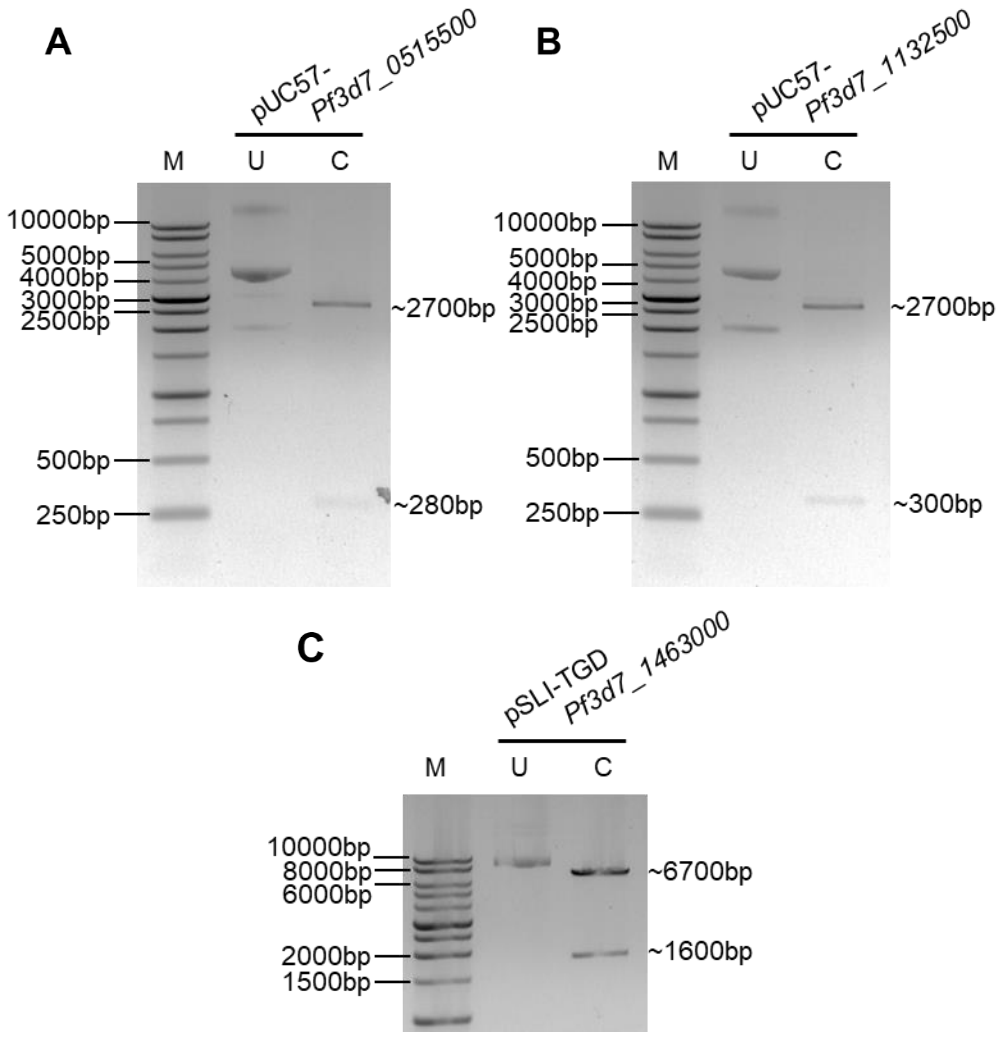

Figure 5.5: Restriction enzyme digestion of 5' gene fragments and pSLI-TGD.
Restriction enzyme digestion of pUC57 plasmids containing the 5' gene fragment of **A)** *Pf3d7_0515500* and **B)** *Pf3d7_1132500* and **C)** pSLI-TGD plasmid with *Not*I and *Mlu*I, evaluated on a 1 % (w/v) agarose/TAE gel and stained with EtBr (0.5 µg/mL). U: Undigested controls and C: digested plasmids. Lane M contains a GeneRuler™ 1 kb DNA ladder (Promega). The complete electrophoresis gels are located in Supplementary Figure 9.1 and Figure 9.2.

After obtaining digested products corresponding to the expected 5' gene fragment and pSLI-TGD plasmid backbone, the respective gene fragments were isolated and purified from the agarose/TAE gels. The purified gene fragments were used for downstream ligation reactions.

5.3.2. Identification of recombinant pSLI-TGD plasmids

The 5' gene fragments for *Pf3d7_0515500* and *Pf3d7_1132500* were sticky end ligated to the backbone of the pSLI-TGD vector, and putative recombinant plasmids were transformed into competent *E. coli* cells as described in 4.4.3. Colony screen PCR was performed on the 4 – 8 colonies obtained from the transformation reaction, with vector backbone specific primer pairs

(Table 4.2). Four of the five colonies screened for the ligation reaction containing the 5' gene fragment for *Pf3d7_0515500* with the pSLI-TGD vector backbone produced the expected PCR product band of ~ 400 bp (Figure 5.6A). All the colonies screened for the ligation reaction containing the 5' gene fragment for *Pf3d7_1132500* produced the expected PCR product of ~ 550 bp (Figure 5.6B). Colony 1 from the putative pSLI-TGD_*Pf3d7_0515500* and colony 3 from the putative pSLI-TGD_*Pf3d7_1132500* were chosen for subsequent confirmation experiments and DNA sequencing.

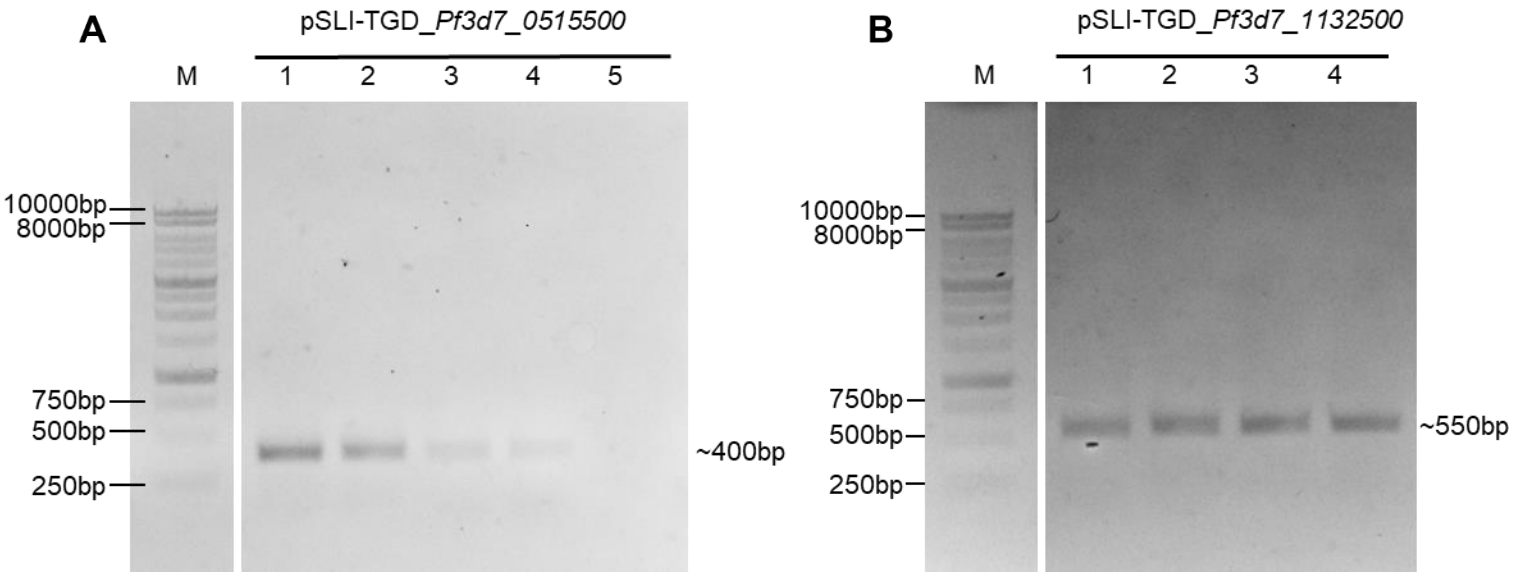

Figure 5.6: Colony screening for recombinant pSLI-TGD_*gene* plasmids.
PCR products were evaluated on a 1 % (w/v) agarose/TAE gel and stained with EtBr (0.5 µg/mL). Lane M contains a GeneRuler™ 1 kb DNA ladder (Promega). **A)** Lanes 1-5 contain amplified 5' gene fragments of *Pf3d7_0515500*. **B)** Lanes 1 – 4 contain amplified 5' gene fragments of *Pf3d7_1132500*. The complete electrophoresis gels are located in Supplementary Figure 9.4.

The putative recombinant plasmids were also digested with *Not*I and *Mlu*I to validate the presence and size of 5' gene fragments (Figure 5.7). The expected insert sizes for pSLI-TGD-*Pf3d7_0515500* (~ 280 bp) and pSLI-TGD-Pf3d7_*1132500* (~ 300 bp) were obtained.

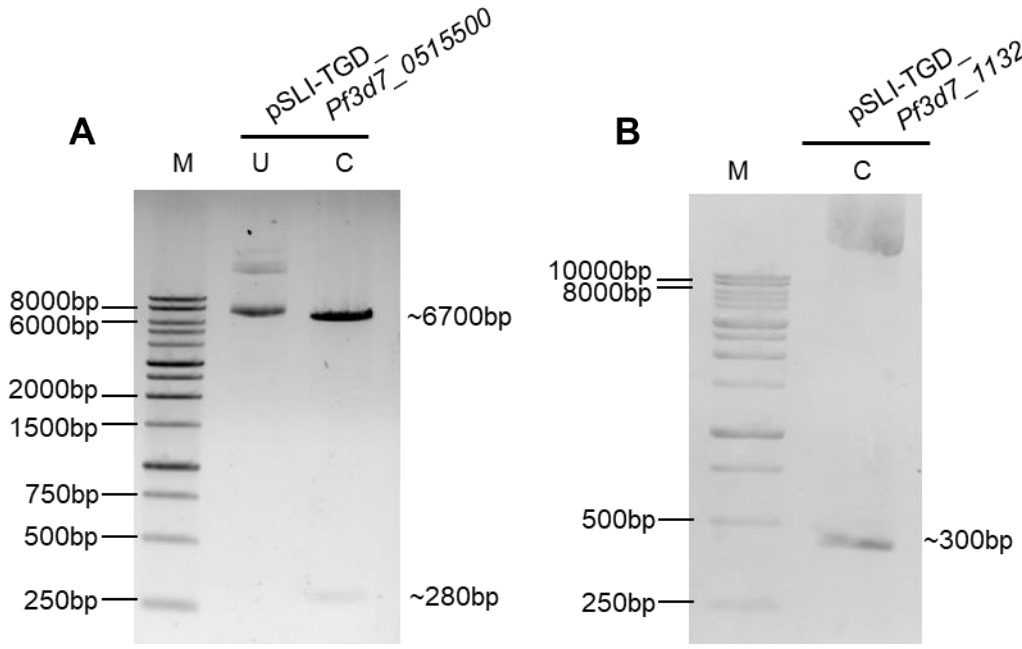

Figure 5.7: Restriction enzyme digestion of recombinant pSLI-TGD_*gene* plasmids.
RE confirmation of **A)** pSLI-TGD-*Pf3d7_0515500* and **B)** pSLI-TGD-*Pf3d7_1132500* on 1 % (w/v) agarose/TAE gel and stained with EtBr (0.5 µg/mL). Lane M contains a GeneRuler™ 1 kb DNA ladder (Promega). U: Undigested controls and C: digested plasmids. The complete electrophoresis gels are in Supplementary Figure 9.3.

These results indicate that both genes were successfully cloned into the pSLI-TGD vector. Next, the sequences of these plasmids were evaluated to confirm that the cloning was successful and that no point or frameshift mutations occurred in the gene fragments.

5.3.3. Sequence validation of recombinant pSLI-TGD

DNA Sanger sequencing was performed to ensure that the correct nucleotide sequence and orientation of the gene fragments were cloned into the pSLI-TGD vector backbone. Backbone specific primers Lz_116 and Lz_114 were used to sequence the entire gene fragment inserted into the SLI-TGD vector backbone. Using overlapping forward and reverse sequences, the chromatogram and consensus sequence, generated using an open-source online software tool, Benchling (www.benchling.com), were used to evaluate the nucleotide sequence of the gene insert. The 5' gene fragments found in the recombinant pSLI-TGD plasmids were identical to the genomic DNA of a 3D7 *P. falciparum* parasite. The 5' gene fragment regions were also in-frame with other elements of the pSLI-TGD plasmid, such as the GFP-tag, and neomycin resistance gene that can be used to select for integrants. Therefore, successful cloning of the plasmids pSLI-TGD-*Pf3d7_0515500* and pSLI-TGD-*Pf3d7_1132500* was achieved.

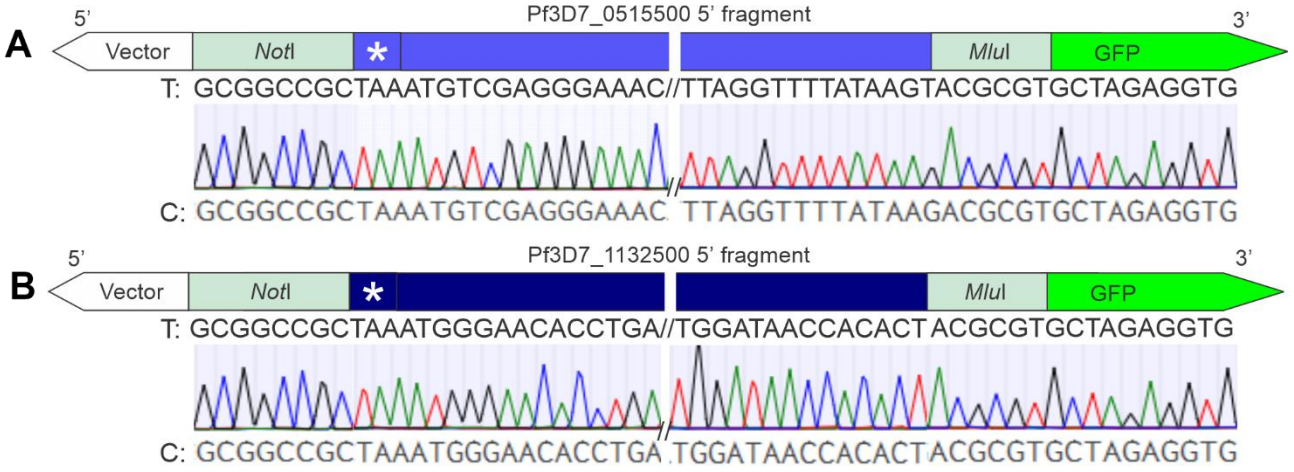

Figure 5.8: Sequence validation of recombinant pSLI-TGD_*gene* plasmid clones.
Sequence alignments of the recombinant pSLI-TGD plasmid with 5' gene fragment inserts to confirm nucleotide identity. T: template sequence of **A)** pSLI_TGD_*Pf3d7_0515500* and **B)** pSLI-TGD_*Pf3d7_1132500* indicated with associated chromatogram and C: consensus sequence determined by Sanger sequencing, with white gaps where sequences are not shown. The asterisks (*) indicate the stop codon.

5.4. Transfection and selection for episomal uptake of pSLI-TGD

For transfection experiments, large quantities (~ 50 – 200 µg) of plasmid DNA was required (94). Pure plasmid DNA was isolated for each of the SLI-TGD recombinant plasmids from saturated *E. coli* cultures, and a small portion of the purified plasmid was digested with *Not*I and *Mlu*I, to validate the identity of the isolated plasmids.

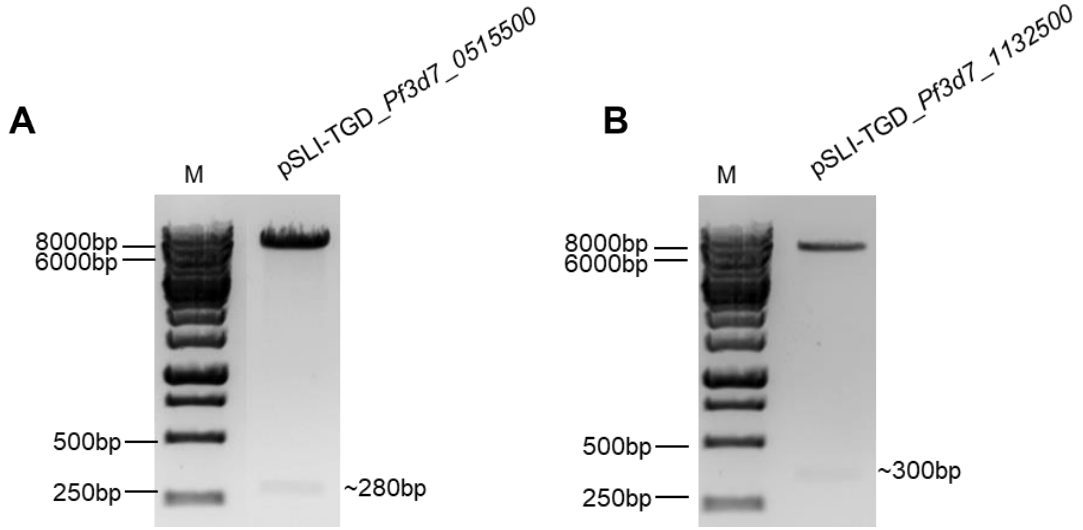

Figure 5.9: Restriction enzyme digestion of isolated SLI-TGD plasmids.
*Not*I and *Mlu*I restriction enzyme digestion of recombinant pSLI-TGD plasmids for **A)** *Pf3d7-0515500* and **B)** *Pf3d7-1132500* plasmids after plasmid isolation, visualised on 1 % (w/v) agarose/TAE gel with EtBr (0.5 µg/mL), Lane M contains a GeneRuler™ 1 kb DNA ladder (Promega). Complete electrophoresis gels are located in Supplementary Figure 9.6.

The expected vector (6760 bp) and gene insert fragments for pSLI-TGD-*Pf3d7_0515500* (~ 280 bp) and pSLI-TGD-Pf3d7_*1132500* (~ 300 bp) were observed, confirming that the correct plasmids were isolated (Figure 5.9). The isolated plasmids were subsequently concentrated and precipitated, as described in section 4.5, for transfection into *P. falciparum* parasites. The electroporation was performed at 305 – 330 V and produced acceptable time constants of > 13 for both transfection reactions.

The transfected parasites were subjected to 10 consecutive days of WR99210 (4 nM) drug pressure to select for parasites that had successfully taken up the recombinant plasmid episomally and therefore expressed the hDHFR gene that allows resistance to WR99210. For two biological parasite cultures transfected with either pSLI-TGD-*Pf3d7_0515500* or pSLI-TGD-Pf3d7_*1132500*, selection with WR99210 was started 24 h after electroporation and maintained for 10 consecutive days (94, 123), followed by a period, where the parasites were maintained under normal culture conditions to allow recovery (Figure 5.10). During transfection, electroporation exerted a large amount of stress on erythrocytes, leading to a degree of erythrocyte lysis and a rapid drop in parasitaemia within the first few days after transfection. This is evident with the 3 – 4 % drop in parasitaemia from day 0 to 1 after transfection with recombinant pSLI-TGD. Treatment with WR99210 resulted in a further reduction in parasitaemia until no parasites were visible on a thin blood smear. After 20 to 22 days in drug free media, no viable parasites reappeared, indicating that episomal uptake of the recombinant plasmids was unsuccessful (Figure 5.10).

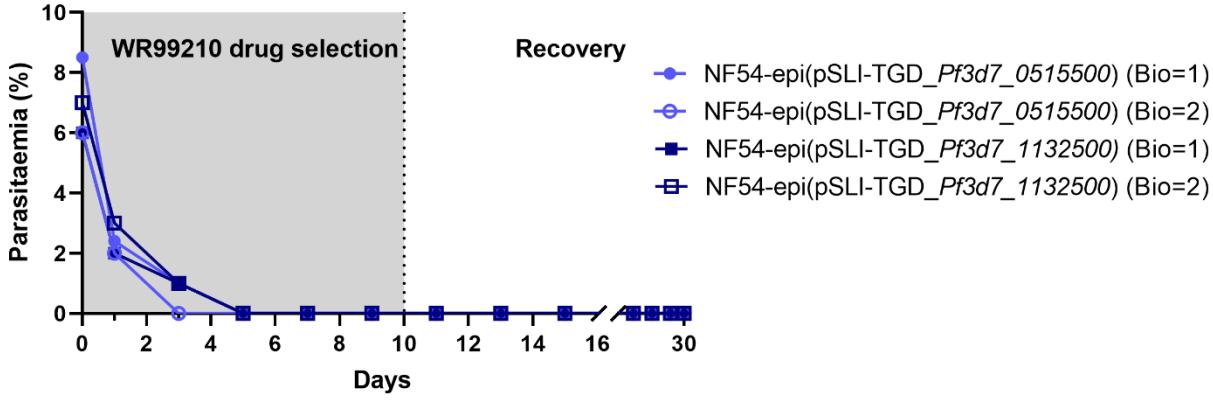

Figure 5.10: Parasitaemia of *P. falciparum* parasites transfected with pSLI-TGD with episomal selection 24 h after transfection.
The parasites of NF54 strain *P. falciparum* were transfected with pSLI-TGD-*Pf3d7_0515500* and pSLI-TGD-*Pf3d7*_1132500 (day 0). Transfection was followed by selection of WR99210 drugs (grey box, from day 1) to select parasites with episomal uptake of plasmids. Parasitaemia was monitored every second day after transfection with RapidDiff stained thin blood smears.

After this, an alternative approach was used where, for one biological repeat, selection with WR99210 (4 nM) was only started 48 h after electroporation (112) and was maintained for 8 consecutive days (Figure 5.11). Here, pSLI-TGD-*Pf3d7_0515500* and pSLI-TGD-Pf3d7_*1132500* were transfected into independent NF54 cultures, and an initial decrease in parasitaemia was observed after electroporation. It was expected that the parasitaemia would drop to undetectable levels under WR99210 drug selection and that parasite recovery would only occur after WR99210 was removed, however after 5 – 7 days of drug selection, the parasitaemia of both transfected cultures started increasing.

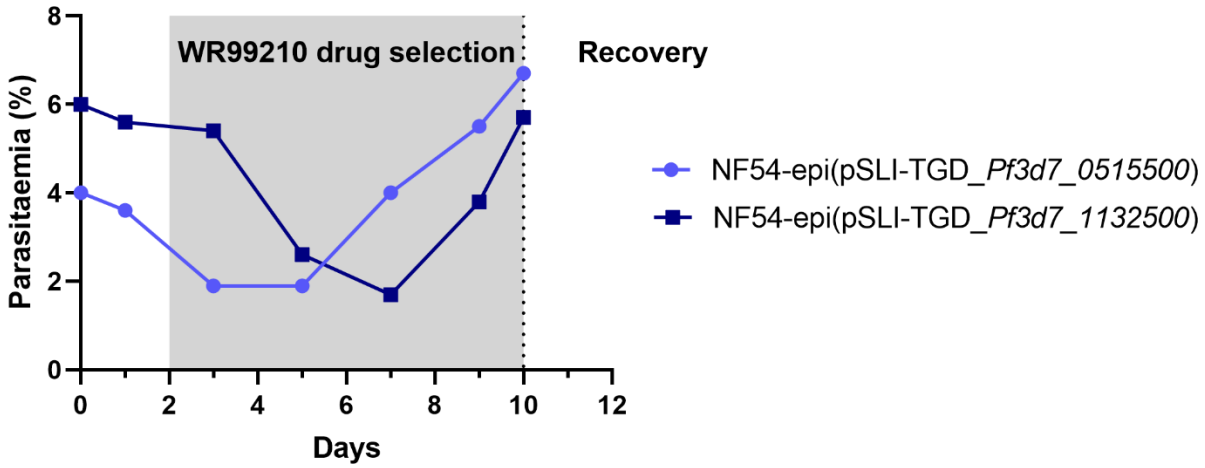

Figure 5.11: Parasitaemia of *P. falciparum* parasites transfected with pSLI-TGD with episomal selection 48 h after transfection and recovery.
NF54 strain *P. falciparum* parasites were transfected with pSLI-TGD-*Pf3d7_0515500* and pSLI-TGD-*Pf3d7_1132500* followed by WR99210 drugs selection (grey box, from day 2) to select for parasites with episomal uptake of plasmids. Parasitaemia was monitored every second day after transfection with RapidDiff stained thin blood smears.

To confirm the episomal presence of pSLI-TGD-*Pf3d7_0515500* and pSLI-TGD-Pf3d7_*1132500*, samples from the recovered parasite cultures (> 4 % trophozoite cultures, 5 % haematocrit) were used to isolate DNA. Vector backbone specific primers that amplify the gene fragments of interest were used in a PCR screen and produced a single band at ~ 500 bp for pSLI-TGD-*Pf3d7_0515500.* Furthermore, a band of ~ 500 bp for pSLI-TGD-*Pf3d7_1132500,* was visualised on an agarose/TAE gel, confirming the episomal uptake of this recombinant plasmid (Figure 5.12).

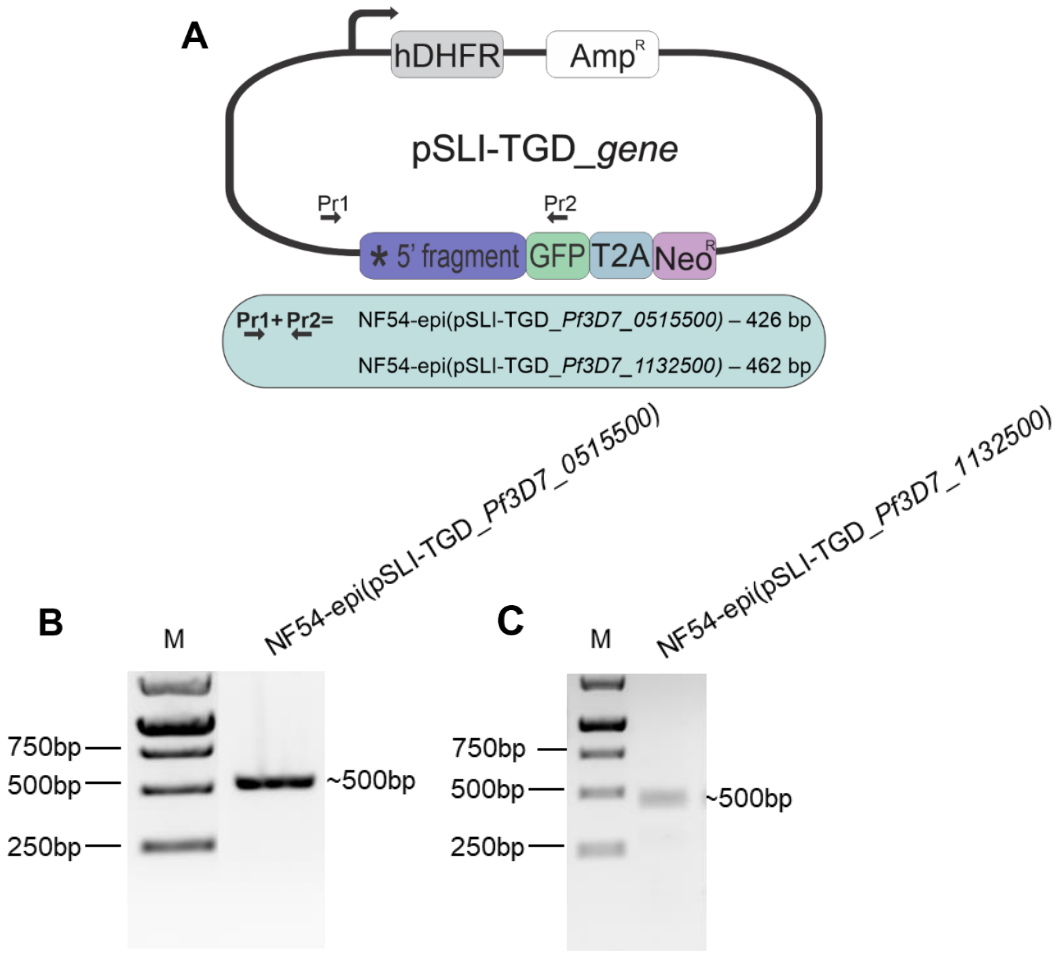

Figure 5.12: Confirmation of episomal presence of recombinant pSLI-TGD plasmids.
A) Representation of primer pairs used to detect episomal presence. **B** and **C)** PCR screen to validate the episomal presence of **B)** *Pf3d7_0515500* and **C)** *Pf3d7_1132500* in pSLI-TGD. The PCR products were visualised on a 1 % (w/v) agarose/TAE gel with (0.5 µg/mL), Lane M contains a GeneRuler™ 1 kb DNA ladder (Promega). The complete electrophoresis gels are located in Supplementary Figure 9.8 and Figure 9.9.

Successful episomal uptake of both recombinant plasmids indicated that the parasite cultures could be placed under G418 drug selection to select for integration of the plasmid into the parasitic genome.

5.5. Transgenic SLI-TGD line selection with G418

To integrate recombinant plasmids into the parasite genome, two biological parasites cultures with confirmed episomal uptake of the recombinant SLI plasmids were subjected to a second cycle of drug selection with G418. Drug selection with 400 µg/mL G418, a neomycin derivative, was maintained for 16 days, after which drug pressure was removed and parasitaemia was monitored every 3 to 4 days. Here, the SLI system should aid in the efficacy of genomic integration as the neomycin resistance can only be expressed under the GOI promoter after

integration of the recombinant plasmid into the parasite genome. The second drug selection cycle, with G418, will allow for the selection of integrated lines only, as the parasite population with episomal expression of the recombinant plasmids does not produce the neomycin resistant protein. If the integration of pSLI-TGD-*Pf3d7_0515500* and pSLI-TGD-*Pf3d7_1132500* occurred and no parasites were recovered after 4 weeks, this could indicate that these amino acid transporters are essential for the proliferation of asexual parasites. However, based on previous gene essentiality studies (88), it is expected that the parasites will be able to recover after gene disruption, as these transporters are not essential for asexual parasites (Table 1.1) and might only be essential for the sexual differentiation of *P. falciparum*.

Unexpectedly, during the first 10 - 11 days of G418 drug selection, the parasites proliferated normally in contrast to the expected steady decrease of parasitaemia. The parasitaemia for each of the NF54-epi(pSLI-TGD-*Pf3d7_0515500*) and NF54-epi(pSLI-TGD-*Pf3d7_1132500*) lines that underwent integration selection to produce the modified lines NF54-*Pf3d7_0515500*-GFP and NF54-*Pf3d7_1132500*-GFP, only decreased from day 12, with minimal to no parasites being detected after day 16 of drug selection. No viable parasites appeared after 34 days without drug selection (Figure 5.13A), indicating that homologous recombination did not occur, and that genomic integration was unsuccessful. To ensure that the batch of G418 was active and effective against *P. falciparum* parasites at 400 µg/mL, an independent culture with episomal uptake of NF54-epi(pSLI-*glmS-myb1*) and NF54-epi(pSLI-M9-*myb1*) was placed under G418 drug selection for 16 days (124). The expected decrease in parasitaemia was observed from the start of the drug selection cycle, and parasite recovery was observed from 30 days onwards (Figure 5.13B). Therefore, the G418 batch was active, and results seen during integration selection for NF54-*Pf3d7_0515500*-GFP and NF54-*Pf3d7_1132500*-GFP were not due to an inactive G418 but specific for these transgenic lines.

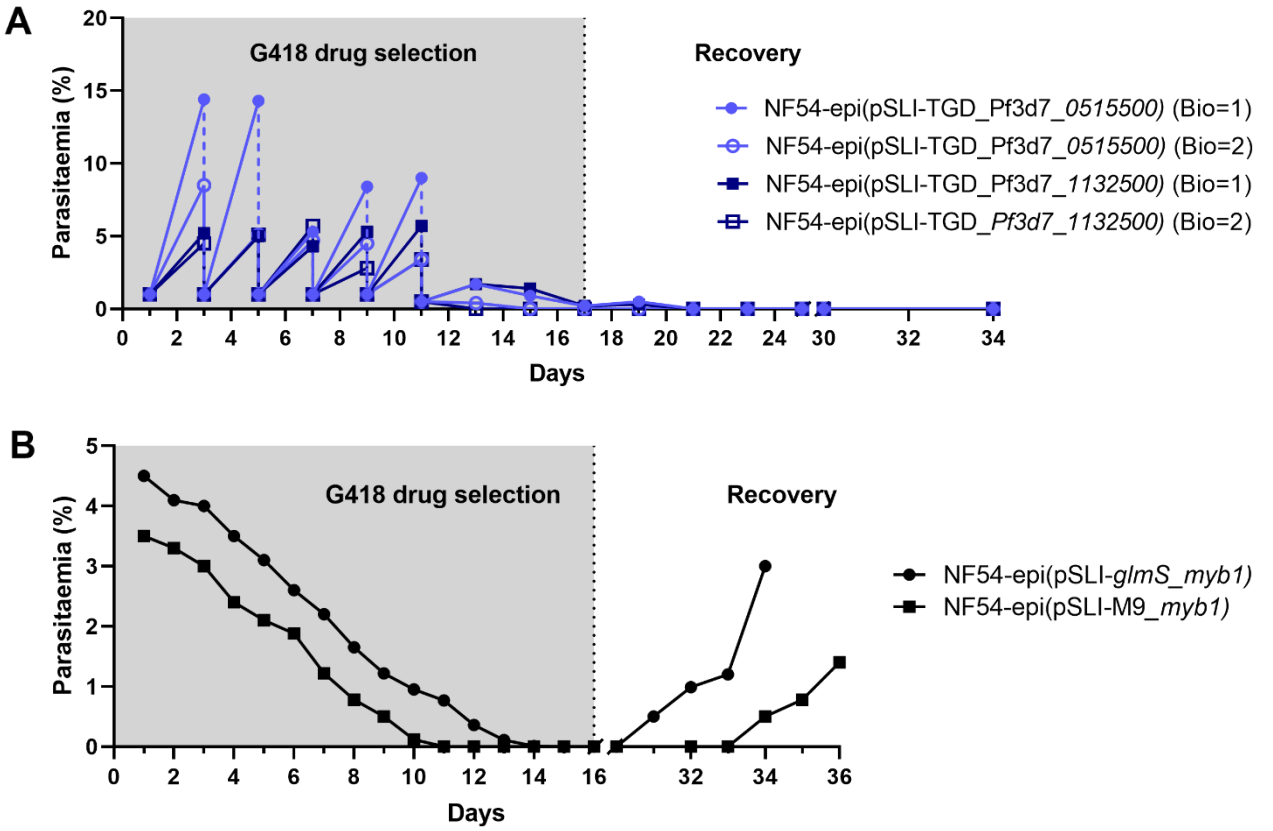

Figure 5.13: Parasitaemia of *P. falciparum* during SLI-TGD integration selection with G418. Episomal confirmation of NF54-epi(pSLI-TGD-*Pf3d7_0515500*) and NF54-epi(pSLI-TGD-*Pf3d7_1132500*) was followed by the selection of G418 drugs (grey box) to select parasites with integration of recombinant plasmids for **A)** Biological 1 and Biological 2. **B)** Control for G418 drug selection on cultures with episomal pSLI-*glmS*/-M9. Parasitaemia was determined from RapidDiff stained thin blood smears and adjusted by diluting the parasite culture to obtain the required parasitaemia (dash lines) every second day.

Given that transgenic lines with non-functional amino acid transporters could not be established, an inducible knockdown system was investigated to potentially evaluate the essentiality of these transporters in asexual proliferation and gametocyte differentiation of *P. falciparum* parasites.

5.6. Cloning and validation of pSLI-*glmS*/-M9 plasmids

The SLI-*glmS* conditional knockdown system allows for the reduction of Pf3d7_0515500 and Pf3d7_1132500 expression at various stages of the parasite's life cycle through the inducible degradation of the mRNA to investigate the phenotypic effect and function of these putative amino acid transporters. The 3' gene fragment of *Pf3d7_0515500* (426 bp) and *Pf3d7_1132500* (853 bp) was cloned into plasmids containing a GFP tag and the riboswitch (pSLI-*glmS*). A control plasmid, with nonfunctional *glmS* ribozyme (pSLI-M9) was also generated.

5.6.1. Cloning of 3' gene fragments into SLI-*glmS*/-M9 vector backbone

Due to the AT-richness of *Pf3d7_1132500*, commercial synthesis was unsuccessful, and alternatively, the 3' fragment for *Pf3d7_1132500* was amplified from gDNA with primers that incorporate *Not*I and *Mlu*I cut sites. The PCR products were digested with *Not*I and *Mlu*I, and subsequently evaluated on an agarose/TAE gel. A single band, corresponding to the expected gene fragment size of *Pf3d7_1132500* (~ 800 bp) was obtained (Figure 5.14), indicating that optimised conditions and gene-specific primers were used to amplify the 3' gene fragment.

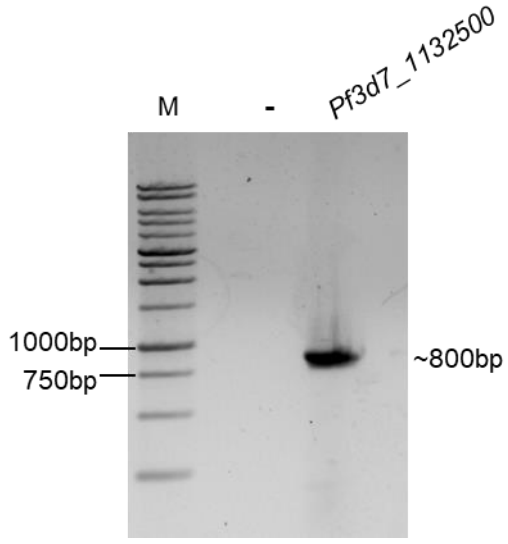

Figure 5.14: Amplification of *Pf3d7_1132500* 3' gene fragment.
PCR amplification of *Pf3d7_1132500* was evaluated on a 1 % (w/v) agarose/TAE gel and stained with EtBr (0.5 µg/mL). -) blank control. Lane M contains a GeneRuler™ 1 kb DNA ladder (Promega).

The gene fragment for *Pf3d7_0515500*, corresponding to the 3' coding strand of this putative amino acid transporter, was synthesised by Gene Universal (USA). After purification of the pUC57 plasmid containing the 3' gene fragment, *Not*I and *Mlu*I digestion was performed to confirm the identity of the isolated plasmid and obtain the gene insert. Two bands,

corresponding to the expected fragment sizes for the synthesised *Pf3d7_0515500* gene fragment (~400 bp) and vector (~ 2700 bp), were obtained (Figure 5.15A). Similarly, the SLI-*glmS* and SLI-M9 plasmids were isolated from *E. coli* stocks and after *Not*I and *Mlu*I digestion to confirm the plasmid identity, the expected bands corresponding to the vector backbone (~ 7000 bp) the original gene insert (*Pf3d7_1406300*, ~ 900 bp) was observed (Figure 5.15B).

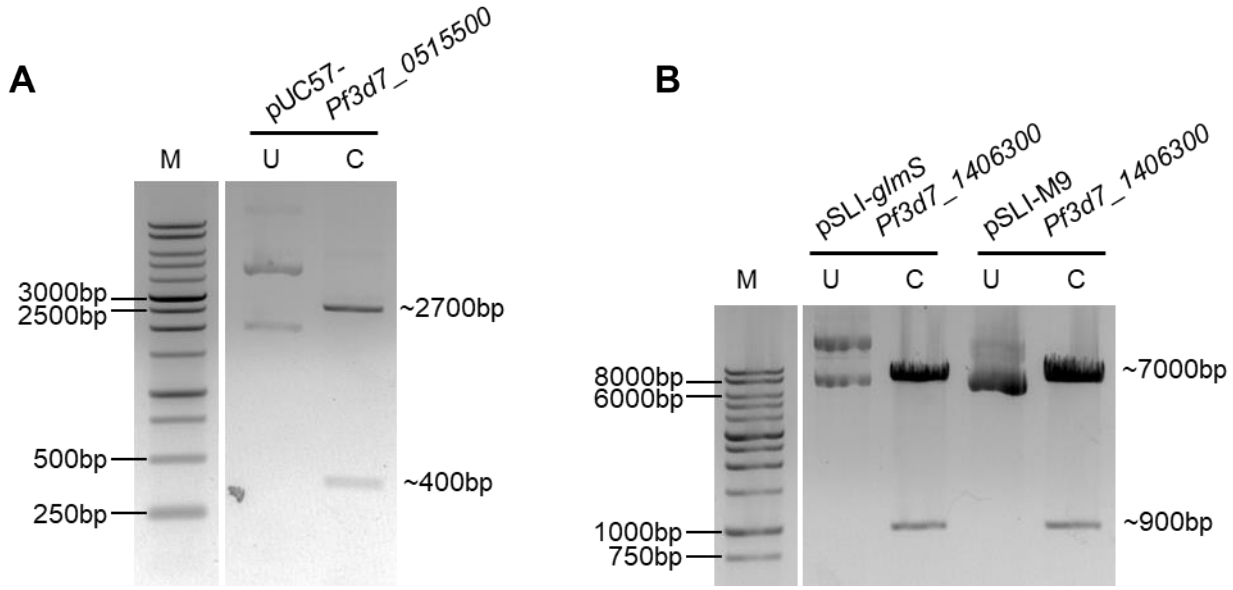

Figure 5.15: Restriction enzyme digestion of *Pf3d7_0515500* 3' gene fragment.
Restriction enzyme digestion of **A)** pUC57-*Pf3d7_0515500* and **B)** SLI-*glmS* (7806 bp) and SLI-M9 (7806 bp) plasmids with *Not*I and *Mlu*I, evaluated on a 1 % (w/v) agarose/TAE gel and stained with EtBr (0.5 µg/mL). U: Undigested controls and C: digested plasmids. Lane M contains a GeneRuler™ 1 kb DNA ladder (Promega). The complete electrophoresis gels are located in Supplementary Figure 9.1 and Figure 9.2.

The band sizes for the 3' gene fragments of both genes, *Pf3d7_0515500* and *Pf3d7_1132500,* and the vector backbone SLI-*glmS* and SLI-M9, were as expected and were purified from the gel to be used in subsequent cloning experiments.

5.6.2. Identification of recombinant pSLI-*glmS*/-M9 plasmids

The 3' gene fragments for both *Pf3d7_0515500* and *Pf3d7_1132500,* were cloned into the pSLI-*glmS* and pSLI-M9 plasmids, thus allowing the GFP-tag and *glmS* ribozyme to be in-frame with the gene fragment. After ligation, the putative recombinant plasmids were transformed into competent *E. coli* cells, and the subsequent colonies were PCR screened for the amplification of selected gene fragments with vector specific primer pair (Table 4.2). For each gene fragment, the expected band size of ~ 500 bp for *Pf3d7_0515500* and ~ 1000 bp for *Pf3d7_1132500* for

colony screen PCR was obtained, indicating that the 3' gene fragments were successfully cloned into the vectors (Figure 5.16).

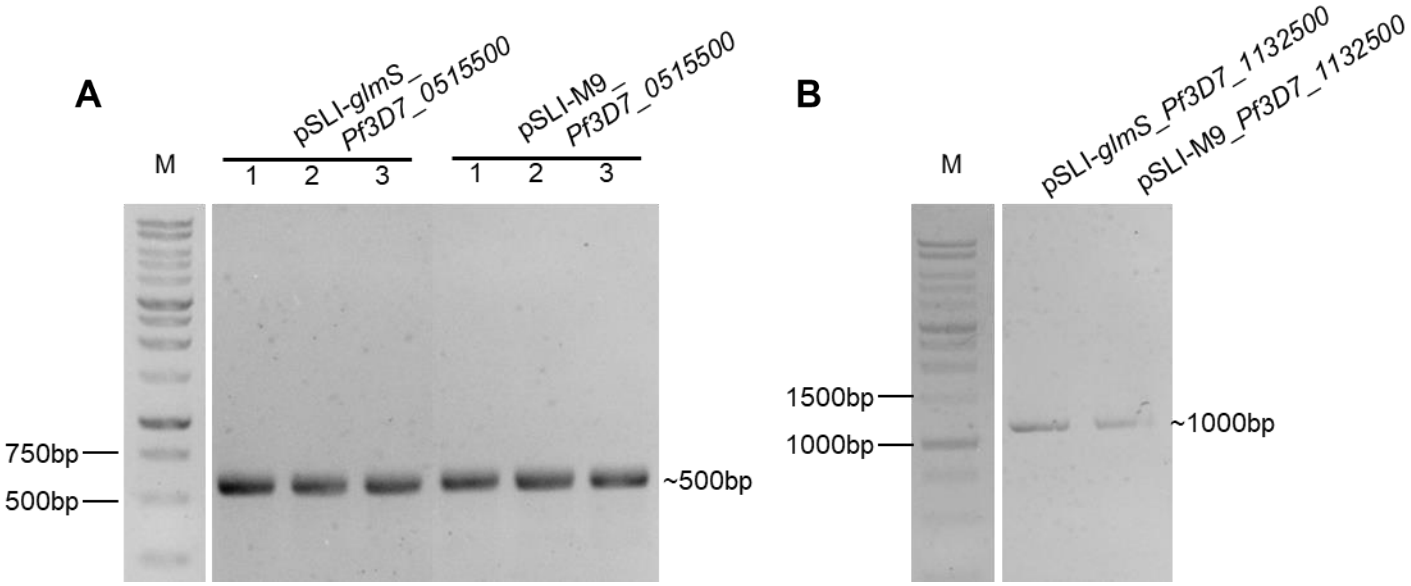

Figure 5.16: Colony screening for recombinant pSLI-*glmS*/-M9_*gene* plasmids.
The products of PCR screening with backbone specific primers were evaluated on a 1 % (w/v) agarose/TAE gel and stained with EtBr (0.5 µg/mL). Lane M contains a GeneRuler™ 1 kb DNA ladder (Promega). **A)** Lanes 1-3 contain the amplified gene insert fragment of *Pf3d7_0515500* cloned into pSLI-*glmS*, while lane 4-6 was cloned into pSLI-M9. **B)** Lanes 1 and 2 contain amplified gene insert fragments of *Pf3d7_1132500* cloned into pSLI-*glmS* and pSLI-M9, respectively. The complete electrophoresis gels are located in Supplementary Figure 9.5.

Recombinant plasmids were also evaluated with RE mapping, to confirm that the *Not*I and *Mlu*I sites surrounding the gene insert were not disrupted. The band sizes for *Pf3d7_0515500* (~ 400 bp) and *Pf3d7_1132500* (~ 800 bp) were observed from the digested plasmids of the digested SLI-*glmS* and SLI-M9 recombinant plasmids (Figure 5.17). This colony screen and restriction enzyme results indicate that both gene fragments were successfully cloned into the respective SLI-*glmS* and SLI-M9 plasmids. To confirm the identity of the recombinant SLI-*glmS* and SLI-M9 plasmids, Sanger sequencing was performed.

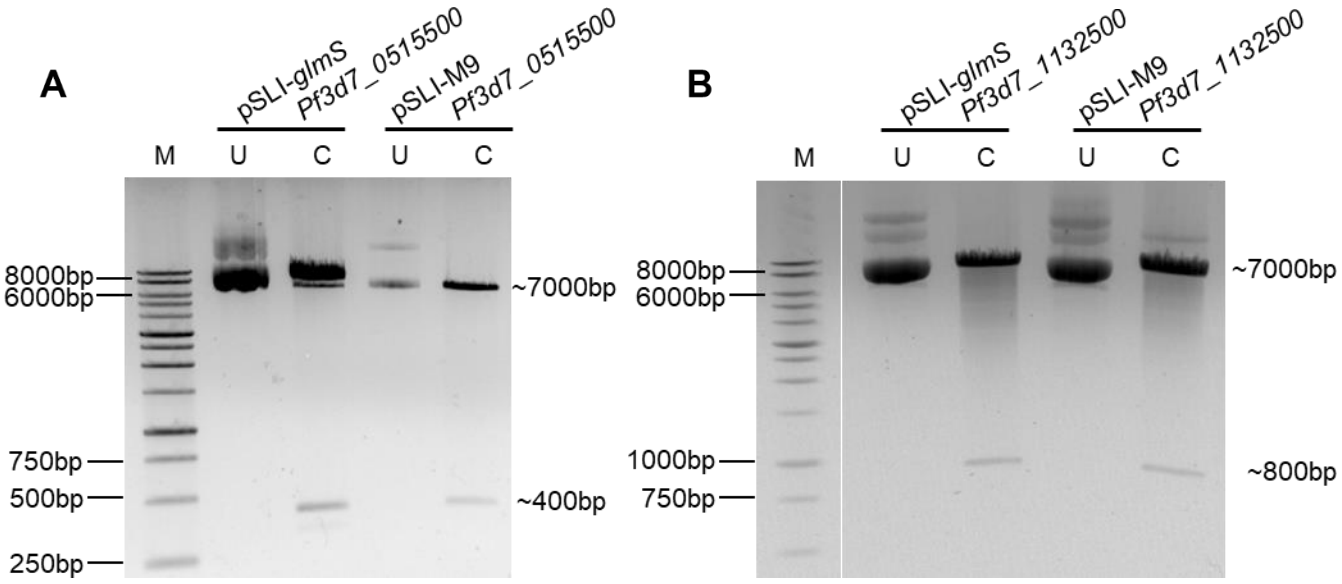

Figure 5.17: Restriction enzyme digestion of recombinant pSLI-*glmS*-M9 plasmids.
The confirmation of RE digestion of recombinant plasmids for **A**) *Pf3d7_0515500* and **B)** *Pf3d7_1132500* was evaluated on a 1 % (w/v) agarose/TAE gel and stained with EtBr (0.5 µg/mL). Lane M contains a GeneRuler™ 1 kb DNA ladder (Promega). U: Undigested controls and C: digested plasmids. The complete electrophoresis gels are in Supplementary Figure 9.3.

5.6.3. Sequence validation of recombinant pSLI-*glmS*-M9

Lastly, the nucleotide sequence of the 3' gene fragments was evaluated with Sanger sequencing as described in 4.4.7. The combination of the chromatogram data and the consensus sequence, produced from overlapping forward and reverse sequences produced with backbone-specific primers, confirmed that there were no mutations or deletions in the gene inserts of pSLI-*glmS-Pf3d7_0515500*, pSLI-M9-*Pf3d7_0515500,* pSLI-*glmS-Pf3d7_1132500* and pSLI-M9-*Pf3d7_1132500* (Figure 5.18). The 3' gene fragments were in-frame with both the GFP and *glmS* ribozyme sequences found in the vector backbone, therefore conditional knockdown of the protein will be possible once genomic integration occurs.

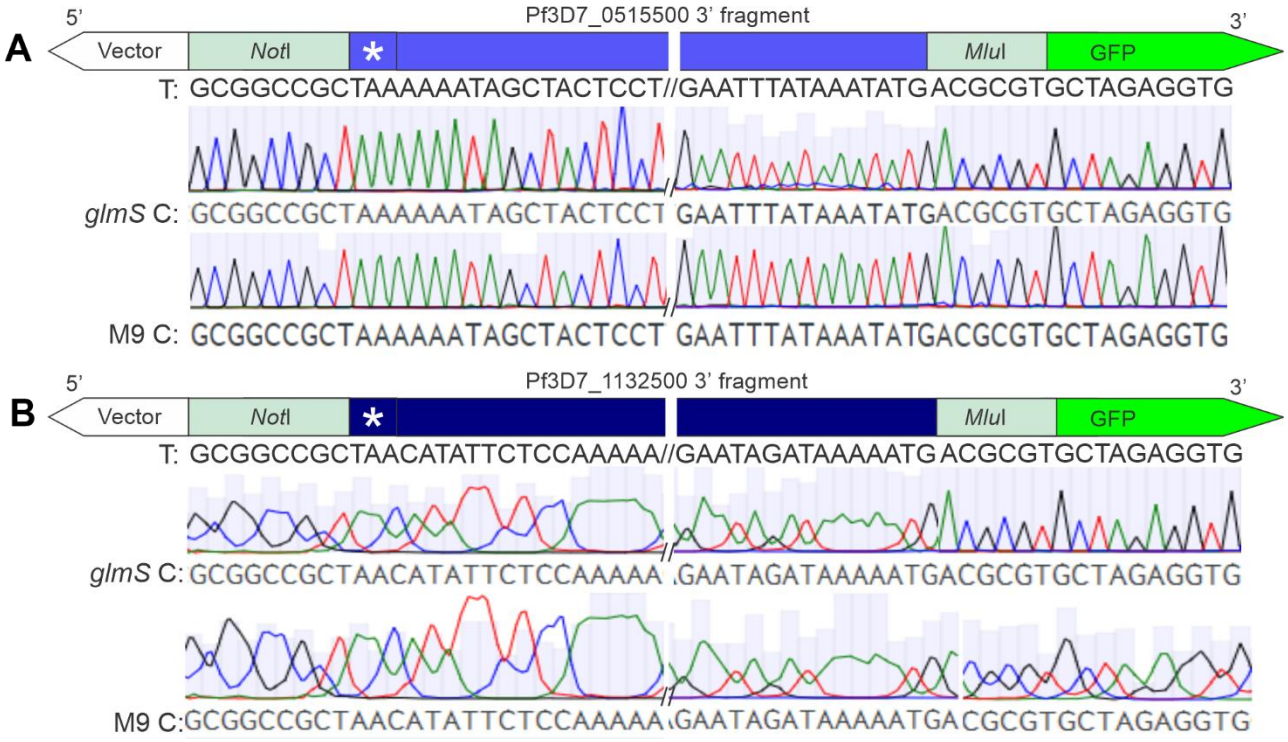

Figure 5.18: Sequence validation of recombinant pSLI-*glmS*-M9 plasmids.
Sequence chromatogram and C: consensus sequence of recombinant pSLI-*glmS*-M9 plasmids with .3' gene fragments of **A)** pSLI_TGD_*Pf3d7_0515500* and **B)** *pSLI-TGD_Pf3d7_1132500* compared to the T: template sequence. White gaps indicate where sequences are not shown, and the asterisk (*) indicates the stop codon.

Successful cloning of recombinant plasmids pSLI-*glmS-Pf3d7_0515500*, pSLI-M9-*Pf3d7_0515500,* pSLI-*glmS-Pf3d7_1132500* and pSLI-M9-*Pf3d7_1132500* was achieved and can be used to generate transgenic parasite lines with inducible expression of these putative amino acid transporters.

5.7. Transfection and selection for episomal uptake of pSLI-*glmS*-M9

Large quantities of plasmid DNA from pSLI-*glmS_Pf3d7_0515500*, pSLI-M9_*Pf3d7_0515500,* pSLI-*glmS_Pf3d7_1132500* and pSLI-M9_*Pf3d7_1132500* were successfully isolated from saturated *E. coli* cultures. The digested products were analysed on agarose/TAE gel, and the band sizes were as expected for the SLI-*glmS* and SLI-M9 vectors (7000 bp) and 3' gene fragments: *Pf3d7_0515500* (~ 400 bp) and *Pf3d7_1132500* (~ 800 bp) (Figure 5.19).

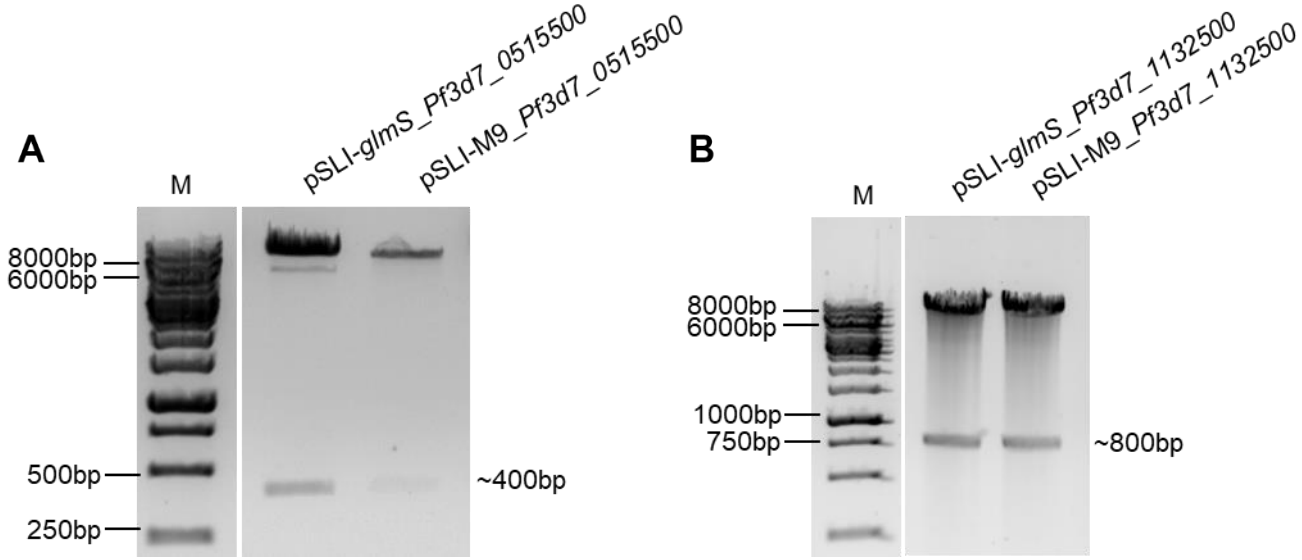

Figure 5.19: Restriction enzyme digestion of isolated SLI-*glmS*/-M9 plasmids.
The enzyme digestion of pSLI-*glmS*/-M9 for **A)** *Pf3d7-0515500* and **B)** *Pf3d7-1132500* plasmids after plasmid isolation was visualised on 1 % (w/v) agarose/TAE gel with EtBr (0.5 µg/mL), Lane M contains a GeneRuler™ 1 kb DNA ladder (Promega). Complete electrophoresis gels are located in Supplementary Figure 9.6 and Figure 9.7.

An NF54 parasite culture was electroporated at 310 V to allow for the uptake of recombinant plasmids, and a sufficient time constant of > 15 was obtained. Transfected parasites were subjected to 10 consecutive days of WR99210 (4 nM) drug selection after electroporation. For two biological parasite cultures transfected with the respective recombinant plasmids, WR99210 drug selection was started 24 h after electroporation (94, 123). This was followed by a recovery period, where parasites were kept under normal culture conditions (Figure 5.20). Electroporation and subsequent treatment with WR99210 resulted in the expected reduction of parasitaemia until no parasites were visible on a thin blood smear at ~ 5 days later. As was observed with the SLI-TGD system, viable parasites did not reappear for transfected parasites placed under drug selection 24 h after electroporation, indicating that the uptake of recombinant plasmids was unsuccessful (Figure 5.20A and B). An alternative approach was also used where one biological repeat was subjected to WR99210 drug pressure that was only started 48 h after electroporation as previously described (112). Here, the pSLI-*glmS*/-M9_*Pf3d7_0515500* and pSLI-*glmS*/-M9_*Pf3d7_1132500* were transfected into separate NF54 parasite cultures, and when WR99210 drug selection was only started 48 h after transfection. Again, the parasitaemia started increasing during WR99210 drug selection as the transfected parasites were able to withstand drug pressure, indicating possible episomal uptake of the recombinant plasmids (Figure 5.21C).

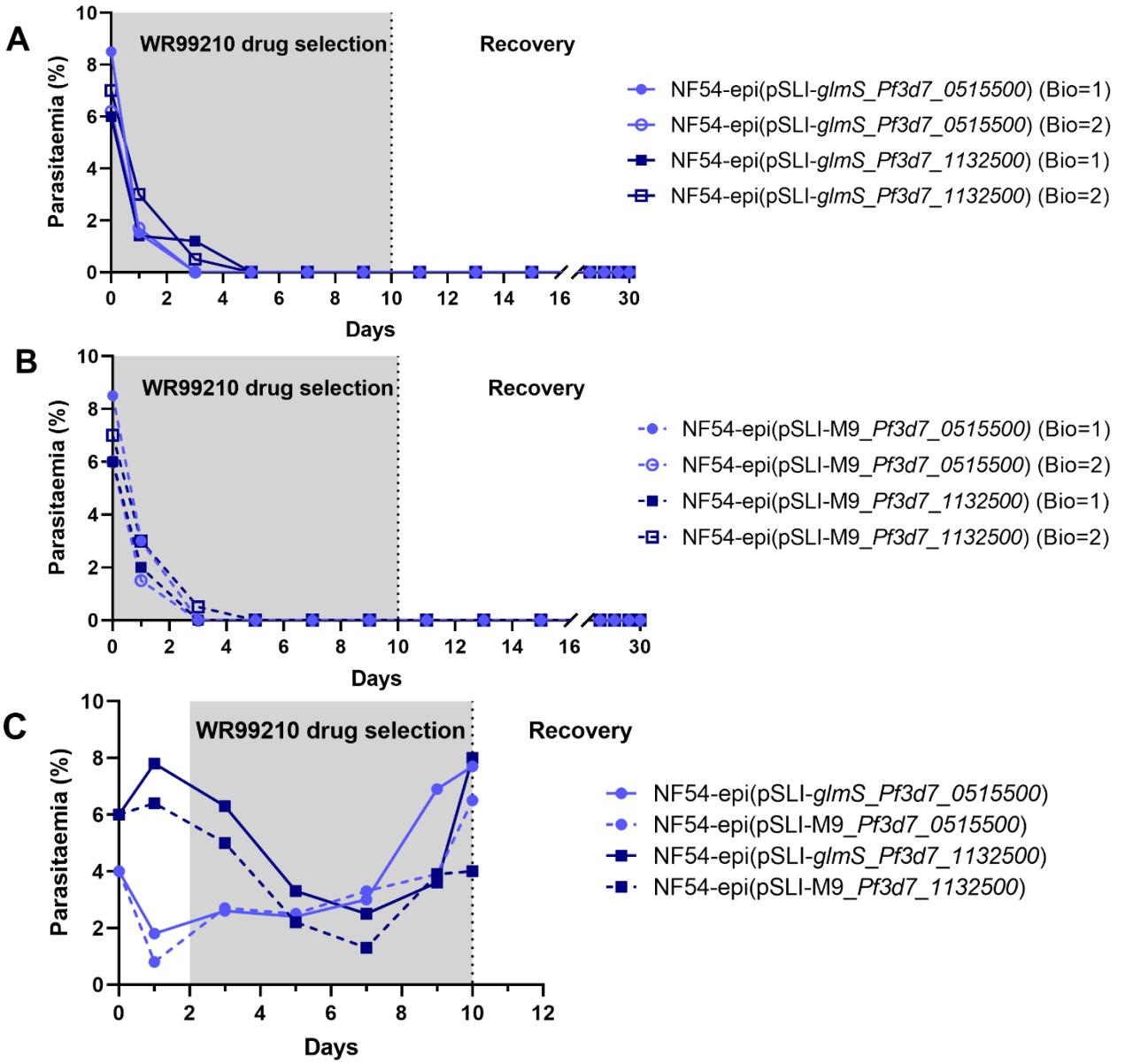

Figure 5.20: Parasitaemia of *P. falciparum* parasites transfected with pSLI-*glmS*/-M9 with episomal selection 48 h after transfection.
Transfection with pSLI-*glmS*/-M9-*Pf3d7_0515500* and pSLI- *glmS*/-M9-*Pf3d7_1132500* was followed by WR99210 drug selection (grey box) from **A and B)** 24 h for two biological and **C)** 48 h to select for parasites with episomal uptake of plasmids. Parasitaemia was monitored every second day after transfection with RapidDiff stained thin blood smears.

Genomic DNA was isolated from the recovered parasites and was PCR screened to confirm the episomal presence of recombinant SLI-*glmS*/-M9 plasmids (Figure 5.21).

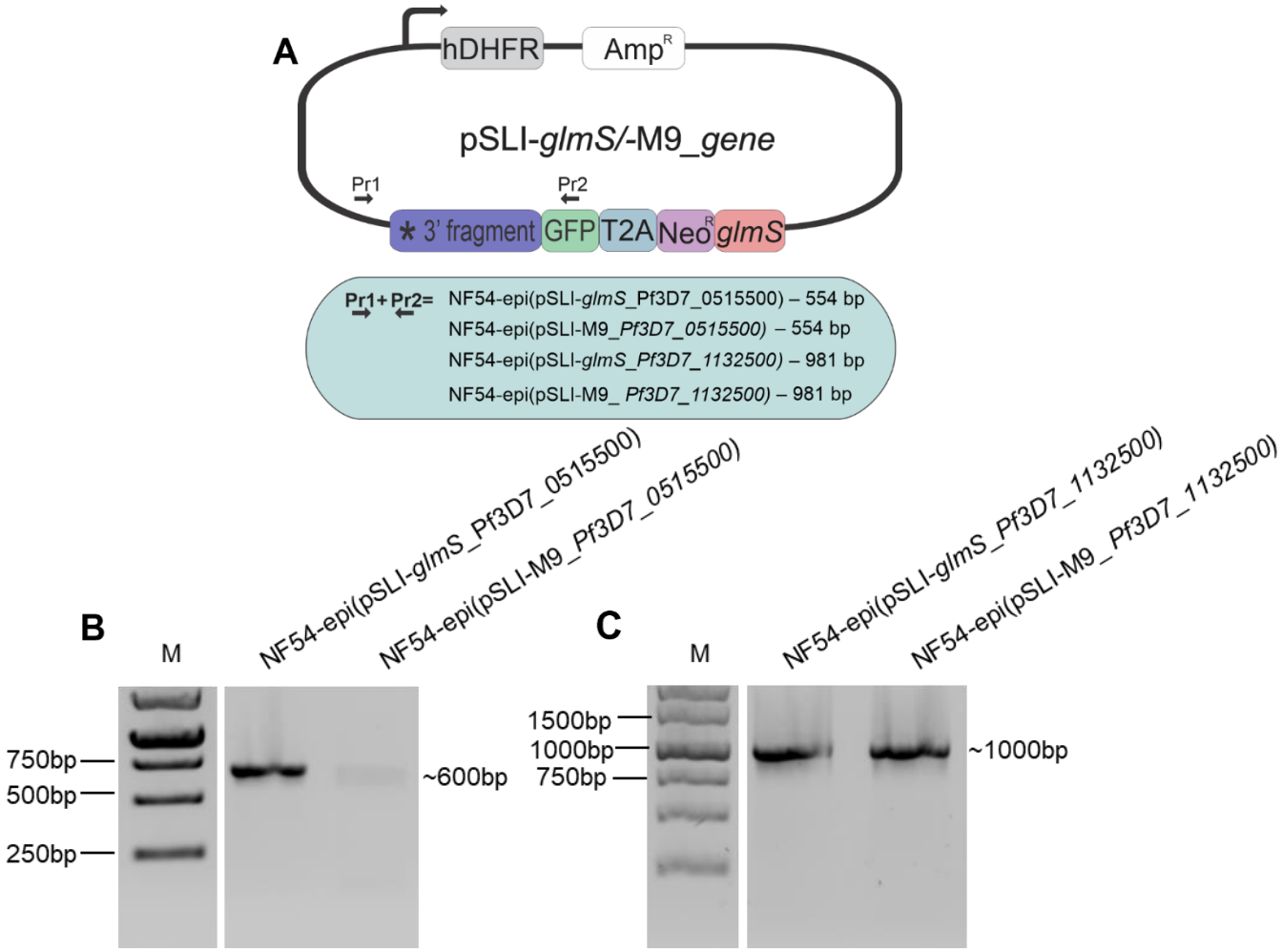

Figure 5.21: Confirmation of episomal presence of recombinant pSLI-*glmS*/-M9 plasmids.
A) Representation of primer pairs and expected amplicon sizes used to detect episomal presence. **B** and **C)** Episomal presence of pSLI-*glmS*/-M9 recombinant plasmids for **B)** *Pf3d7_0515500* and **C)** *Pf3d7_1132500.* Products were visualised on a 1 % (w/v) agarose/TAE gel with (0.5 µg/mL), Lane M contains a GeneRuler™ 1 kb DNA ladder (Promega). The complete electrophoresis gels are found in Supplementary Figure 9.8 and Figure 9.9.

PCR screening, with vector specific primers, detected the episomal presence of pSLI-*glmS_Pf3d7_0515500* and pSLI-M9*_Pf3d7_0515500* by producing a single band at the expected size of ~ 600 bp. Furthermore, a single band of ~ 1000 bp were detected for pSLI-*glmS_Pf3d7_1132500* and pSLI-M9*_Pf3d7_1132500*, confirming the episomal uptake of recombinant plasmids. Subsequently, this parasite culture could be placed under G418 drug pressure to select for the integration of recombinant plasmids into the parasite's genome.

5.8. Transgenic SLI-*glmS* line selection with G418

The NF54-epi(pSLI-*glmS_Pf3d7_0515500*), NF54-epi(pSLI-M9_*Pf3d7_0515500*), NF54-epi(pSLI-*glmS_Pf3d7_1132500*), and NF54-epi(pSLI-M9_*Pf3d7_1132500*) parasite cultures were subjected to a second round of drug pressure, using G418. Surprisingly, parasitaemia only started to decrease after day 13 of G418 drug pressure, until no parasites were detected microscopically (Figure 5.22). For recovery, the cultures were kept under standard conditions as described in section 4.3. Here, the first biological repeat did not generate transgenic lines, and no recovered parasites were ever observed (Figure 5.22A). In the second biological repeat, the recovered parasites appeared after 30 days without drug pressure, and genomic DNA was isolated to determine if genomic integration occurred (Figure 5.22B).

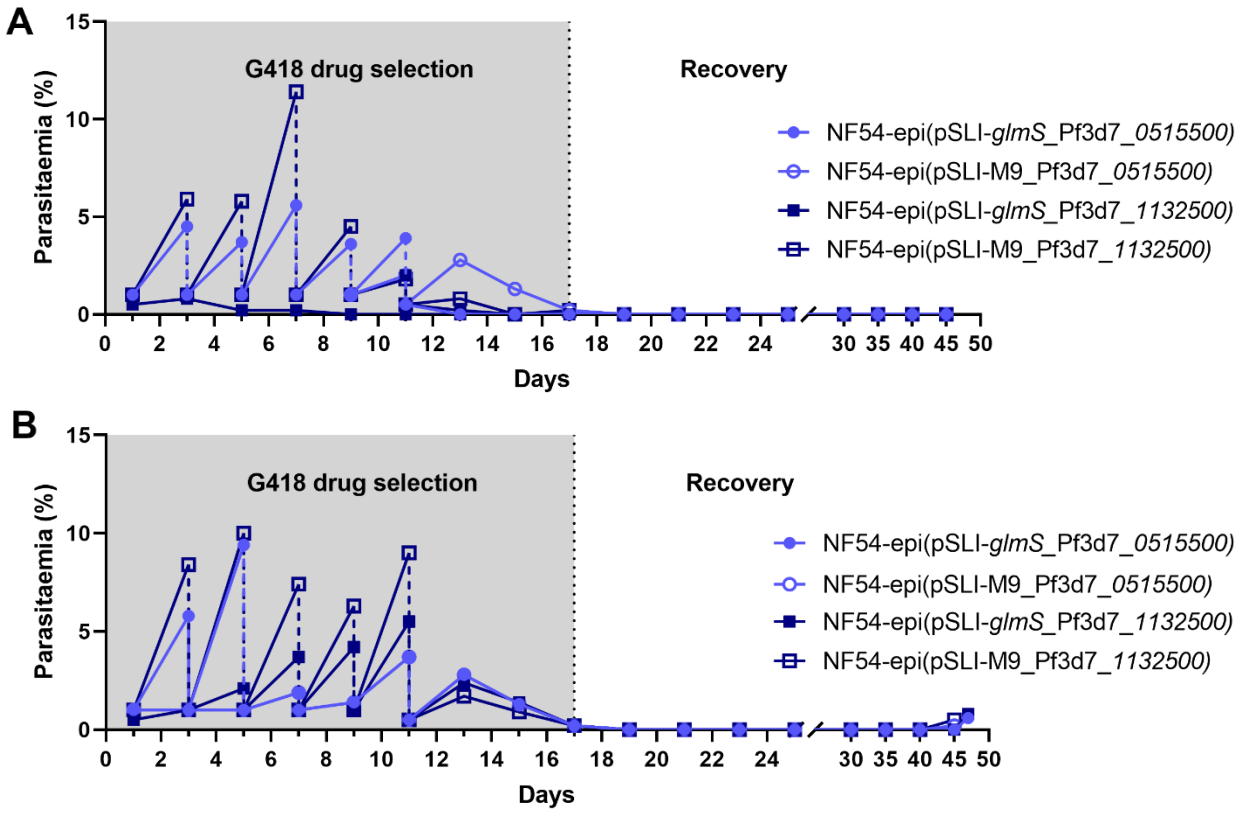

Figure 5.22: Parasitaemia of *P. falciparum* parasites during SLI-*glmS*-M9 integration selection. Confirmation of episomal uptake was followed by selection of G418 drug selection (grey box) for **A)** Biological 1 and **B)** Biological 2 to select for genomic integration. Parasitaemia was monitored every second day and adjusted accordingly (dashed line) with RapidDiff stained thin blood smears.

In order to assess if transgenic lines NF54-*Pf3d7_0515500-glmS*-GFP, NF54-*Pf3d7_1132500-glmS*-GFP, NF54-*Pf3d7_0515500*-M9-GFP and NF54-*Pf3d7_1132500*-M9-GFP were created, genomic integration of the recovered parasite cultures were assessed by PCR using primers,

described in Table 4.3, to amplify regions at the 5' and 3' regions of the GOI locus (Figure 5.23). If genomic integration occurred, WT locus amplification would be absent because the modified locus size is not able to amplify under selected PCR conditions. Also, amplification in the 5' and 3' regions flanking the modified site will be detected. However, from the recovered parasite culture, a band was observed at the WT locus and no amplification was observed in the 5' and 3' regions, indicating that integration at the GOI locus was unsuccessful (Figure 5.23).

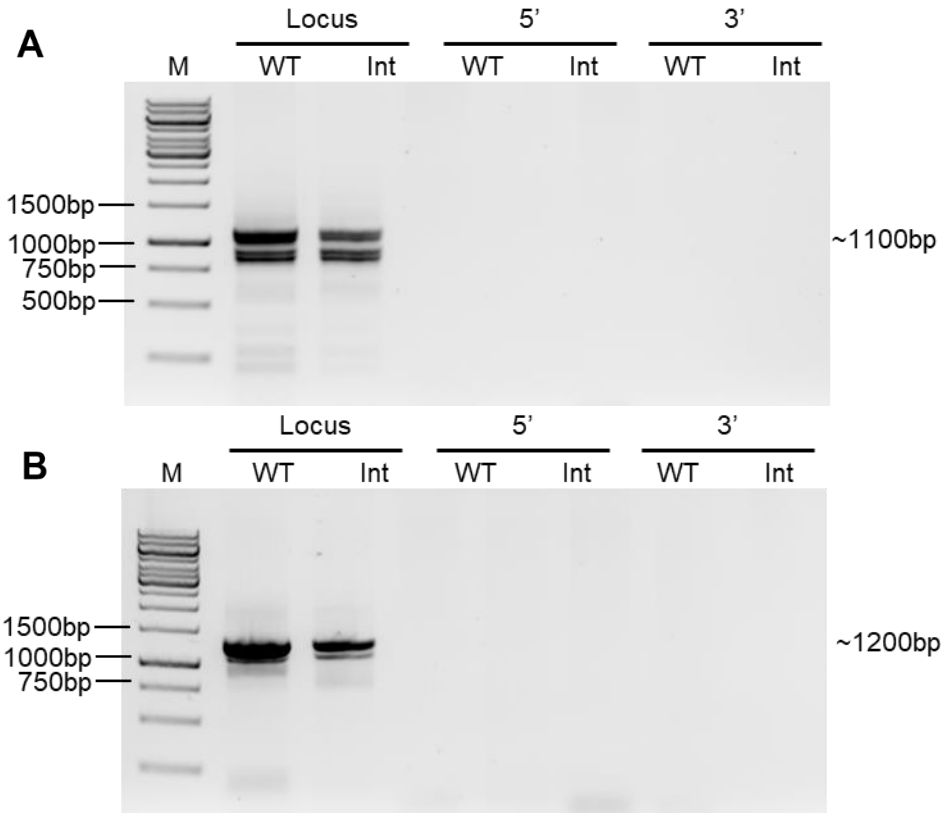

Figure 5.23: Screening of possible SLI-*glmS* transgenic lines.
Genomic integration of pSLI-*glmS* was performed with primers flanking the 5' and 3' regions of **A)** *Pf3d7_0515500* and **B)** *Pf3d7_1132500.* Products were visualised on a 1 % (w/v) agarose/TAE gel with (0.5 µg/mL), Lane M contains a GeneRuler™ 1 kb DNA ladder (Promega).

Although a population of parasites were able to recover from G418 drug selection and thus neomycin resistance must be present, no positive PCR results were obtained when investigating integration at the amino acid transporter locus. Since the activity of the G418 was previously confirmed (Figure 5.13), an alternative reason for the recovery from G418 selection was investigated. One explanation is that the PCR reaction is faulty since the efficacy of the specific primer pairs cannot be tested until integration is obtained. Alternatively, it has been reported that integration of recombinant plasmids can occur into an incorrect locus (94). If in-frame integration of the recombinant plasmid occurred at a different locus with similarity to the

GOI, it would still result in the expression of the GFP fluorescence tag. Therefore, the recovered parasite cultures were evaluated with fluorescence microscopy. Green fluorescence was confirmed for NF54-*Pf3d7_0515500-glmS*-GFP (Figure 5.24).

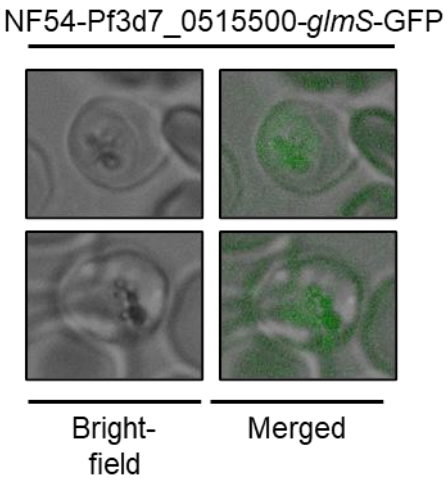

Figure 5.24: Fluorescence analysis of NF54-Pf3d7_0515500-*glmS*-GFP.
Green fluorescence was measured with excitation wavelength 488 nm and emission wavelength 500 nm for putative transgenic line, NF54-Pf3d7_0515500-*glmS*-GFP using an EVOS cell imaging system (Thermo Fisher Scientific, USA) at 1000x magnification for both brightfield (left) and merged fluorescent images.

The green fluorescence suggests that the GFP tag is expressed, which requires that genomic integration of the recombinant plasmid occur. At present, it is unclear whether this occurred at the GOI locus, or a different genomic location. This could potentially be due to no random breaks occurring in the parasite genome at the GOI, therefore homologous recombination with the recombinant plasmids occurred at another locus to allow for the expression of neomycin resistance and parasite survival (94). Consequently, whole genome sequencing should be performed to determine the location of the genomic integration.

6. Discussion

The *P. falciparum* parasite has a variety of nutritional requirements throughout its complex life cycle. Amino acids, obtained from host haemoglobin, or taken up from the extracellular environment, are required by all stages of the *P. falciparum* parasite for protein synthesis and DNA replication. Extensive digestion of host haemoglobin is observed in asexual stage parasites; however, the parasite only incorporates a small amount of these amino acids into protein synthesis (77). Excess amino acids are exported out of asexual parasites, while amino acids such as isoleucine, tryptophan, and glutamine are imported. Three of the 11 putative amino acid transporters identified in the parasite genome and expressed in the asexual life stage are essential (84). In contrast, gametocytes undergo extensive transcriptional remodelling and a relative decrease in the expression of putative amino acid transporters is observed (83). Four amino acid transporters are constitutively expressed in gametocytes, of which *Pf3d7_0515500* (GEP1) was identified as an ortholog to a transporter essential to *P. yoellii* gametocytogenesis (92). As such, the essentiality in *P. falciparum* of this putative amino acid transporter, *Pf3d7_0515500* (GEP1), and another transporter from the same superfamily, *Pf3d7_1132500* (NSS3) was investigated.

To identify new therapeutic drug targets, the essentiality of a pathway or protein needs to be validated through genetic manipulation. Various genetic manipulation techniques, to investigate protein essentiality, have been developed for *P. falciparum,* including targeted gene deletion, and conditional knockdown of protein expression. Gene knockout is an effective technique to investigate gene essentiality, given that the parasite is haploid for most of its life cycle, and that irreversible protein loss is observed. Although conditional knockdown of membrane proteins has been achieved with the *glmS* ribozyme, one concern associated with this technique is the lifespan of membrane proteins that have been translated prior to knockdown of the mRNA and whether the level of knockdown achieved will result in a phenotype (125). This study was focused on generating transgenic lines for the subsequent investigation of the essentiality of *Pf3d7_0515500* (GEP1) and *Pf3d7_1132500* (NSS3) in *P. falciparum* asexual proliferation and gametocytogenesis. Here, we attempted to generate transgenic parasite lines which could genetically disrupt and conditionally knockdown the putative amino acid transporters to determine the essentiality of these amino acid transporters in gametocytogenesis. The truncation of the transporter genes with the SLI-TGD system at the 5’ fragment of the gene at its native loci should produce a non-functional transporter. However, after multiple integration

attempts through a dual drug selection cycle, no integrants were obtained for the SLI-TGD system. The lack of integrants obtained for both putative amino acid transporters from this genetic integration approach indicates the inability to genetically modify these genes with SLI-TGD is due to technical difficulties, rather than essentiality, as they were suggested to be non-essential for asexual *P. falciparum* (84). Known difficulties with *P. falciparum* transfections include low efficiencies (0.8 x 10^{-6}) and the loss of episomal presence of the plasmids as they are not equally divided between daughter merozoites during schizogony (126, 127). Furthermore, once integration occurs, the neomycin resistance gene expression is driven by the native amino acid promoters, and as seen by the expression profiles indicated in Table 1.1, *Pf3d7_0515500* has relatively low expression during the IDC. Therefore, insufficient levels of neomycin resistance could be produced for the survival of integrant parasites when 400 µg/mL G418 drug pressure was applied.

Alternatively, the SLI-*glmS* system was used in an attempt to generate conditional knockdown lines, where fully functional transporter proteins are present until the knockdown of the *glmS* ribozyme is induced. For the first biological of G418 selection, parasites were unable to recover. The parasite cultures that were able to recover during another biological repeat of G418 drug selection were analysed by PCR to detect the integration of the 5' and 3' regions, however, amplification of the WT locus was present. As the primer pairs for the integration confirmation PCR could not be tested prior to integration, it remains unclear if genomic integration occurred at the GOI locus to result in the expression of the neomycin selection marker. Furthermore, the presence of green fluorescence was detected in NF54-*Pf3d7_0515500-glmS*-GFP, supporting the hypothesis that integration of the recombinant plasmid occurred. Therefore, future studies should include whole genome sequencing to determine if genomic integration of the recombinant plasmids occurred at the amino acid transporter loci, prior to determining the essentiality of these transporters in *P. falciparum* parasites. If integration of the recombinant plasmids occurred at the incorrect locus, CRISPR-Cas9 could be used to circumvent the stochastic integration of the recombinant plasmids by targeting the GOI.

The transport of free amino acids, and the import of isoleucine and methionine, are crucial for the survival of *P. falciparum* parasites. From this study, we are one step closer to investigating the essentiality of these NSS amino acid transporters in *P. falciparum* parasites that could increase our understanding of parasite biology and help to identify possible therapeutic drug targets. If these putative amino acids transporters prove to be essential for *P. falciparum* parasites, the amino acid specificity and subsequent essential biological pathways could be

identified. Additionally, FDA approved drugs targeting the NSS subfamily, can be tested against *P. falciparum* parasites, and active compounds can be chemically modified to increase the specificity to the parasite.

7. Conclusion

Malaria remains deadly, and drug resistance to current chemotherapeutics has stalled the progress towards reducing the burden of malaria. To identify new chemotherapeutic drug targets that are effective against the pathogenic asexual stage and prevent resistance transmission, the parasite biology needs to be investigated. As it is critical for the parasite to obtain amino acids from the host and to expel excess amino acids from the parasite, this study was directed towards investigating the essentiality of putative amino acid transporters in asexual proliferation and gametocytogenesis of *P. falciparum*, with two genetic modification tools.

Recombinant plasmids, to disrupt and conditionally knockdown the two putative amino acid transporters, were successfully generated and transfected into asexual *P. falciparum* parasites. Episomal uptake for both systems were confirmed, however, only the SLI-*glmS* system resulted in neomycin resistant parasites. In future studies, whole genome sequencing could be used to determine where genomic integration of the recombinant plasmids occurred. Furthermore, the essentiality of these two putative amino acid transporters, *Pf3d7_0515500* (GEP1) and *Pf3d7_1132500* (NSS3) could be investigated to aid in the discovery of essential proteins and pathways in *P. falciparum* parasites that could be targeted by chemotherapeutics.

8. References

1. World Health Organization. World malaria report 2022. Geneva, Switzerland; 2022. Contract No.: 2022.
2. National Institude for Communicable Diseases N. Hope is on the horizon for a malaria-free Africa. National Institude for Communicable Diseases. 2023.
3. South African Department of Health D. Malaria elimination strategic plan for South. Africa 2019–2023. 2019.
4. Lalremruata A, Jeyaraj S, Engleitner T, Joanny F, Lang A, Belard S, et al. Species and genotype diversity of *Plasmodium* in malaria patients from Gabon analysed by next generation sequencing. Malar J. 2017;16(1):398.
5. Calderaro A, Piccolo G, Gorrini C, Rossi S, Montecchini S, Dell'Anna ML, et al. Accurate identification of the six human *Plasmodium spp.* causing imported malaria, including *Plasmodium ovale wallikeri* and *Plasmodium knowlesi*. Malar J. 2013;12:321.
6. Conroy AL, Datta D, John CC. What causes severe malaria and its complications in children? Lessons learned over the past 15 years. BMC Med. 2019;17(1):52.
7. Talapko J, Skrlec I, Alebic T, Jukic M, Vcev A. Malaria: the past and the present. Microorganisms. 2019;7(6).
8. Geleta G, Ketema T. Severe Malaria Associated with *Plasmodium falciparum* and *P. vivax* among Children in Pawe Hospital, Northwest Ethiopia. Malar Res Treat. 2016;2016:1240962.
9. Kochar DK, Saxena V, Singh N, Kochar SK, Kumar SV, Das A. *Plasmodium vivax* malaria. Emerg Infect Dis. 2005;11(1):132-4.
10. Miller LH, Baruch DI, Marsh K, Doumbo OK. The pathogenic basis of malaria. Nature. 2002;415(6872):673-9.
11. Menard R. The journey of the malaria sporozoite through its hosts: two parasite proteins lead the way. Microbes Infect. 2000;2(6):633-42.
12. Vanderberg JP, Frevert U. Intravital microscopy demonstrating antibody-mediated immobilisation of *Plasmodium berghei* sporozoites injected into skin by mosquitoes. Int J Parasitol. 2004;34(9):991-6.
13. Vaughan AM, Kappe SHI. Malaria parasite liver infection and exoerythrocytic biology. Cold Spring Harb Perspect Med. 2017;7(6).
14. Frevert U. Sneaking in through the back entrance: the biology of malaria liver stages. Trends Parasitol. 2004;20(9):417-24.
15. Weiss GE, Gilson PR, Taechalertpaisarn T, Tham WH, de Jong NW, Harvey KL, et al. Revealing the sequence and resulting cellular morphology of receptor-ligand interactions during *Plasmodium falciparum* invasion of erythrocytes. PLoS Pathog. 2015;11(2):e1004670.
16. Sherman IW. Biochemistry of *Plasmodium* (malarial parasites). Microbiol Rev. 1979;43(4):453-95.
17. Hanssen E, Knoechel C, Dearnley M, Dixon MW, Le Gros M, Larabell C, et al. Soft X-ray microscopy analysis of cell volume and hemoglobin content in erythrocytes infected with asexual and sexual stages of *Plasmodium falciparum*. J Struct Biol. 2012;177(2):224-32.
18. Chulay JD, Haynes JD, Diggs CL. *Plasmodium falciparum*: assessment of *in vitro* growth by [3H]hypoxanthine incorporation. Exp Parasitol. 1983;55(1):138-46.

19. Baumeister S, Winterberg M, Przyborski JM, Lingelbach K. The malaria parasite *Plasmodium falciparum*: cell biological peculiarities and nutritional consequences. Protoplasma. 2010;240(1-4):3-12.
20. Kirk K. Membrane transport in the malaria-infected erythrocyte. Physiol Rev. 2001;81(2):495-537.
21. Arnot DE, Gull K. The *Plasmodium* cell-cycle: facts and questions. Ann Trop Med Parasitol. 1998;92(4):361-5.
22. Bozdech Z, Llinas M, Pulliam BL, Wong ED, Zhu J, DeRisi JL. The transcriptome of the intraerythrocytic developmental cycle of *Plasmodium falciparum*. PLoS Biol. 2003;1(1):E5.
23. Bannister LH, Hopkins JM, Fowler RE, Krishna S, Mitchell GH. A brief illustrated guide to the ultrastructure of *Plasmodium falciparum* asexual blood stages. Parasitol Today. 2000;16(10):427-33.
24. Talman AM, Domarle O, McKenzie FE, Ariey F, Robert V. Gametocytogenesis: the puberty of *Plasmodium falciparum*. Malar J. 2004;3:24.
25. Dixon MWA, Tilley L. *Plasmodium falciparum* goes bananas for sex. Mol Biochem Parasitol. 2021;244:111385.
26. Baker DA. Malaria gametocytogenesis. Mol Biochem Parasitol. 2010;172(2):57-65.
27. Billker O, Lindo V, Panico M, Etienne AE, Paxton T, Dell A, et al. Identification of xanthurenic acid as the putative inducer of malaria development in the mosquito. Nature. 1998;392(6673):289-92.
28. Billker O, Dechamps S, Tewari R, Wenig G, Franke-Fayard B, Brinkmann V. Calcium and a calcium-dependent protein kinase regulate gamete formation and mosquito transmission in a malaria parasite. Cell. 2004;117(4):503-14.
29. Ghosh AK, Moreira LA, Jacobs-Lorena M. *Plasmodium*-mosquito interactions, phage display libraries and transgenic mosquitoes impaired for malaria transmission. Insect Biochem Mol Biol. 2002;32(10):1325-31.
30. Guerreiro A, Deligianni E, Santos JM, Silva PA, Louis C, Pain A, et al. Genome-wide RIP-Chip analysis of translational repressor-bound mRNAs in the *Plasmodium* gametocyte. Genome Biol. 2014;15(11):493.
31. Belete TM. Recent progress in the development of new antimalarial drugs with novel targets. Drug Des Devel Ther. 2020;14:3875-89.
32. World Health Organization. World malaria report 2021. Geneva, Switzerland; 2021.
33. Gari T, Lindtjorn B. Reshaping the vector control strategy for malaria elimination in Ethiopia in the context of current evidence and new tools: opportunities and challenges. Malar J. 2018;17(1):454.
34. Phillips MA, Burrows JN, Manyando C, van Huijsduijnen RH, Van Voorhis WC, Wells TNC. Malaria. Nat Rev Dis Primers. 2017;3:17050.
35. Mwangangi JM, Mbogo CM, Orindi BO, Muturi EJ, Midega JT, Nzovu J, et al. Shifts in malaria vector species composition and transmission dynamics along the Kenyan coast over the past 20 years. Malar J. 2013;12:13.
36. South African Department of Health D. National guidelines for the prevention of malaria, South Africa. 2018.
37. Tse EG, Korsik M, Todd MH. The past, present and future of anti-malarial medicines. Malar J. 2019;18(1):93.

38. Stokes BH, Dhingra SK, Rubiano K, Mok S, Straimer J, Gnadig NF, et al. *Plasmodium falciparum* K13 mutations in Africa and Asia impact artemisinin resistance and parasite fitness. Elife. 2021;10.
39. Witmer K, Dahalan FA, Delves MJ, Yahiya S, Watson OJ, Straschil U, et al. Transmission of artemisinin-resistant malaria parasites to mosquitoes under antimalarial drug pressure. Antimicrob Agents Chemother. 2020;65(1).
40. Siqueira-Neto JL, Wicht KJ, Chibale K, Burrows JN, Fidock DA, Winzeler EA. Antimalarial drug discovery: progress and approaches. Nat Rev Drug Discov. 2023;22(10):807-26.
41. Clinical Trials Partnership RS. Malaria vaccine approval: a step change for global health. Lancet. 2021;398(10309):1381.
42. Laurens MB. RTS,S/AS01 vaccine (Mosquirix): an overview. Hum Vaccin Immunother. 2020;16(3):480-9.
43. WHO recommends R21/Matrix-M vaccine for malaria prevention in updated advice on immunization [press release]. Geneva, 2 October 2023 2023.
44. Sinha S, Medhi B, Sehgal R. Challenges of drug-resistant malaria. Parasite. 2014;21:61.
45. Muller IB, Hyde JE. Antimalarial drugs: modes of action and mechanisms of parasite resistance. Future Microbiol. 2010;5(12):1857-73.
46. Martin RE, Henry RI, Abbey JL, Clements JD, Kirk K. The 'permeome' of the malaria parasite: an overview of the membrane transport proteins of *Plasmodium falciparum*. Genome Biol. 2005;6(3):R26.
47. Martin RE. The transportome of the malaria parasite. Biol Rev Camb Philos Soc. 2020;95(2):305-32.
48. Staines HM, Derbyshire ET, Slavic K, Tattersall A, Vial H, Krishna S. Exploiting the therapeutic potential of *Plasmodium falciparum* solute transporters. Trends Parasitol. 2010;26(6):284-96.
49. Krishnan A, Soldati-Favre D. Amino acid metabolism in apicomplexan parasites. Metabolites. 2021;11(2).
50. Kirk K, Lehane AM. Membrane transport in the malaria parasite and its host erythrocyte. Biochem J. 2014;457(1):1-18.
51. Lodish H. Molecular cell biology. 6th ed. 6th ed2008.
52. Monteiro Junior JC, Kruger A, Palmisano G, Wrenger C. Transporter-mediated solutes uptake as drug target in *Plasmodium falciparum*. Front Pharmacol. 2022;13:845841.
53. Untaroiu AM, Carey MA, Guler JL, Papin JA. Leveraging the effects of chloroquine on resistant malaria parasites for combination therapies. BMC Bioinformatics. 2019;20(1):186.
54. Cowell AN, Istvan ES, Lukens AK, Gomez-Lorenzo MG, Vanaerschot M, Sakata-Kato T, et al. Mapping the malaria parasite druggable genome by using *in vitro* evolution and chemogenomics. Science. 2018;359(6372):191-9.
55. LaMonte G, Lim MY, Wree M, Reimer C, Nachon M, Corey V, et al. Mutations in the *Plasmodium falciparum* cyclic amine resistance locus (PfCARL) confer multidrug resistance. mBio. 2016;7(4).
56. Spillman NJ, Allen RJ, McNamara CW, Yeung BK, Winzeler EA, Diagana TT, et al. Na^+ regulation in the malaria parasite *Plasmodium falciparum* involves the cation ATPase PfATP4 and is a target of the spiroindolone antimalarials. Cell Host Microbe. 2013;13(2):227-37.

57. McCarthy JS, Abd-Rahman AN, Collins KA, Marquart L, Griffin P, Kummel A, et al. Defining the antimalarial activity of Cipargamin in healthy volunteers experimentally infected with blood-stage *Plasmodium falciparum*. Antimicrob Agents Chemother. 2021;65(2).
58. Dennis ASM, Lehane AM, Ridgway MC, Holleran JP, Kirk K. Cell swelling induced by the antimalarial KAE609 (Cipargamin) and other PfATP4-associated antimalarials. Antimicrob Agents Chemother. 2018;62(6).
59. Rottmann M, McNamara C, Yeung BK, Lee MC, Zou B, Russell B, et al. Spiroindolones, a potent compound class for the treatment of malaria. Science. 2010;329(5996):1175-80.
60. Armstrong JF, Campo B, Alexander SPH, Arendse LB, Cheng X, Davenport AP, et al. Advances in malaria pharmacology and the online guide to MALARIA PHARMACOLOGY: IUPHAR review 38. Br J Pharmacol. 2023;180(15):1899-929.
61. Marchesini N, Vieira M, Luo S, Moreno SN, Docampo R. A malaria parasite-encoded vacuolar H(+)-ATPase is targeted to the host erythrocyte. J Biol Chem. 2005;280(44):36841-7.
62. Hameed PS, Solapure S, Patil V, Henrich PP, Magistrado PA, Bharath S, et al. Triaminopyrimidine is a fast-killing and long-acting antimalarial clinical candidate. Nat Commun. 2015;6:6715.
63. Istvan ES, Das S, Bhatnagar S, Beck JR, Owen E, Llinas M, et al. *Plasmodium* Niemann-Pick type C1-related protein is a druggable target required for parasite membrane homeostasis. Elife. 2019;8.
64. Jiang X. An overview of the *Plasmodium falciparum* hexose transporter and its therapeutic interventions. Proteins. 2022;90(10):1766-78.
65. Ortiz D, Guiguemde WA, Johnson A, Elya C, Anderson J, Clark J, et al. Identification of selective inhibitors of the *Plasmodium falciparum* hexose transporter PfHT by screening focused libraries of anti-malarial compounds. PLoS One. 2015;10(4):e0123598.
66. Hapuarachchi SV, Cobbold SA, Shafik SH, Dennis AS, McConville MJ, Martin RE, et al. The malaria parasite's lactate transporter PfFNT is the target of antiplasmodial compounds identified in whole cell phenotypic screens. PLoS Pathog. 2017;13(2):e1006180.
67. Divo AA, Geary TG, Davis NL, Jensen JB. Nutritional requirements of *Plasmodium falciparum* in culture. I. Exogenously supplied dialyzable components necessary for continuous growth. J Protozool. 1985;32(1):59-64.
68. Wu G. Functional amino acids in growth, reproduction, and health. Adv Nutr. 2010;1(1):31-7.
69. Payne SH, Loomis WF. Retention and loss of amino acid biosynthetic pathways based on analysis of whole-genome sequences. Eukaryot Cell. 2006;5(2):272-6.
70. Yadav MK, Swati D. Comparative genome analysis of six malarial parasites using codon usage bias based tools. Bioinformation. 2012;8(24):1230-9.
71. Babbitt SE, Altenhofen L, Cobbold SA, Istvan ES, Fennell C, Doerig C, et al. *Plasmodium falciparum* responds to amino acid starvation by entering into a hibernatory state. Proc Natl Acad Sci U S A. 2012;109(47):E3278-87.
72. Loria P, Miller S, Foley M, Tilley L. Inhibition of the peroxidative degradation of haem as the basis of action of chloroquine and other quinoline antimalarials. Biochem J. 1999;339 (Pt 2):363-70.

73. Zarchin S, Krugliak M, Ginsburg H. Digestion of the host erythrocyte by malaria parasites is the primary target for quinoline-containing antimalarials. Biochem Pharmacol. 1986;35(14):2435-42.
74. Lew VL, Tiffert T, Ginsburg H. Excess haemoglobin digestion and the osmotic stability of *Plasmodium falciparum*-infected red blood cells. Blood. 2003;101(10):4189-94.
75. Lamour SD, Straschil U, Saric J, Delves MJ. Changes in metabolic phenotypes of *Plasmodium falciparum in vitro* cultures during gametocyte development. Malar J. 2014;13:468.
76. Olszewski KL, Morrisey JM, Wilinski D, Burns JM, Vaidya AB, Rabinowitz JD, et al. Host-parasite interactions revealed by *Plasmodium falciparum* metabolomics. Cell Host Microbe. 2009;5(2):191-9.
77. Krugliak M, Zhang J, Ginsburg H. Intraerythrocytic *Plasmodium falciparum* utilizes only a fraction of the amino acids derived from the digestion of host cell cytosol for the biosynthesis of its proteins. Mol Biochem Parasitol. 2002;119(2):249-56.
78. Ginsburg H. Transport pathways in the malaria-infected erythrocyte. Their characterization and their use as potential targets for chemotherapy. Biochem Pharmacol. 1994;48(10):1847-56.
79. MacRae JI, Dixon MW, Dearnley MK, Chua HH, Chambers JM, Kenny S, et al. Mitochondrial metabolism of sexual and asexual blood stages of the malaria parasite *Plasmodium falciparum*. BMC Biol. 2013;11:67.
80. Cobbold SA, Martin RE, Kirk K. Methionine transport in the malaria parasite *Plasmodium falciparum*. Int J Parasitol. 2011;41(1):125-35.
81. Parker KER, Fairweather SJ, Rajendran E, Blume M, McConville MJ, Broer S, et al. The tyrosine transporter of *Toxoplasma gondii* is a member of the newly defined apicomplexan amino acid transporter (ApiAT) family. PLoS Pathog. 2019;15(2):e1007577.
82. Wichers JS, van Gelder C, Fuchs G, Ruge JM, Pietsch E, Ferreira JL, et al. Characterization of apicomplexan amino acid transporters (ApiATs) in the malaria parasite *Plasmodium falciparum*. mSphere. 2021;6(6):e0074321.
83. van Biljon R, van Wyk R, Painter HJ, Orchard L, Reader J, Niemand J, et al. Hierarchical transcriptional control regulates *Plasmodium falciparum* sexual differentiation. BMC Genomics. 2019;20(1):920.
84. Zhang M, Wang C, Otto TD, Oberstaller J, Liao X, Adapa SR, et al. Uncovering the essential genes of the human malaria parasite *Plasmodium falciparum* by saturation mutagenesis. Science. 2018;360(6388).
85. van Biljon R. Integrative transcriptome and phenome analysis reveal unique regulatory cascades controlling the intraerythrocytic asexual and sexual development of human malaria parasites: University of Pretoria; 2019.
86. Balestra AC, Koussis K, Klages N, Howell SA, Flynn HR, Bantscheff M, et al. Ca^{2+} signals critical for egress and gametogenesis in malaria parasites depend on a multipass membrane protein that interacts with PKG. Sci Adv. 2021;7(13).
87. Bushell E, Gomes AR, Sanderson T, Anar B, Girling G, Herd C, et al. Functional profiling of a *Plasmodium* genome reveals an abundance of essential genes. Cell. 2017;170(2):260-72 e8.
88. Jiang Y, Wei J, Cui H, Liu C, Zhi Y, Jiang Z, et al. An intracellular membrane protein GEP1 regulates xanthurenic acid induced gametogenesis of malaria parasites. Nat Commun. 2020;11(1):1764.

89. Rajendran E, Hapuarachchi SV, Miller CM, Fairweather SJ, Cai Y, Smith NC, et al. Cationic amino acid transporters play key roles in the survival and transmission of apicomplexan parasites. Nat Commun. 2017;8:14455.
90. Kenthirapalan S, Waters AP, Matuschewski K, Kooij TW. Functional profiles of orphan membrane transporters in the life cycle of the malaria parasite. Nat Commun. 2016;7:10519.
91. Anand A, Chandana M, Ghosh S, Das R, Singh N, Vaishalli PM, et al. Significance of *Plasmodium berghei* amino acid transporter 1 in food vacuole functionality and its association with cerebral pathogenesis. Microbiol Spectr. 2023;11(2):e0494322.
92. Kuehnel RM, Ganga E, Balestra AC, Suarez C, Wyss M, Klages N, et al. A *Plasmodium* membrane receptor platform integrates cues for egress and invasion in blood forms and activation of transmission stages. Sci Adv. 2023;9(24):eadf2161.
93. Overington JP, Al-Lazikani B, Hopkins AL. How many drug targets are there? Nat Rev Drug Discov. 2006;5(12):993-6.
94. Birnbaum J, Flemming S, Reichard N, Soares AB, Mesen-Ramirez P, Jonscher E, et al. A genetic system to study *Plasmodium falciparum* protein function. Nat Methods. 2017;14(4):450-6.
95. Briquet S, Gissot M, Silvie O. A toolbox for conditional control of gene expression in apicomplexan parasites. Mol Microbiol. 2022;117(3):618-31.
96. Okombo J, Kanai M, Deni I, Fidock DA. Genomic and genetic approaches to studying antimalarial drug resistance and *Plasmodium* biology. Trends Parasitol. 2021;37(6):476-92.
97. Prommana P, Uthaipibull C, Wongsombat C, Kamchonwongpaisan S, Yuthavong Y, Knuepfer E, et al. Inducible knockdown of *Plasmodium* gene expression using the *glmS* ribozyme. PLoS One. 2013;8(8):e73783.
98. Armstrong CM, Goldberg DE. An FKBP destabilization domain modulates protein levels in *Plasmodium falciparum*. Nat Methods. 2007;4(12):1007-9.
99. Fierro MA, Hussain T, Campin LJ, Beck JR. Knock-sideways by inducible ER retrieval enables a unique approach for studying *Plasmodium*-secreted proteins. Proc Natl Acad Sci U S A. 2023;120(33):e2308676120.
100. Kyte J, Doolittle RF. A simple method for displaying the hydropathic character of a protein. J Mol Biol. 1982;157(1):105-32.
101. Trager W, Jensen JB. Human malaria parasites in continuous culture. Science. 1976;193(4254):673-5.
102. Zolg JW, MacLeod AJ, Dickson IH, Scaife JG. *Plasmodium falciparum*: modifications of the *in vitro* culture conditions improving parasitic yields. J Parasitol. 1982;68(6):1072-80.
103. Lambros C, Vanderberg JP. Synchronization of *Plasmodium falciparum* erythrocytic stages in culture. J Parasitol. 1979;65(3):418-20.
104. Radfar A, Mendez D, Moneriz C, Linares M, Marin-Garcia P, Puyet A, et al. Synchronous culture of *Plasmodium falciparum* at high parasitemia levels. Nat Protoc. 2009;4(12):1899-915.
105. Hatefi Y, Hanstein WG. Solubilization of particulate proteins and nonelectrolytes by chaotropic agents. Proc Natl Acad Sci U S A. 1969;62(4):1129-36.
106. Woodcock DM, Crowther PJ, Doherty J, Jefferson S, DeCruz E, Noyer-Weidner M, et al. Quantitative evaluation of *Escherichia coli* host strains for tolerance to cytosine methylation in plasmid and phage recombinants. Nucleic Acids Res. 1989;17(9):3469-78.

107. Asif A, Mohsin H, Tanvir R, Rehman Y. Revisiting the mechanisms involved in calcium chloride induced bacterial transformation. Front Microbiol. 2017;8:2169.
108. Weston A, Brown MG, Perkins HR, Saunders JR, Humphreys GO. Transformation of *Escherichia coli* with plasmid deoxyribonucleic acid: calcium-induced binding of deoxyribonucleic acid to whole cells and to isolated membrane fractions. J Bacteriol. 1981;145(2):780-7.
109. Panja S, Aich P, Jana B, Basu T. How does plasmid DNA penetrate cell membranes in artificial transformation process of *Escherichia coli*? Mol Membr Biol. 2008;25(5):411-22.
110. Doherty AJ, Suh SW. Structural and mechanistic conservation in DNA ligases. Nucleic Acids Res. 2000;28(21):4051-8.
111. Wong TK, Neumann E. Electric field mediated gene transfer. Biochem Biophys Res Commun. 1982;107(2):584-7.
112. Govindarajalu G, Rizvi Z, Kumar D, Sijwali PS. Lyse-reseal erythrocytes for transfection of *Plasmodium falciparum*. Sci Rep. 2019;9(1):19952.
113. Skinner-Adams TS, Lawrie PM, Hawthorne PL, Gardiner DL, Trenholme KR. Comparison of *Plasmodium falciparum* transfection methods. Malar J. 2003;2:19.
114. Rug M, Maier AG. Transfection of *Plasmodium falciparum*. Methods Mol Biol. 2013;923:75-98.
115. Mamoun CB, Gluzman IY, Goyard S, Beverley SM, Goldberg DE. A set of independent selectable markers for transfection of the human malaria parasite *Plasmodium falciparum*. Proc Natl Acad Sci U S A. 1999;96(15):8716-20.
116. Tsirigos KD, Peters C, Shu N, Kall L, Elofsson A. The TOPCONS web server for consensus prediction of membrane protein topology and signal peptides. Nucleic Acids Res. 2015;43(W1):W401-7.
117. Viklund H, Elofsson A. OCTOPUS: improving topology prediction by two-track ANN-based preference scores and an extended topological grammar. Bioinformatics. 2008;24(15):1662-8.
118. Reynolds SM, Kall L, Riffle ME, Bilmes JA, Noble WS. Transmembrane topology and signal peptide prediction using dynamic bayesian networks. PLoS Comput Biol. 2008;4(11):e1000213.
119. Kall L, Krogh A, Sonnhammer EL. An HMM posterior decoder for sequence feature prediction that includes homology information. Bioinformatics. 2005;21 Suppl 1:i251-7.
120. Bernsel A, Viklund H, Falk J, Lindahl E, von Heijne G, Elofsson A. Prediction of membrane-protein topology from first principles. Proc Natl Acad Sci U S A. 2008;105(20):7177-81.
121. Viklund H, Bernsel A, Skwark M, Elofsson A. SPOCTOPUS: a combined predictor of signal peptides and membrane protein topology. Bioinformatics. 2008;24(24):2928-9.
122. Amara SG, Arriza JL. Neurotransmitter transporters: three distinct gene families. Curr Opin Neurobiol. 1993;3(3):337-44.
123. Moon RW, Hall J, Rangkuti F, Ho YS, Almond N, Mitchell GH, et al. Adaptation of the genetically tractable malaria pathogen *Plasmodium knowlesi* to continuous culture in human erythrocytes. Proc Natl Acad Sci U S A. 2013;110(2):531-6.
124. Tshabalala S. Genetic and chemical interrogation of the transcriptional factor PfMyb1 during *Plasmodium falciparum* proliferation and differentiation: University of Pretoria; 2023.

125. Kudyba HM, Cobb DW, Vega-Rodriguez J, Muralidharan V. Some conditions apply: Systems for studying *Plasmodium falciparum* protein function. PLoS Pathog. 2021;17(4):e1009442.
126. O'Donnell RA, Freitas-Junior LH, Preiser PR, Williamson DH, Duraisingh M, McElwain TF, et al. A genetic screen for improved plasmid segregation reveals a role for Rep20 in the interaction of *Plasmodium falciparum* chromosomes. EMBO J. 2002;21(5):1231-9.
127. van Dijk MR, Vinkenoog R, Ramesar J, Vervenne RA, Waters AP, Janse CJ. Replication, expression and segregation of plasmid-borne DNA in genetically transformed malaria parasites. Mol Biochem Parasitol. 1997;86(2):155-62.

9. Supplementary

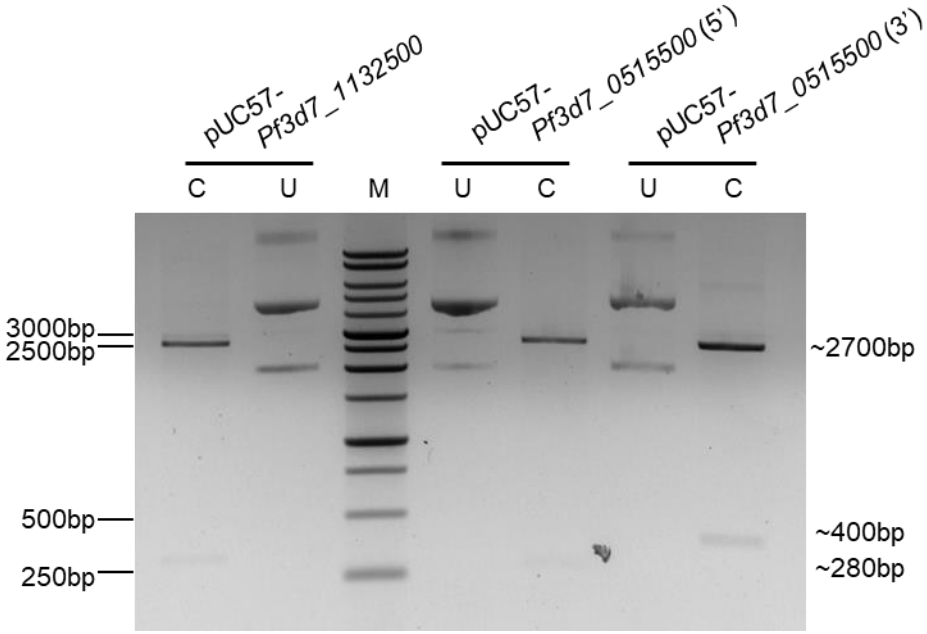

Figure 9.1: RE digestion of synthesised pUC57 for Figure 5.5 and Figure 5.15.
pUC57 plasmids syntheised by Gene Universal, digested with *Not*I and *Mlu*I and visualised on 1 % (w/v) agarose/TAE gel with 0.5 µg/mL EtBr to isolate respective gene fragments. Lane M contains a GeneRuler™ 1 kb DNA ladder (Promega), U: undigested plasmids, C: digested plasmids.

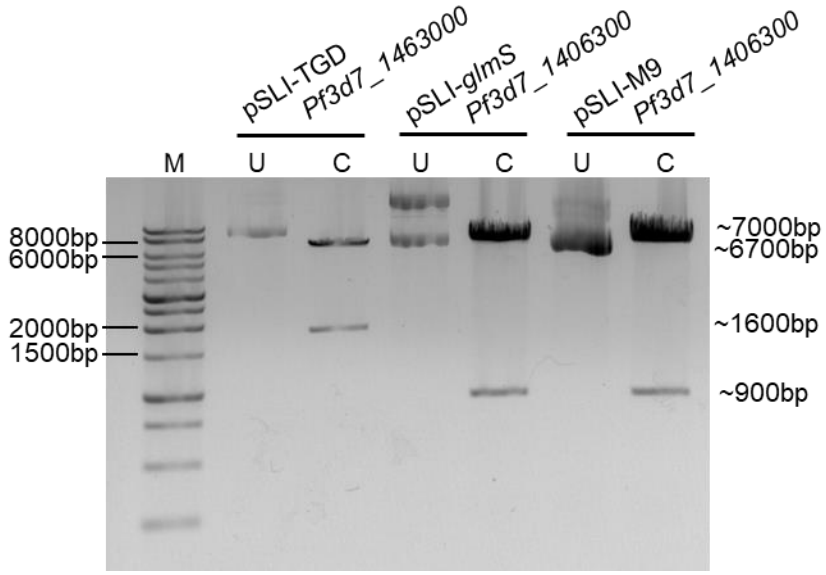

Figure 9.2: RE digestion of pSLI-TGD, pSLI-*glmS* and pSLI-M9 vectors for Figure 5.5 and Figure 5.15.

Vectors were digested with *Not*I and *Mlu*I and visualised on 1 % (w/v) agarose/TAE gel with 0.5 µg/mL EtBr to isolate respective vector backbones. Lane M contains a GeneRuler™ 1 kb DNA ladder (Promega), U: undigested plasmids, C: digested plasmids.

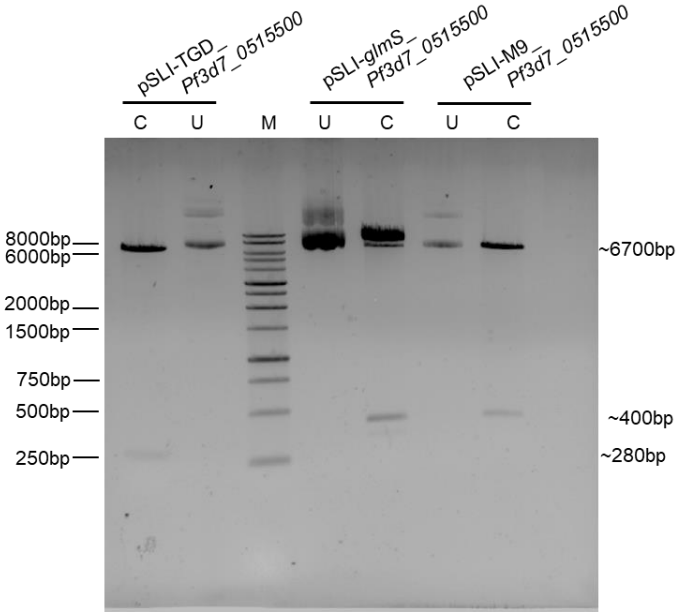

Figure 9.3: RE digestion of pSLI-TGD and pSLI-*glmS*-M9 plasmids with *Pf3d7_0515500* fragments for Figure 5.7 and Figure 5.17.
Plasmids were digested with *Not*I and *Mlu*I and visualised on 1 % (w/v) agarose/TAE gel with 0.5 µg/mL EtBr to confirm fragment sizes of recombinant plasmids. Lane M contains a GeneRuler™ 1 kb DNA ladder (Promega), U: undigested plasmids, C: digested plasmids.

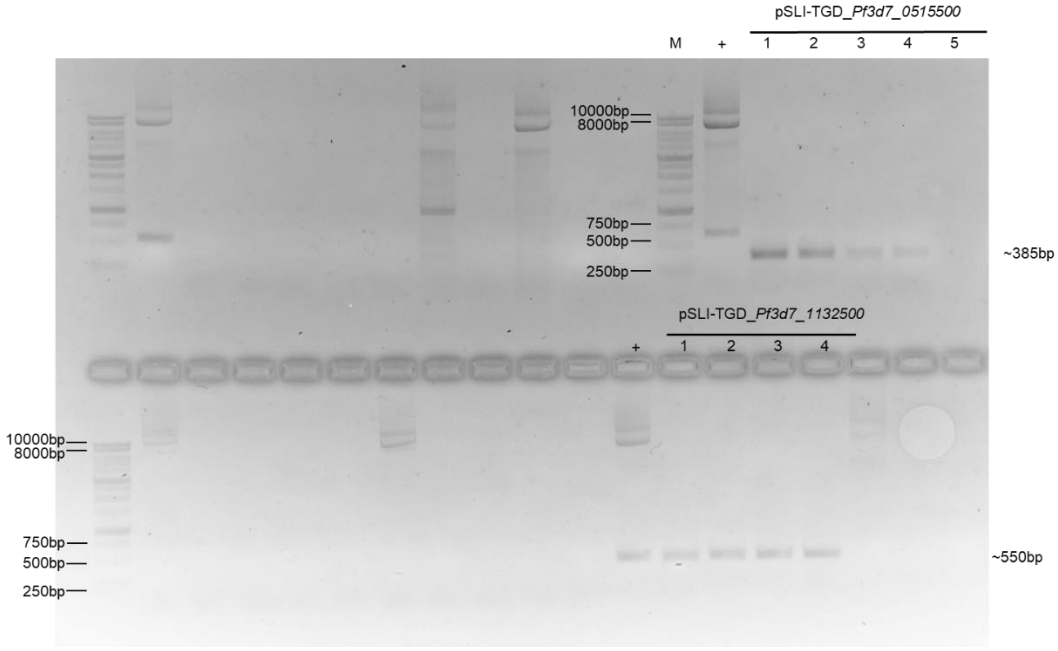

Figure 9.4: PCR screening for recombinant pSLI-TGD_*gene* for Figure 5.6.
Bacterial colonies PCR screened for recombinant plasmids were visualised on 1 % (w/v) agarose/TAE gel with 0.5 µg/mL EtBr. Lane M contains a GeneRuler™ 1 kb DNA ladder (Promega), and the positive control (+) contained the pSLI-TGD plasmid with the original insert.

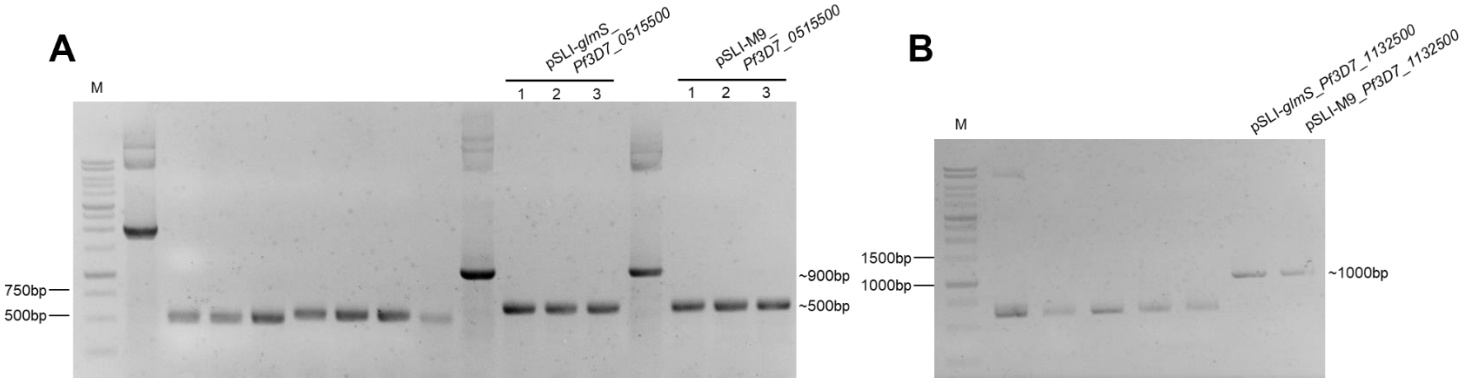

Figure 9.5: PCR screening for recombinant pSLI-*glmS*-M9_*gene* for Figure 5.16.
Bacterial colonies screened with vector specific primers for recombinant plasmids were visualised on 1 % (w/v) agarose/TAE gel with 0.5 µg/mL EtBr. Lane M contains a GeneRuler™ 1 kb DNA ladder (Promega).

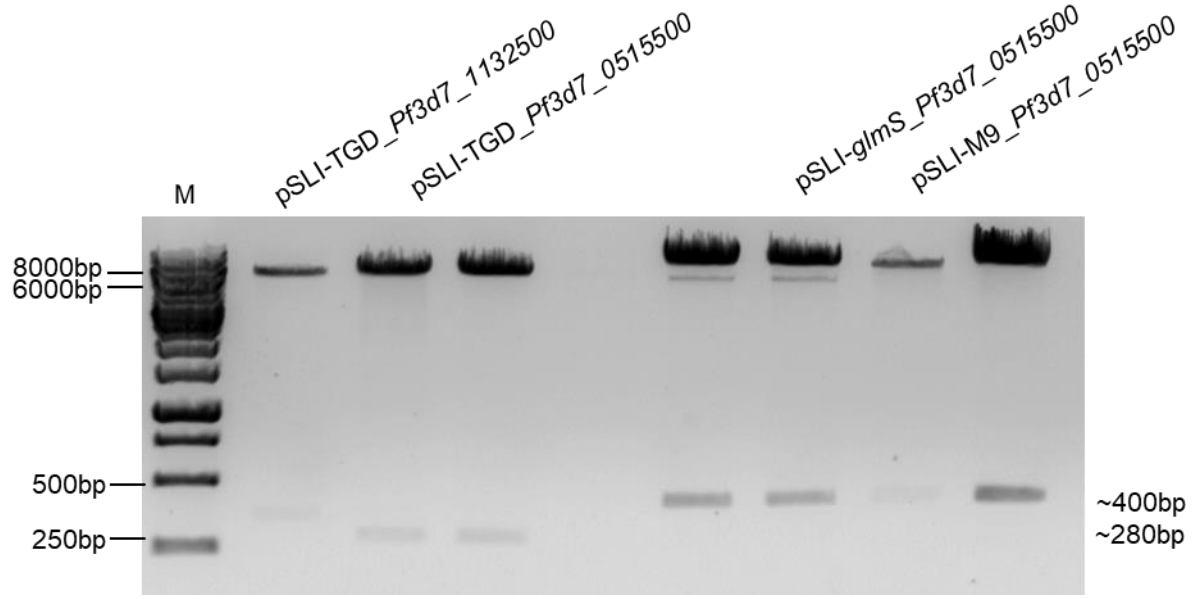

Figure 9.6: Validation of recombinant pSLI-TGD and pSLI-*glmS*-M9 plasmids for transfection for Figure 5.9 and Figure 5.19.
Large scale isolated plasmids were digested with *Not*I and *Mlu*I and visualised on 1 % (w/v) agarose/TAE gel with 0.5 µg/mL EtBr. Lane M contains a GeneRuler™ 1 kb DNA ladder (Promega).

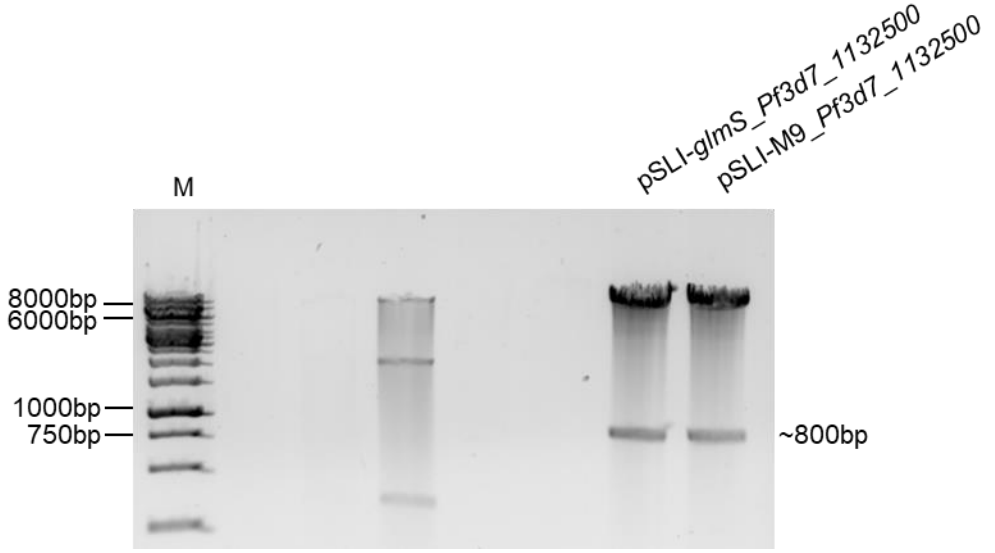

Figure 9.7: Validation of recombinant pSLI-*glmS*/-M9 plasmids for transfection for Figure 5.19.
Large scale isolated plasmids for *Pf3d7_1132500* were digested with *Not*I and *Mlu*I and visualised on 1 % (w/v) agarose/TAE gel with 0.5 µg/mL EtBr. Lane M contains a GeneRuler™ 1 kb DNA ladder (Promega).

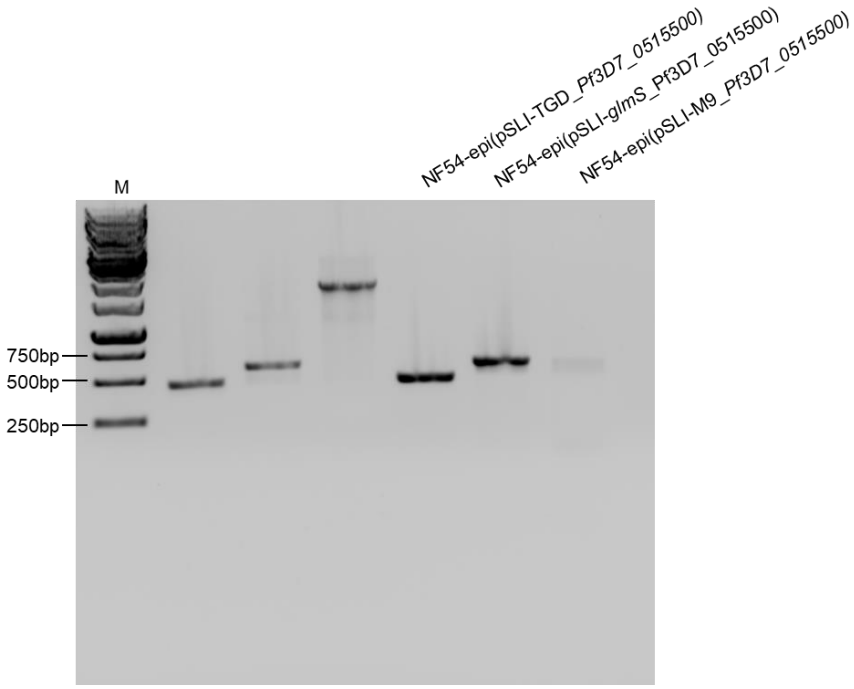

Figure 9.8: Validation of *Pf3d7_0515500* plasmid episomal presence for Figure 5.12 and Figure 5.21.
PCR screen for episomal presence of pSLI-TGD and pSLI-*glmS*/-M9 and visualised on 1 % (w/v) agarose/TAE gel with 0.5 µg/mL EtBr. Lane M contains a GeneRuler™ 1 kb DNA ladder (Promega).

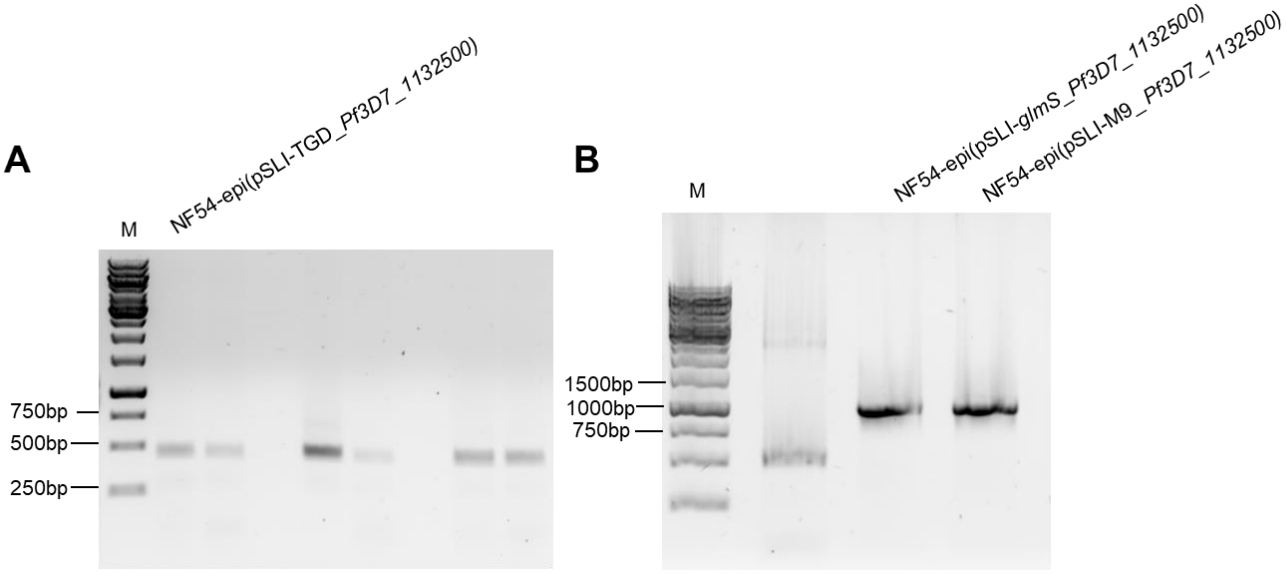

Figure 9.9: Validation of *Pf3d7_1132500* plasmid episomal presence for Figure 5.12 and Figure 5.21.
Screen for episomal presence of **A)** pSLI-TGD and **B)** pSLI-*glmS*/-M9 and visualised on 1 % (w/v) agarose/TAE gel with 0.5 µg/mL EtBr. Lane M contains a GeneRuler™ 1 kb DNA ladder (Promega).